Università degli Studi di Ferrara

DOTTORATO DI RICERCA IN
BIOCHIMICA, BIOLOGIA MOLECOLARE E BIOTECNOLOGIE

CICLO XXII

COORDINATORE Prof. FRANCESCO BERNARDI

HUMAN HERPESVIRUS 8 UPREGULATES ACTIVATING TRANSCRIPTION FACTOR 4 (ATF4)
and
REAL TIME PCR TO ASSESS TOTAL BACTERIAL LOAD IN CHRONIC WOUNDS

Settore Scientifico Disciplinare MED/07

Dottorando Dott.ssa GENTILI VALENTINA

Tutore Prof. DI LUCA DARIO

Anni 2007/2009

INDEX

ABSTRACT

I. Human Herpesvirus 8 Upregulates Activator Transcription Factor 4

BACKGROUND: Human herpesvirus 8 (HHV-8) is the primary etiologic agent of Kaposi's sarcoma, a highly vascularised neoplasm of endothelial origin characterized by inflammation, neoangiogenesis, and by the presence of characteristic spindle cells. HHV-8 angiogenic activity is due to the activation of NF-kB and the subsequent induction of MCP-1 synthesis. MCP-1 is a chemokine produced by macrophages and endothelial cells in response to different stimuli, and is a direct mediator of angiogenesis. HHV-8-induced angiogenesis is MCP-1 dependent. However, HHV-8 activation of MCP-1 is not completely dependent on NF-kB induction and another cellular factor is involved. A potential candidate is the cellular activating transcription factor 4 (ATF4), a stress responsive gene. ATF4 is upregulated in several condition, including ER-stress, viral infection (e.g. CMV) and in tumours.

AIM: The aim of the research is to study the interaction between HHV-8 and ATF4, and verify whether ATF4 is involved in angiogenesis characteristic of HHV-8 infection.

METHODS: To demonstrate the effect of HHV-8 on ATF4 expression, Jurkat cells were infected with a cell-free viral inoculum, obtained in our laboratory by stimulating reactivation of latent HHV-8 in chronically infected cells (PEL-derived). HHV-8 reactivation from latency was assessed by transfection of BC-3 and BCBL-1 cells (PEL-derived) with pCG-ATF4 recombinant plasmid. DNA or RNA were analysed by PCR, rtPCR or quantitative real time PCR. Promoters activation was assessed by luciferase assays.

RESULTS: HHV-8 upregulates the expression of ATF4 gene, and overexpression of ATF4 is able to increase replication and transcription of HHV-8, but not to reactivate HHV-8 from latency. Preliminary results show that ATF4 activates the MCP-1 promoter in absence of the NF-kB binding sites.

CONCLUSION: HHV-8 induces ATF4 expression during the productive infection, probably to obtain advantage for its replication and neoplastic development. ATF4 might be implicated in HHV-8 induced tumorigenesis, being involved in several aspects of viral

replication, and could represent a potential therapeutic target for HHV-8 induced transformation.

II. Real Time PCR To Assess Total Bacterial Load in Chronic Wounds

BACKGROUND: Wounds and wound healing are important issues in chronic patients (i.e. diabetes, pressure). Critical colonization and infection are strictly linked to a delay in wound healing. Analysis of pathogens present in chronic wound is an essential aspect for the wound care. Classic microbiologic methods have several limits to ensure the correct analysis of ulcer environment.

AIM: To analyse total bacterial load by a single quantitative real time PCR reaction in swabs and biopsies obtained from infected chronic wounds treated with an innovative hydrophobic dressing.

METHODS: Biopsies were collected at the beginning and after 4 weeks of treatment, and swabs were collected once a week for 4 weeks. Real time PCR was carried out on DNA extracted from biopsies and swabs amplifying a region of the 16s rRNA gene, highly conserved among bacteria. Moreover, DNA extracted from biopsies was also analysed for the detection of 2 anaerobic bacteria (*B. Fragilis*, *F. necrophorum*, frequently associated with delayed healing) by real time PCR amplifying specific unique regions of their genome. In parallel, classical culturing methods were performed on biopsies searching for *Staphylococcus* and *Pseudomonas* species.

RESULTS: We evaluated the correlation between the molecular data obtained by real time PCR and the clinical data, in particular considering the area of the wound. We observed a mean 253-fold decrease of the total bacterial load in 10/20 wounds those also showed an average 58% decrease of their area. This 10 wounds showed a positive correlation between clinical and molecular data. In 5/20 wound, we found a non significant 5,2-fold decrease of the total bacterial load, correlate with a 27% increase of the wound's area. Thus, 75% of molecular results (15/20 wounds) were correlate to the clinical data. In contrast, classical culturing method did not correlate with the clinical data, confirming that classical methods have several limits and disadvantages. *B. Fragilis* was present in 10/20 wounds, and *F. necrophorum* in 2/20 wounds.

CONCLUSION: The molecular approach can be considered a reliable and rapid test to assess infection levels in chronic wounds, being more sensitive than the classic cultural techniques. The research of specific pathogens is not sufficient to assess the outcome of the wounds, whereas total bacterial load can give a prognostic value to the wound care.

RIASSUNTO

I. L'herpesvirus umano 8 (HHV-8) "upregola" il fattore d'attivazione trascrizionale ATF4.

INTRODUZIONE: HHV-8 è l'agente eziologico del Sarcoma di Kaposi, un tumore altamente vascolarizzato di origine endoteliale caratterizzato da infiammazione, neoangiogenesi, e dalla presenza di cellule dalla caratteristica forma *spindle*. L'attività angiogenica di HHV-8 è dovuta all'attivazione del fattore NF-kB e dalla conseguente induzione della sintesi di MCP-1, una chemochina prodotta da macrofagi e cellule endoteliali in risposta a diversi stimoli. MCP-1 è un mediatore diretto dell'angiogenesi. L'angiogenesi indotta da HHV-8 è MCP-1-dipendente, ed è in parte dovuta all'attivazione di NF-kB. Dato che l'attivazione di MCP-1 da parte di HHV-8 non è completamente dipendente da NF-kB, si è ipotizzato che fosse coinvolto un altro fattore cellulare. Un potenziale candidato è ATF4, un fattore cellulare di attivazione trascrizionale, ubiquitario, sovraespresso nei tumori e normalmente attivato in risposta a diversi stimoli di stress cellulare, come ad esempio lo stress del reticolo endoplasmatico, l'infezione virale.

SCOPO: Lo scopo della ricerca è stato quello di studiare le interazioni tra HHV-8 e ATF4, e di verificare se ATF4 fosse coinvolto nell'angiogenesi indotta da HHV-8.

METODI: Per dimostrare l'effetto di HHV-8 sull'espressione di ATF4, cellule Jurkat sono state infettate con un inoculo virale *cell-free* prodotto nel nostro laboratorio tramite la riattivazione di HHV-8 in cellule latentemente infettate dal virus (derivate da PEL). Per verificare l'azione di ATF4 sull'infezione virale, cellule derivate da PEL, BC-3 e BCBL-1, sono state transfettate con il plasmide ricombinante pCG-ATF4. I DNA e gli RNA estratti sono stati analizzati tramite la PCR, la rtPCR o la real time PCR quantitativa. Per analizzare l'attivazione su promotori genici è stato utilizzato il saggio della Luciferasi.

RISULTATI: HHV-8 "upregola" l'espressione di ATF4, e la sovraespressione di ATF4 è in grado di aumentare la replicazione e la trascrizione di HHV-8. Nonostante ciò, ATF4 non è in grado di riattivare il virus dalla latenza, dal momento che non attiva i principali promotori di HHV-8. ATF4 è però in grado di attivare il promotore di MCP-1 in assenza dei siti di legame per NF-kB.

CONCLUSIONE: HHV-8 induce l'espressione di ATF4 durante l'infezione produttiva, probabilmente per trarne vantaggio per la replicazione e per lo sviluppo neoplastico. ATF4 potrebbe quindi essere coinvolto nella tumorigenesi indotta da HHV-8, essendo implicato in diversi aspetti della replicazione virale, e potrebbe rappresentare un potenziale *target* terapeutico contro la trasformazione indotta da HHV-8.

II. Utilizzo della tecnica della real time PCR per quantificare la carica batterica totale in ulcere croniche.

INTRODUZIONE: Le ulcere croniche più comuni includono le ulcere venose, diabetiche e da pressione. La condizione cronica indica la mancanza di guarigione per mesi o addirittura anni, gravando pesantemente a livello fisico e psicologico sul paziente. La colonizzazione e l'infezione di ferite croniche sono strettamente correlate alla mancata guarigione. L'analisi dei patogeni presenti è un aspetto fondamentale per il trattamento delle ulcere croniche. I metodi della microbiologia classica presentano diversi limiti per una corretta analisi del microambiente di un'ulcera, tra cui il maggior tempo impiegato per effettuare l'analisi, la minor sensibilità dei risultati, ma soprattutto l'impossibilità di coltivare tutti i patogeni presenti in una lesione. Per questi motivi, recentemente sono stati considerati con crescente interesse approcci molecolari per quantificare ed identificare i patogeni presenti nelle lesioni croniche.

SCOPO: Lo scopo della ricerca è stato quello di analizzare la carica batterica totale attraverso un'unica reazione di real time PCR in tamponi e biopsie di ulcere croniche infette trattate con una medicazione idrofobica innovativa.

METODI: Le biopsie sono state effettuate all'inizio e al termine di 4 settimane di trattamento e i tamponi una volta alla settimana per 4 settimane. Il DNA estratto da tali campioni è stato processato attraverso la real time PCR amplificando una regione del gene codificante per 16S rRNA, altamente conservato in tutti i batteri. Inoltre, il DNA estratto dalle biopsie è stato analizzato per la ricerca di 2 batteri anaerobi frequentemente associati alla mancanza di guarigione delle ulcere, *B. fragilis* e *F. necrophorum.* Parallelamente, le biopsie sono state analizzate tramite la microbiologia classica per verificare la presenza di *Staphylococcus* e *Pseudomonas spp.*

RISULTATI: Abbiamo valutato la correlazione tra i dati molecolari ottenuti mediante real time PCR e i risultati clinici riguardanti l'area dell'ulcera. E' stata osservata una diminuzione di 253 volte della carica batterica in 10 ulcere su 20, le quali hanno mostrato anche una diminuzione media dell'area ulcerosa del 58%. In 5 ulcere su 20, non è stata osservata variazione tra la carica batterica all'inizio e al termine del trattamento, e anche il risultato clinico è stato negativo, con un aumento medio dell'area dell'ulcera del 27%. Quindi, il 75% dei risultati molecolari era correlato con i risultati clinici, mentre i dati ottenuti con la microbiologia classica non concordavano con l'andamento delle lesioni, confermando che i metodi culturali presentano diversi limiti e svantaggi. Per quanto riguarda gli anaerobi, il *B. fragilis* era presente in 10 ulcere su 20, ed il *F. necrophorum* in 2 su 20.

CONCLUSIONI: La tecnica molecolare può essere considerata un test più rapido, sensibile ed affidabile dei metodi microbiologici classici, per valutare i livelli d'infezione in ferite croniche e l'efficacia di trattamenti terapeutici. La ricerca di specifici patogeni all'interno di una lesione cutanea non è sufficiente per monitorare l'andamento delle ulcere, mentre sembra essere molto più rilevante la carca batterica totale, che può dare un valore prognostico all'esito della malattia.

PART I

HUMAN HERPESVIRUS 8 UPREGULATES ACTIVATING TRANSCRIPTION FACTOR 4 (ATF4)

INTRODUCTION

1. Herpesviruses: general features

1.1. Classification of herpesviruses

More than 100 herpesviruses have been discovered, all of them are double-stranded DNA viruses that can establish latent infections in their respective hosts. Eight herpesviruses infect humans. The *Herpesvirinae* family is subdivided into three subfamilies: the *Alpha-*, *Beta-*, or *Gammaherpesvirinae*[1].

The *Alphaherpesvirinae* are defined by variable cellular host range, shorter viral reproductive cycle, rapid growth in culture, high cytotoxic effects, and the ability to establish latency in sensory ganglia. Human alpha-herpesviruses are herpes simplex viruses 1 and 2 (HSV-1 and HSV-2) and varicella zoster virus (VZV), and are officially designated human herpesviruses 1, 2, and 3.

The *Betaherpesvirinae* have a more restricted host range with a longer reproductive viral cycle and slower growth in culture. Infected cells show cytomegalia (enlargement of the infected cells). Latency is established in secretory glands, lymphoreticular cells, and in different tissues, such as the kidneys and others. In humans, these are human cytomegalovirus (HCMV or herpesvirus 5) and roseoloviruses (causing the disease roseola infantum in children) including human herpesviruses 6A and 6B (HHV-6A and -6B) and human herpesvirus 7 (HHV-7).

The *Gammaherpesvirinae* in vitro replication occurs in lymphoblastoid cells, but lytic infections may occur in epithelial and fibroblasts for some viral species in this subfamily. Gammaherpesviruses are specific for either B or T cells with latent virus found in lymphoid tissues. Only two human gammaherpesviruses are known, human herpesvirus 4, or Epstein-Barr virus (EBV), and human herpesvirus 8, referred to as HHV-8 or Kaposi's sarcoma-associated herpesvirus (KSHV). The gammaherpesviruses subfamily contains two genera that include both the gamma-1 or *Lymphocryptovirus* (LCV) and the gamma-2 or *Rhadinovirus* (RDV) virus genera. EBV is the only *Lymphocryptovirus* and HHV-8 is the only *Rhadinovirus* discovered in humans. LCV

are found only in primates but RDV can be found in both primates and subprimate mammals. RDV DNAs are more diverse across species and are found in a broader range of mammalian species.

HHV-8 has sequence homology and genetic structure similar to another RDV, *Herpesvirus saimiri* (HVS). The T-lymphotropic *Herpesvirus saimiri* establishes specific replicative and persistent infection in different primate host species, causes fulminant T-cell lymphoma in its primate host and can immortalize infected T-cells.

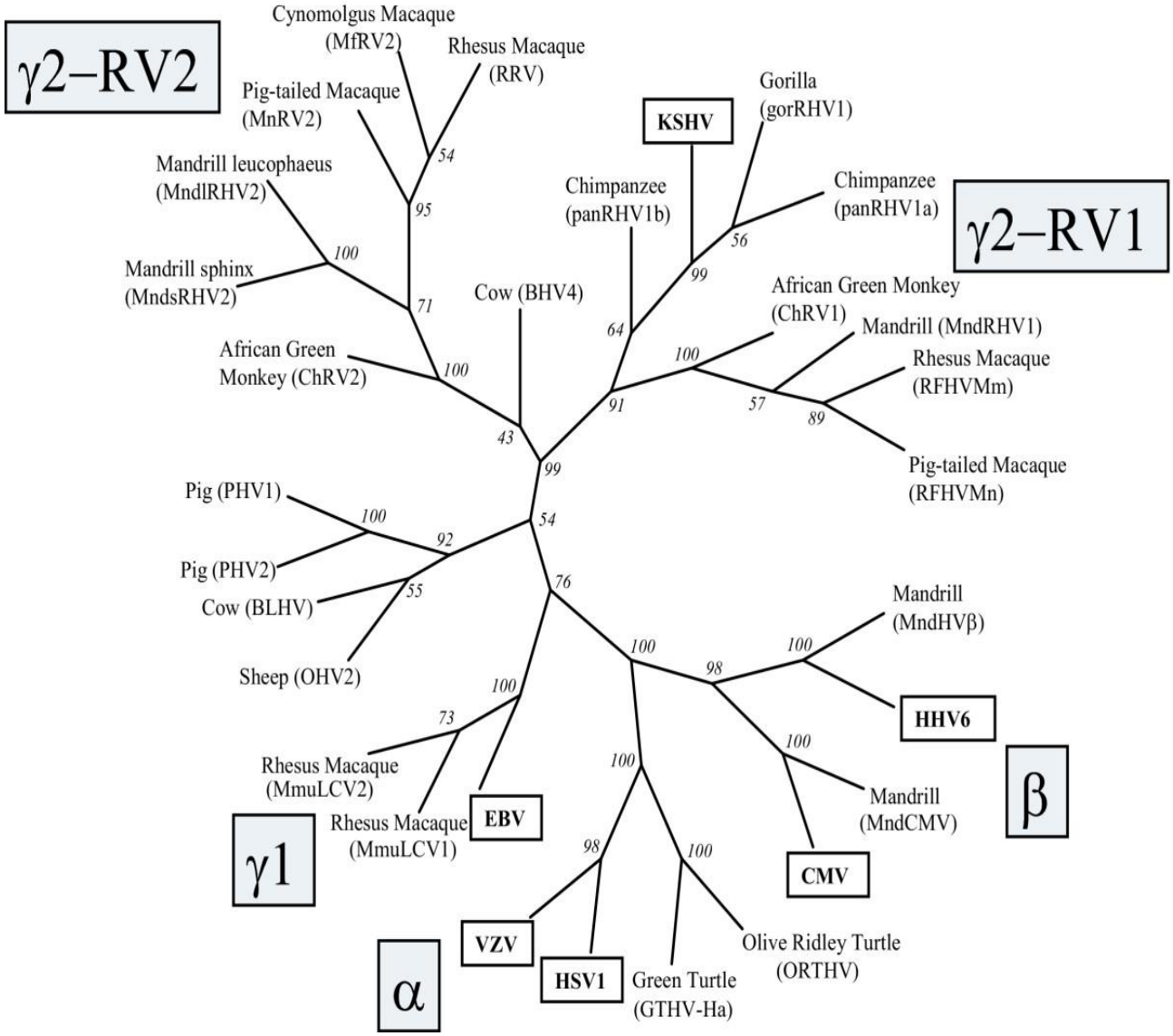

Figure 1: Phylogenetic tree of *herpesviridae*.

Human herpesvirus type	Sub Family	Target cell type	Latency sites	Pathologies
Herpes simplex-1 (HSV-1)	Alpha	Mucoepithelial cells	Neuron	Oral and genital herpes (predominantly orofacial)
Herpes simplex-2 (HSV-2)	Alpha	Mucoepithelial cells	Neuron	Oral and genital herpes (predominantly genital)
Varicella Zoster virus (VSV)	Alpha	Mucoepithelial cells	Neuron	chickenpox
Epstein-Barr Virus (EBV)	Gamma	B lymphocyte, epithelial cells	B lymphocytes	Infectious mononucleosis, Burkitt's lymphoma
Cytomegalovirus (CMV)	Beta	Epithelial cells, monocytes, lymphocytes	Monocytes, lymphocytes	Mononucleosis-like syndrome
Human herpes virus-6 (HHV-6)	Beta	T lymphocytes and others	T lymphocytes	Roseola infantum
Human herpes virus-7 (HHV-7)	Beta	T lymphocytes and others	T lymphocytes	Roseola infantum
Human herpes virus-8 (HHV-8) Kaposi's sarcoma-associated herpes virus (KSHV)	Gamma	Endothelial cells B lymphocytes monocytes	B lymphocytes and endothelial cells	Kaposi's sarcoma, Multicentric Castleman disease, Primary effusion lymphoma

Table 1: Human herpesviruses classification and characteristics.

1.2. Structure of herpesviruses

Herpesviruses have a central toroidal-shaped viral core containing a linear double stranded DNA. This DNA is embedded in a proteinaceous spindle[2]. The capsid is icosadeltahedral (16 surfaces) with 2-fold symmetry and a diameter of 100-120 nm that is partially dependent upon the thickness of the tegument. The capsid has 162 capsomeres.

The herpesvirus tegument, an amorphorous proteinaceous material that under EM lacks distinctive features, is found between the capsid and the envelope; it can have asymmetric distribution. Thickness of the tegument is variable depending on the location in the cell and varies among different herpesviruses[3].

The herpesvirus envelope contains viral glycoprotein protrusions on the surface of the virus. As shown by EM there is a lipid trilaminar structure derived from the cellular membranes. Glycoproteins protrude from the envelope and are more numerous and shorter than those found on other viruses.

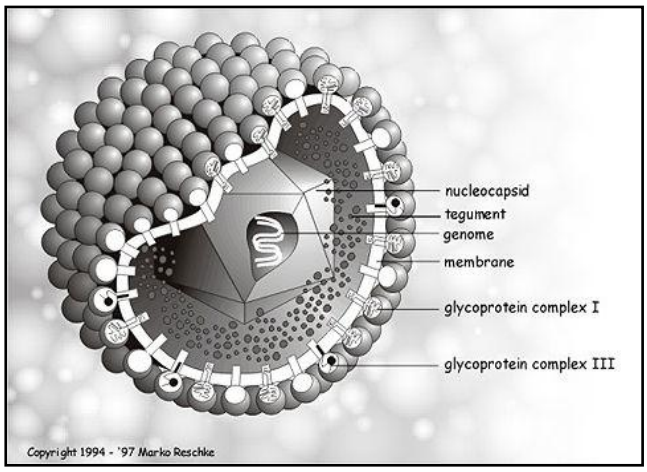

Figure 2: Representation of a herpesvirus virion.

1.3. Herpesviruses genome

Herpesvirus genome studied to date ranges in size from 130 to 235 kbp.

Herpesvirus DNA is characterized by two unique components, unique long (UL) and unique small (US) regions, each flanked by identical inverted repeat sequences. Herpesvirus genome also contains multiple repeated sequences

All known herpesviruses have capsid packaging signals at their termini[4]. The majority of herpes genes contain upstream promoter and regulatory sequences, an initiation site followed by a 5' nontranslated leader sequence, the open reading frame (ORF) itself, some 3' nontranslated sequences, and finally, a polyadenylation signal. Gene overlaps

are common, whereby the promoter sequences of antisense strand (3') genes are located in the coding region of sense strand (5') genes; ORFs can be antisense to one another.

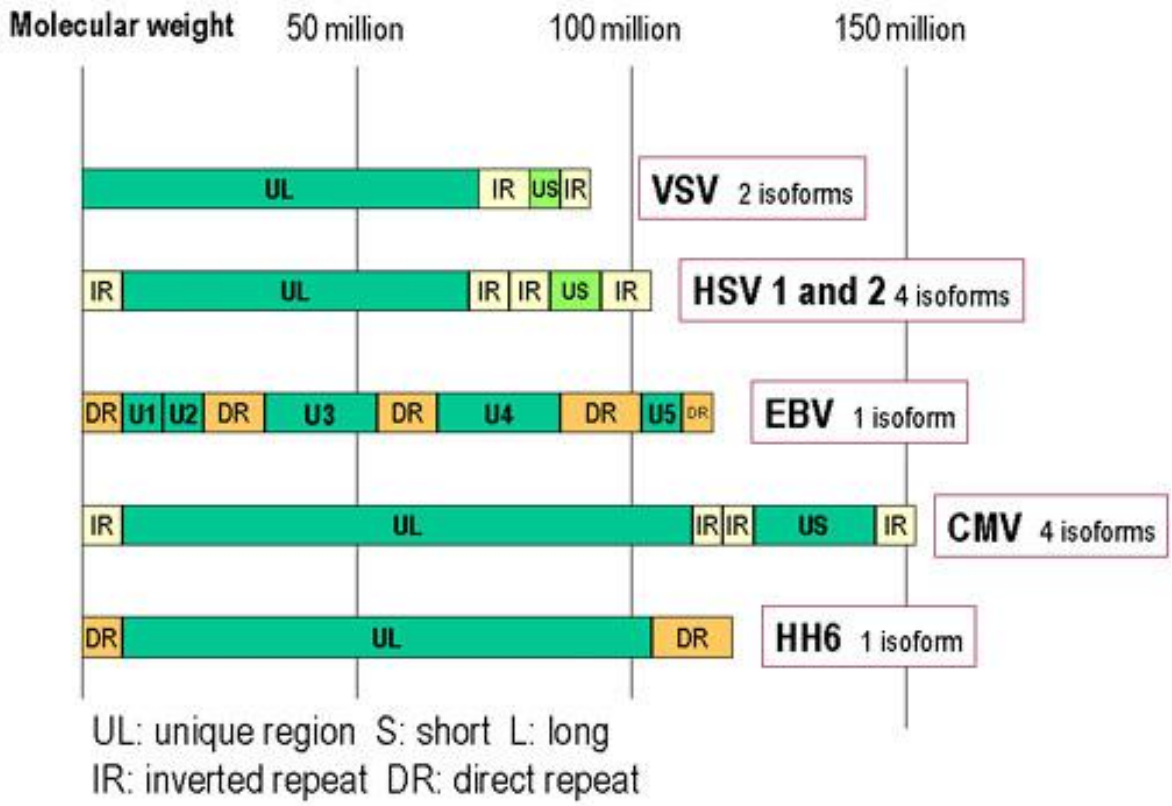

Figure 3: Genomic organization of some herpesviruses. HSV, VZV and CMV have inverted repeated sequences.

Proteins can be embedded within larger coding sequences and yet have different functions. Most genes are not spliced and therefore are without introns and sequences for noncoding RNAs are present.

Herpesviruses code for genes that synthetize proteins involved in establishment of latency, production of DNA, and structural proteins for viral replication, nucleic acid packaging, viral entry, capsid envelopment, for blocking or modifying host immune defences, and for transition from latency to lytic growth. Although all herpesviruses

establish latency, some (e.g., HSV) do not necessarily require latent protein expression to remain latent, unlike others (e.g., EBV and HHV-8).

1.4. Replication of herpesviruses

Herpesviruses can establish lytic or latent infection.

The lytic stage is divided in 6 phases:

1. Binding to the cell surface. As many other viruses, cell tropism is determined by the availability of the correct receptor on the surface of the cell
2. Envelope fusion with the plasma membrane
3. Uncoating. Degradation of the tegument. Capsid is carried to the nuclear membrane.
4. Transcription. The DNA genome then enters the nucleus. This is a very complex process, as expected considering the large size of viral genome. Viral DNA replicates by circularization followed by production of concatemers and cleavage of unit-length genome during packaging. The herpesvirus lytic replicative phase can be divided into four stages:

- α or immediate early (IE), requiring no prior viral protein synthesis. The genes expressed in this stage are involved in transactivating transcription from other viral genes.
- β or early genes (E), whose expression is independent of viral DNA synthesis.
- Following the E phase, γ1 or partial late genes are expressed in concert with the beginning of viral DNA synthesis.
- γ2 or late genes (L), where protein expression is totally dependent upon synthesis of viral DNA and expression of structural genes encoding for capsid proteins and envelope glycoproteins occurs.

Herpesvirus DNA is transcribed to RNA by cellular RNA polymerase I. The neo-formed viral mRNAs block cellular protein synthesis and activate the replication of viral DNA. Herpesviruses encode their own DNA-dependent DNA polymerase and other enzymes and proteins necessary to replication, such as ori-Lyt (replication start for the lytic phase), major DNA binding protein (MDBP) and origin DNA binding protein

(OBP). Herpesviruses can alter their environment by affecting host cell protein synthesis and host cell DNA replication, immortalizing the host cell, and altering the host's immune responses (e.g., blocking apoptosis, cell surface MHC I expression, modulation of the interferon pathway).

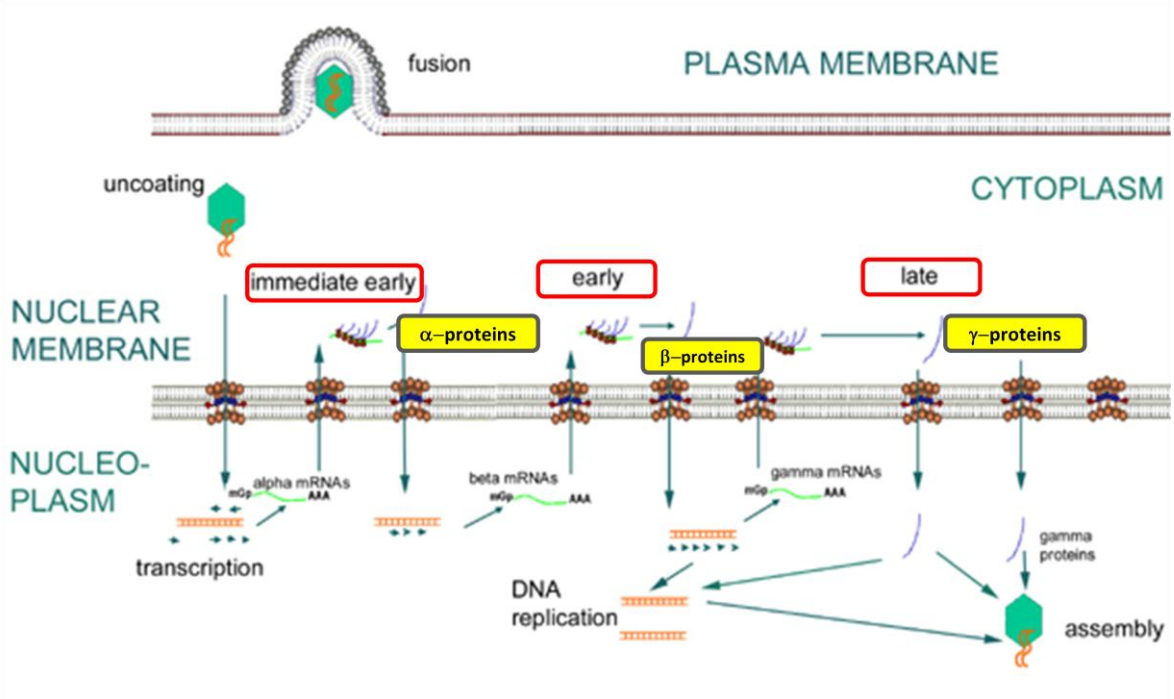

Figure 4: Representation of lytic phase of herpesviruses.

5. Assembly: capsids are assembled in the nucleus.
6. The viral particles bud through the inner lamella of the nuclear membrane which has been modified by the insertion of viral glycoproteins and leave the cell via the exocytosis pathway.

In the latent phase, the virus genome depends on the host replication machinery and replicates as closed circular episome. Latency typically involves the expression of only a few latency specific genes. Generally, most infected host cells harbour latent virus, as in the case of HHV-8: when KS tissue or HHV-8 infected cultured cells are analyzed, the virus is latent in majority of infected cells. Different signals such as inflammation and immunosuppression may cause the virus to enter into a new lytic phase.

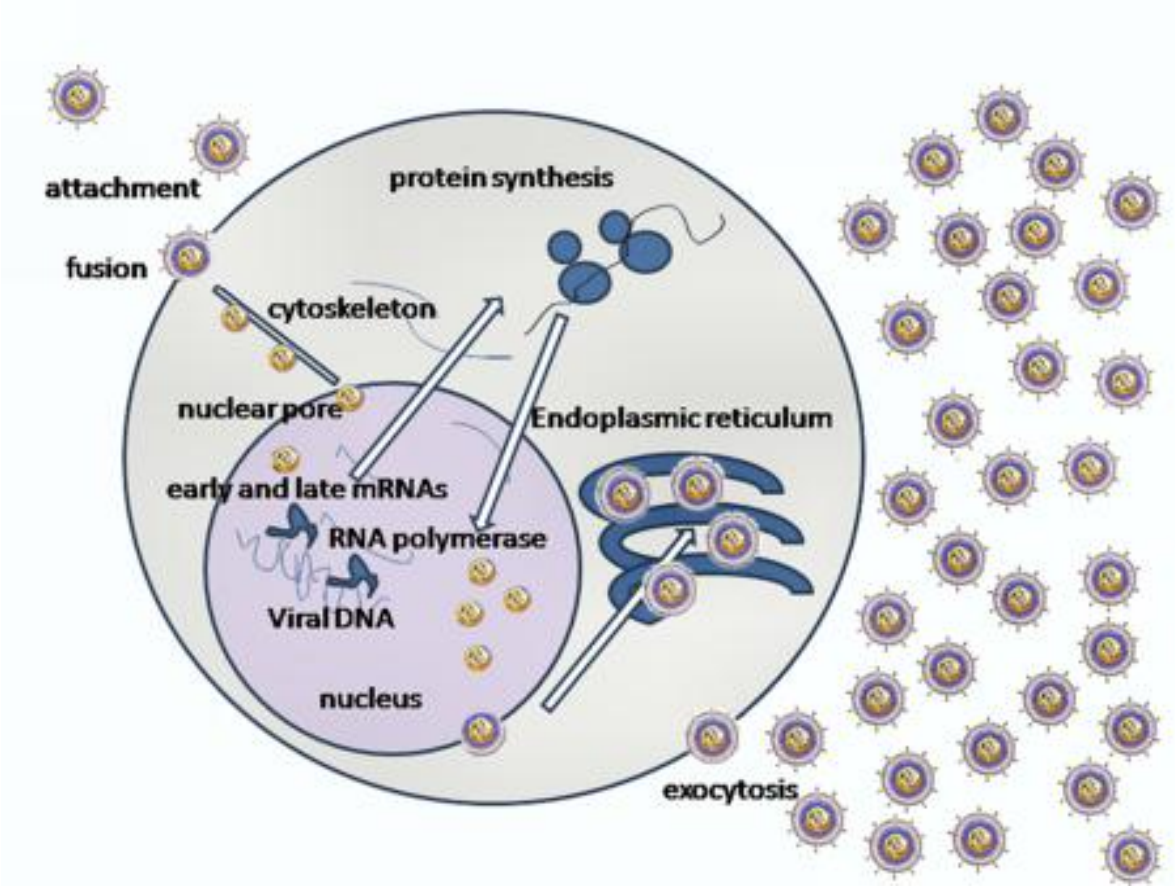

Figure 5: Herpesviruses replication cycle.

2. Human herpesvirus 8

Human herpesvirus 8 (HHV-8), also known as Kaposi's sarcoma associated herpesvirus (KSHV), is a member of the Rhadinovirus genus in the gamma-herpesvirus subfamily, first detected in 1994 in a patient affected by Kaposi sarcoma (KS)[5], a neoplasm of endothelial origin. Since then, HHV-8 has been identified as the etiologic agent of all epidemiologic forms of KS, including classical, endemic African, iatrogenic and AIDS types. In addition, HHV-8 has been implicated in the pathogenesis of other neoplastic disorders affecting immunocompromised hosts: primary effusion lymphoma (PEL, a rare form of B-cell lymphoma)[6], multicentric Castleman disease (MCD, a B-cell

lymphoproliferative disease)[7], other lymphoproliferative disorders affecting patients infected with HIV[8], and neoplastic complications in patients after transplantation[9].

2.1. Structure of human herpesvirus 8

HHV-8 has the typical morphology of the herpesviruses.

The envelope contains proteins of cellular origin and virus-specific glycoproteins, such as gB, gM, gH and K8.1.

The tegument is an amorphous asymmetric proteinaceous layer between envelope and capsid and contains proteins encoded by ORFs 19, 63, 64, 67, 75.

Each capsid, 125 nm in diameter, contains 12 pentons and 150 hexons which are interconnected by 320 triplexes. These capsomers or structural components are arranged in a icosahedral lattice with 20 triangular faces. Each asymmetric unit (one-third of a triangular face) of the capsid contains one-fifth of a penton at the vertex. Several proteins are involved in capsid assembling: the major capsid protein (MCP), three capsid proteins encoded by ORF62, ORF26, ORF65 and a protease encoded by ORF17. Hexons and pentons contain 5 or 6 MCPs, and triplexes contain ORF62 monomer and ORF26 dimer[10].

The core contains the linear double stranded DNA.

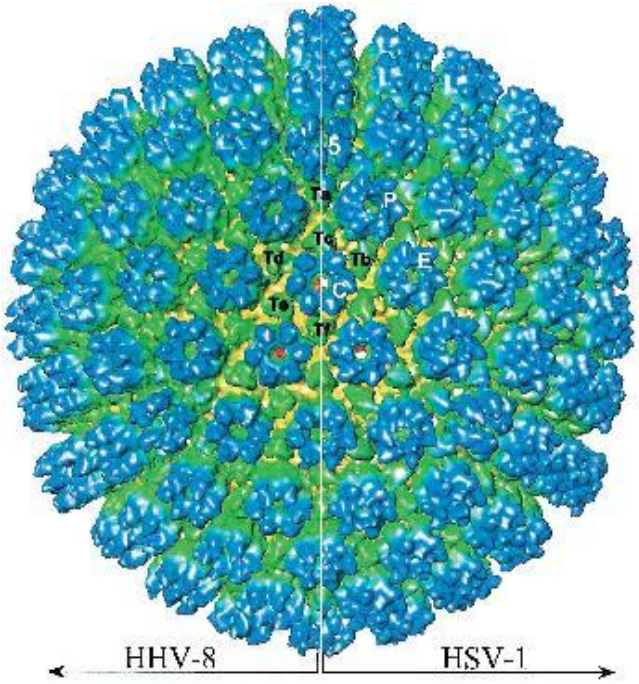

Figure 6: Structural comparison of HHV-8 capsid and HSV-1 B capsid. The two capsid maps are radially coloured and are shown in a montage as viewed along the icosahedral threefold axis. One penton (5), three types of hexon (P, E, and C), and six types of triplexes (Ta to Tf) are labelled.

2.2. HHV-8 genome structure

In the viral capsid, HHV-8 DNA is linear and double stranded, but upon infection of the host cell and release from the viral capsid, it circularizes. Reports of the length of the HHV-8 genome have been complicated by its numerous, hard-to-sequence, terminal repeats. Renne et al.[11] reported a length of 170 kilobases (Kb) but Moore et al.[12] suggested a length of 270 Kb after analysis with clamped homogeneous electric field (CHEF) gel electrophoresis.

Base pair composition on average across the HHV-8 genome is 59% G/C; however, this content can vary in specific areas across the genome.

HHV-8 possesses a long unique region (LUR) of approximately 145 Kb, containing all the known ORFs (open reading frame), flanked by terminal repeats (TRs). Varying amounts of TR lengths have been observed in the different virus isolates. These repeats

are 801 base pairs in length with 85% G/C content, and have packaging and cleavage signals[12]. The LUR is similar to HVS and at least 66 ORFs have homology with the HSV genes. New genes are still being discovered through transcription experiments with alternative splicing. A "K" prefix denotes no genetic homology to any HVS genes (K1–K15).

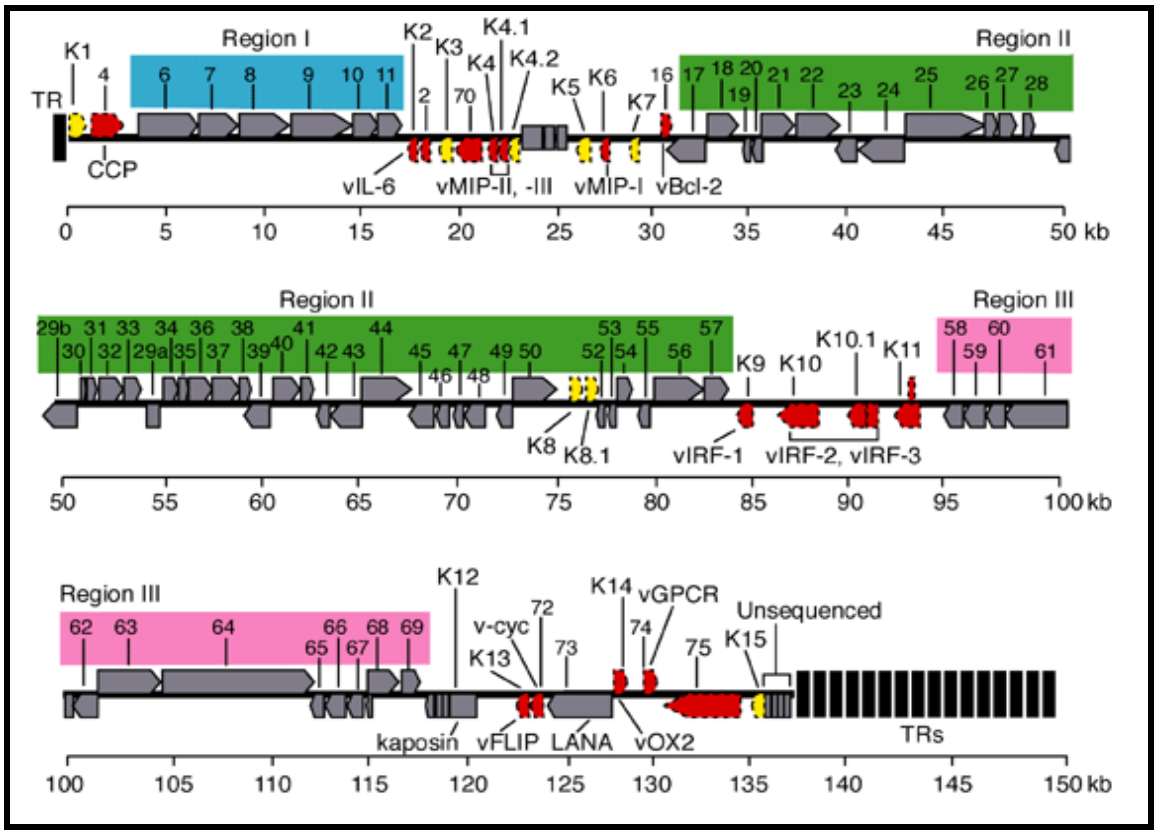

Figure 7: HHV-8 genome. The genome consists of a long unique region (145 kb) encoding for over 80 ORFs, surrounded by terminal repeats regions.

HHV-8 possesses approximately 26 core genes, shared and highly conserved across the *alpha-*, *beta-*, and *gammaherpesviruses*. These genes are in seven basic gene blocks, but the order and orientation can differ between subfamilies. These genes include those for gene regulation, nucleotide metabolism, DNA replication (polymerase ORF9 and

thymidin kinase ORF21), and virion maturation and structure (envelope glycoproteins: ORF8, ORF22, ORF38).

HHV-8 encodes several ORFs homologous to cellular genes (at least 12), not shared by other human herpesviruses[13]. These genes seem to have been acquired from human cellular cDNA as evidenced by the lack of introns. Some retain host function, or have been modified to be constitutively active; an example of this is the viral cyclin-D gene[14]. Cellular homologs related to known oncogenes have been identified in HHV-8, including genes encoding viral Bcl-2 (ORF16), cyclin D (ORF72), interleukin-6 (K2), G-protein-coupled receptor (ORF74), and ribonucleotide reductase (ORF2).

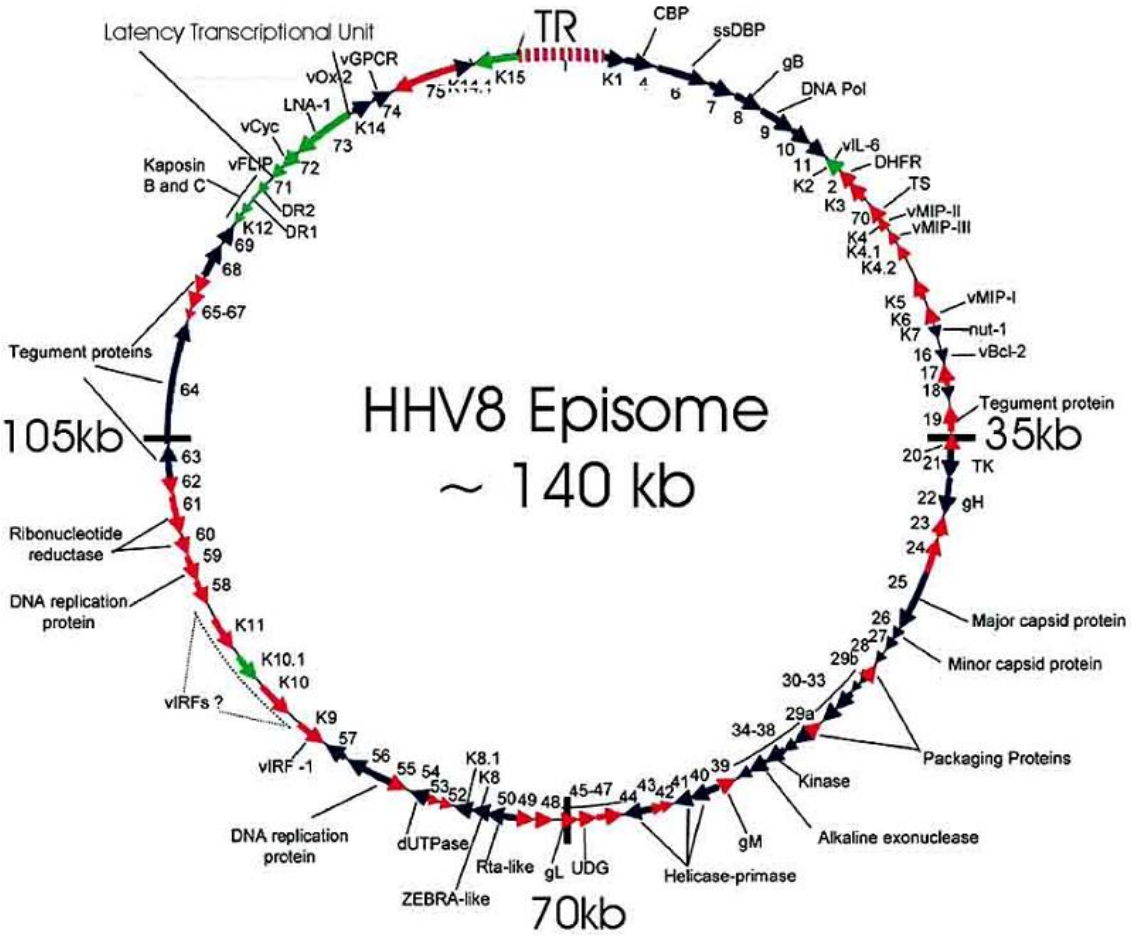

Figure 8: HHV-8 episome.

Other genes have homologues in other members of the RDV genus, such as v-cyclin (ORF72), latency-associated-nuclear antigen (LANA, ORF73), viral G-protein coupled receptor (ORF74). A number of other genes encoding for capsid protein have been identified, including ORF25, ORF26, and ORF65[13]. In addition to virion structural proteins and genes involved in virus replication, HHV-8 has genes and regulatory components (e.g. ORFs K3, K4 and K5) that interact with the host immune system, presumably to counteract cellular host defenses[15].

2.3. Replication cycle of HHV-8

Like other herpesviruses, HHV-8 genome structure and gene expression pattern varies depending on the replication state. The lytic phase consists of 6 steps:

1. Binding to the cell surface mediated by glycoproteins B and K8.1, encoded by ORF8 and K8.1[16]. HHV-8 can use multiple receptor for infection of target cells, and these receptors differ according to the cell type. HHV-8 utilizes the ubiquitous cell surface heparan sulphate (HS) proteoglycan to bind several target cells (e.g. B lymphocytes). Glycoprotein B also interacts with the host cell surface alpha3-beta1-integrin, a heterodimeric receptor containing transmembrane subunits. Another cellular receptor used is the dentritic cell specific intracellular adhesion molecule-3 (ICAM-3) for the binding to the myeloid dendritic cells and macrophages. Moreover, HHV-8 utilizes the transporter protein xCT for entry into cells (but not into the B cells); xCT molecule is a part of the membrane glycoprotein CD98 complex.
2. Fusion between envelope and plasma membrane. The binding between cellular receptors and HHV-8 glycoproteins leads to induction of the host signal cascades critical for maintenance of viral gene expression, such as protein kinase C (PKC), phosphatidylinositol 3-kinase (PI3K), and nuclear factor kB (NF-kB). In fact, HHV-8 reprogrammes the elements of host cell transcriptional machinery that are involved in regulating a variety of processes (apoptosis, cell cycle regulation, signalling, inflammatory response and angiogenesis).
3. Uncoating: capsid degradation by cellular enzymes and viral genome transfer to the cytoplasm.

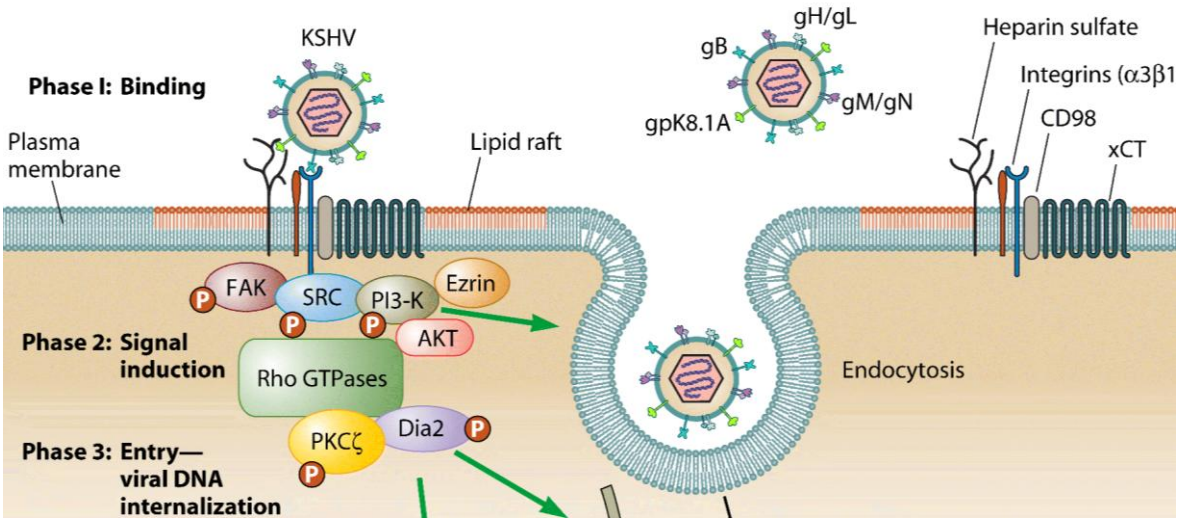

Figure 9: Representation of the first three phases of early events of HHV-8 infection of target cells.

4. Transcription: viral genome migrates to the nucleus and regulator genes are transcribed by host RNA polymerase. mRNAs are translated in virus-specific proteins, able to block cellular synthesis and to start viral replication. Lytic gene expression begins with transcription of immediate-early (IE) genes that regulate the synthesis of other viral genes. Some of the genes transcribed in this step are: ORF6, coding the major DNA binding protein (MDBP), ORFs 9, 56, 59, encoding the DNA polymerase and ORFs 40, 41, 44 (helicase/primase complex). Expression of IE genes occurs independent of viral replication, and afterwards, early and late genes are expressed.

The early genes (E) expression is activated by IE genes within 24 hours after infection or viral reactivation. Early genes encode proteins involved in viral DNA replication, nucleotides metabolism, virus assembly. Some early genes are: K2-5, T1.1, ORFs2, 41, 59, 70, 74.

Expression of late genes (L) begins after viral DNA replication. They encode structural proteins involved in virus assembly, such as glycoproteins B and H (ORF8 and ORF22), capsid proteins (ORFs 25, 26), the small viral capsid antigen (ORF65).

5. Assembly: transcription of genes coding structural proteins and production of viral particle. ORFs26 and 29 proteins are responsible for capsid assembly and viral DNA packaging.

6. The viral particles bud through the inner lamella of the nuclear membrane which has been modified by the insertion of viral glycoproteins and leave the cell via exocytosis.

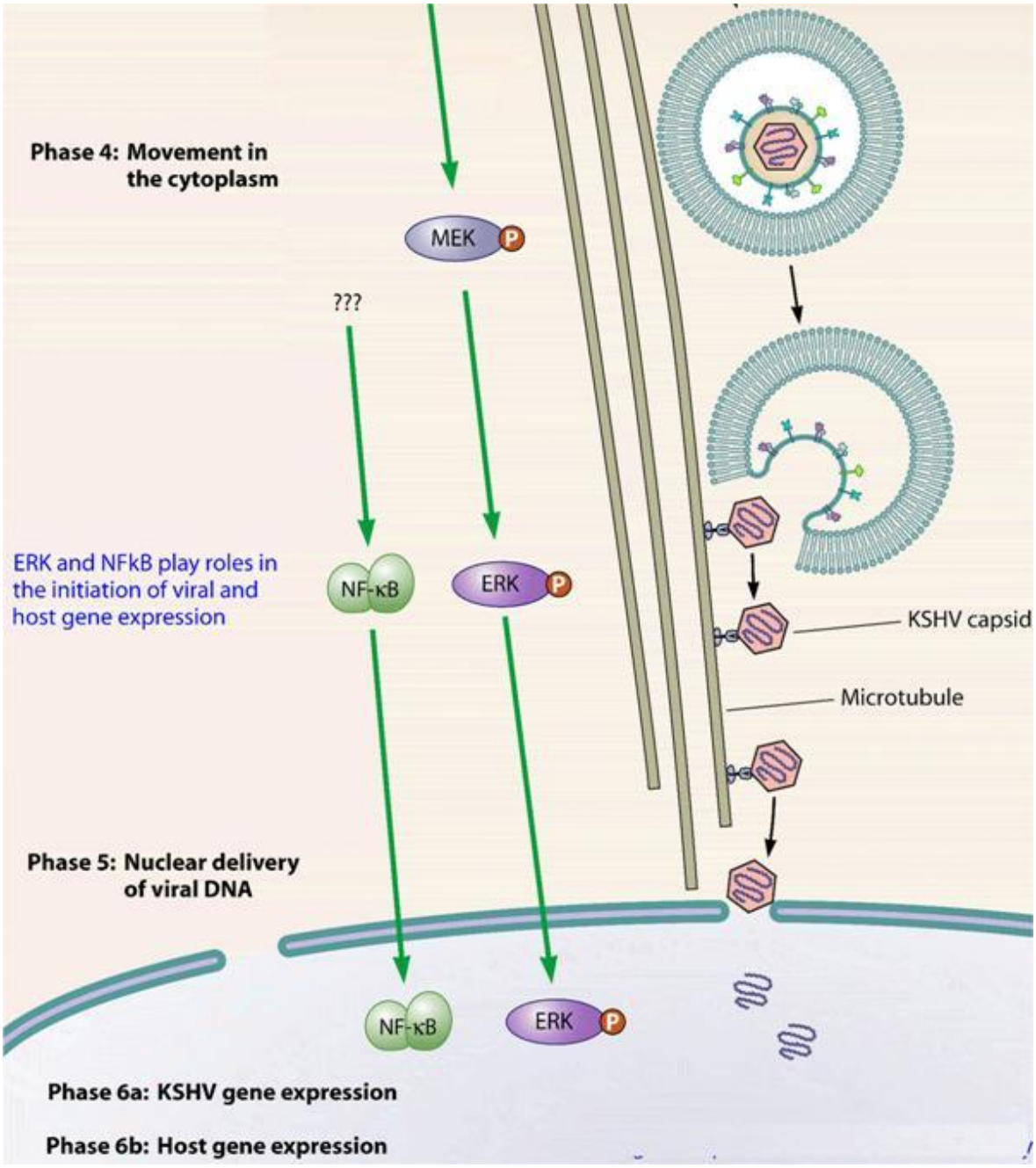

Figure 10: Representation of the last phases of the replication cycle of HHV-8.

After initial infection, HHV-8 may establish lifelong latency. Throughout latency, viral gene expression is tightly regulated and only a few viral genes are expressed. The latent HHV-8 genome is circularized by joining of GC rich terminal repeats (TRs) at the ends of the viral genome to form an extrachromosomal circular episome[17]. The latency associated nuclear antigen (LANA) regulates episome replication by host cell machinery[18]. LANA is a phosphoprotein expressed in latently infected cells and promotes the maintenance of latency by associating with the ORF50 promoter[19] or binding cellular factors which normally interact with ORF50. HHV-8 infection can be reactivated from latency and the lytic gene expression may restart.

2.4. Transactivator genes of HHV-8

Two immediate-early genes play a key role in the reactivation from latent phase to lytic phase: ORF50 and ORF57.

- *ORF50*

ORF50 is an immediate early gene whose product is the major transcriptional transactivator and his activity is required for viral reactivation by all known chemical inducer (e.g. tetradecanoyl phorbol acetate, TPA). The ORF50 gene is rapidly expressed, within 2 to 4 h after induction.

ORF50 belongs to the family of R transactivators, highly conserved among herpesviruses and is related to immediate-early transcriptional activator proteins of other gammaherpesviruses, such as ORF50a encoded by *Herpesvirus saimiri* and Rta encoded by the BRLF1 ORF of Epstein-Barr virus[20].

During latency, ORF50 expression is repressed; however, ORF50 may be activated by physiological conditions, such as hypoxia, or by pharmaceutical agents and the activation triggers the start of the lytic replication cascade.

The genomic sequence of ORF50 is characterized by 5 exons and 4 introns and transcribes an mRNA of 3,6 Kb. The transcript initiates at position 71560, 23 nts downstream a potential TATA box; its first AUG is located at position 71596.

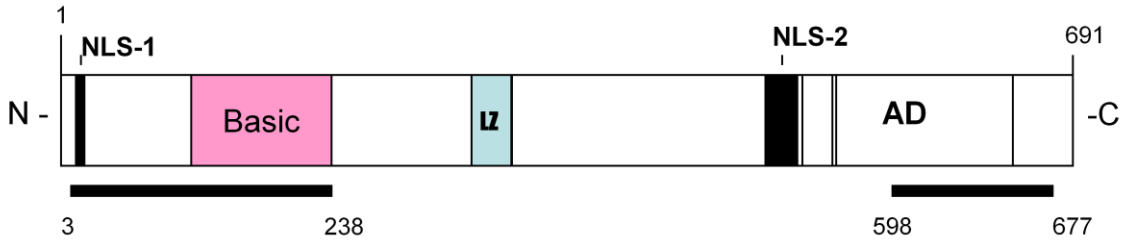

Figure 11: Schematic representation of ORF50 protein.

The ORF50 transcript encodes a 691 aa protein (110 kDa) located in the nucleus during the latent phase for the presence of two nuclear localization signals (NLSs). The N-terminus 272 amino acids of ORF50 binds independently to HHV-8 promoters and mediates sequence-specific DNA binding; N-terminal region is followed by a leucine zipper domain. The C-terminal domain contains multiple charged amino acids alternated with repeated bulky hydrophobic residues, a primary structure conserved in many eukaryotic transcriptional activation domains. The C-terminus is sufficient to activate transcription when targeted to promoters with a heterologous DNA binding domain[21].

This region contains four overlapping domains termed activation domains (AD1, AD2, AD3, AD4), sharing significant homology to the R proteins encoded by other gamma-herpesviruses.

Analysis of the ORF50 amino acids sequence reveals multiple sites of phosphorilation, including a C-terminal region rich in serines and threonines, and 20 other consensus sites for phosphorilation by serine-threonine kinase and protein kinase C (PKC).

R response elements (RREs) have been identified within several lytic gene promoters. The response element contains a 12-bp palindrome with additional sequences flanking the palindrome which are also required for both DNA binding and activation by ORF50. The ORF50 protein binds directly to this palindromic sequence, and the N-terminal 272 aa is sufficient for binding in vitro. ORF50 can directly transactivate the early gene promoters[22].

The ORF50-responsive promoters include the following: ORF 6 (single-stranded DNA binding protein), ORF21 (thymidine kinase [TK]), ORF57 (posttranscriptional activator), ORF59 (DNA polymerase associated processivity factor), K8 (K-bZip), K9 (viral interferon response factor), K12 (kaposin), and nut-1 or PAN or T1.1 (polyadenylated nuclear RNA)[23].

Furthermore, recent studies suggest autoactivation of ORF50 by interaction with the cellular protein octamer-1 (oct-1) and an intact octamer element that is located approximately 200 bp upstream of the ORF50 transcription start site[24].

Expression of ORF50 reactivates viral lytic cycle in cells containing the virus in a latent phase[25], and is also able to activate heterologous viral promoters such as LTR HIV, synergizing with Tat[26]. This molecular transactivation increases cellular susceptibility to HIV infection and could have clinical consequences in patients co-infected with HHV-8 and HIV.

The constitutive expression of ORF50 in stable clones increases expression of several cellular transcription factors, including activating transcriptional factor-4 (ATF4) (Unpublished data).

- *ORF57*

ORF57 is a lytic gene expressed between 2 and 4 h after activation of the lytic phase, immediately following the appearance of ORF50 transcripts but prior to most early mRNAs[21].

ORF57 is homologous to known posttranscriptional regulators in other herpesviruses. One of these, ICP27 of HSV is a regulator whose functions include downregulation of intron containing transcripts and upregulation of some late messages. ICP27 is essential for lytic viral replication, is required for inhibition of host cell splicing and shuttles from the nucleus to the cytoplasm to promote the export of intronless viral RNAs[27]. The other gammaherpesviruses, EBV and *herpesvirus saimiri*, also encode ICP27 homologs.

ORF57 gene is positioned in a unique long region of the HHV-8 genome and is flanked by ORF56 (primase) and K9 (viral interferon regulatory factor, vIRF) genes. ORF56 and ORF57 have their own promoter to initiate transcription, but they share the same polyadenilation signal downstream of ORF57.

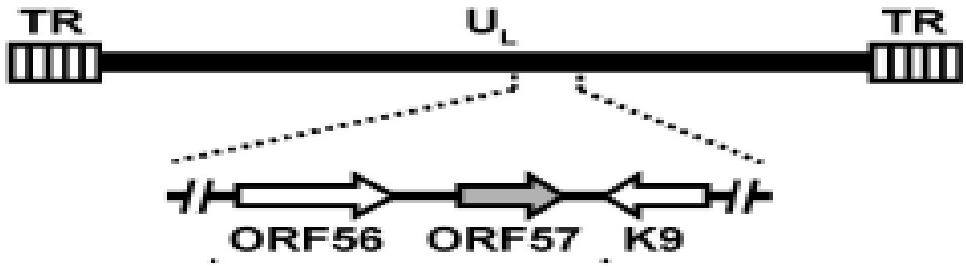

Figure 12: Schematic diagram of ORF57 gene in the context of HHV-8 genome.

ORF57 contains two coding exons and a single 108 bp intron. The exon 1 is relatively small, 114 nts, and has four ATG codons, clustered within a region of 33 nucleotides, in frame with each other and with the first exon and separated from it by a single stop codon. The intron is 109 nts in size and contains consensus splice donor and acceptor sites. The exon 2 is about 1,4 kb long. The transcriptional start site (TSS) is located at nt 82003[27] and polyA signal starts at nt 83608. A TATA box 24 bp is identified upstream the TSS as well as several consensus transcription factor binding sites (NF-kB, AP-1, Oct-1), and at least four R responsive elements involved in the transcriptional activation by ORF50.

ORF57 expression is highly dependent on ORF50, and a RRE in the ORF57 promoter is responsible for ORF57 binding.

ORF57 is expressed predominantly in the nucleus and nuclear localization is driven by three independent nuclear localization signals (NLS) that form a cluster in the N-terminal.

ORF57 encodes a protein of 455 aa residues.

Analyses of amino acid sequence reveals several structural and functional motifs. The N-terminus contains a long stretch of arginine residues, two separate RGG-motifs, which are typical of RNA-binding proteins and four serine/arginine dipeptides, characteristic of SR proteins, the major cellular splicing factors. The three NLSs overlap the arginine rich region.

The C terminus of ORF57 is enriched in leucine residues and contains a leucine zipper motif, typical of cellular transcriprion factors. The C-terminus also contains the zinc-finger-like motif.

ORF57 promotes the expression of HHV-8 intronless genes, including several viral early and late genes, such as ORF59, T1.1 (PAN or nut-1), gB, MPC. ORF59 is an early gene encoding a viral DNA polymerase processivity factor involved in viral DNA replication. T1.1 is a non-coding RNA that accumulates at unusually high levels in the nucleus of lytically infected cells.

ORF50 and ORF57 have a synergic activity that is promoter specific: expression of some promoters that are upregulated by ORF50 can be synergistically enhanced by coexpression with ORF57. This synergy results from a post-translational enhancement of the transcriptional activity of ORF50. ORF57 transactivates specific viral promoters in synergy with ORF50, such as promoters of T1.1, ori-Lyt and Kaposin. ORF57 interacts with ORF50 via its N-terminal region and the central region of ORF50.

2.5. Epidemiology and transmission of HHV-8

The serologic prevalence of HHV-8 infection has been explored in most continents worldwide and in different populations with different levels of risk of HHV-8 infection. It should be noted that the comparisons of prevalence are limited by the fact that either antibodies to latent or lytic HHV-8 antigens were detected and by the test formats used. Several studies have confirmed that there is a low seroprevalence in central and northern Europe, North America and most of Asia, intermediate prevalence in the Middle East and Mediterranean, and high prevalence in southern Africa.

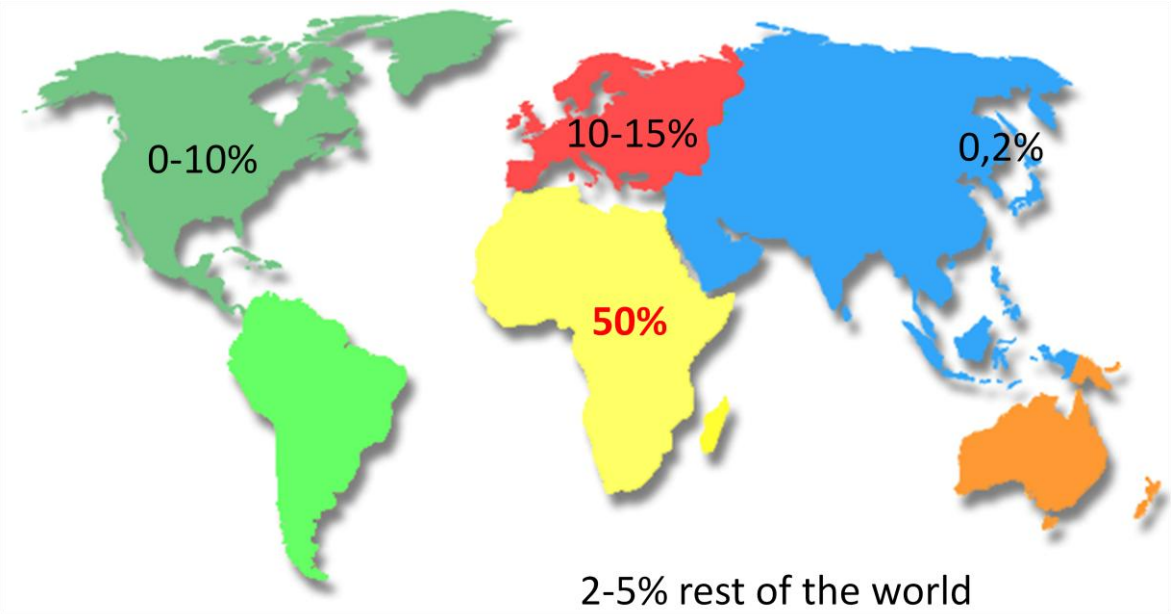

Figure 13: Worldwide geographic distribution of HHV-8 infection.

The virus, first thought to be transmitted only sexually, is now also considered transmissible through low risk or more casual behaviours. Important risk factors for transmission of the virus are a spouse's seropositivity and maternal seropositivity. Of all anatomic sites, HHV-8 DNA is found most frequently in saliva, which also has higher viral concentrations than other secretions[28]. For this reason, it has been hypothesized that saliva could be the route of casual transfer of infectious virus among family members.

Other possible transmissions are blood-borne and organ transplantation.

2.6. HHV-8 pathogenesis

Human herpesvirus 8 is associated with proliferative disorders including Kaposi's sarcoma (KS), multicentric Castleman disease (MCD), primary effusion lymphoma (PEL), and other lymphoadenopathologies.

HHV-8 induces the formation of neoplasias in natural or experimental hosts, and reactivation from latency is essential for this activity.

Latent viral proteins, such as vFLIP and LANA, inactivate tumour suppressors and block apoptosis[29].

However, lytic replication is also important for transmission of the virus in the population and in the pathogenesis of KS. HHV-8 vIL-6 is highly expressed during the lytic cycle, and promotes cellular growth and angiogenesis, while protecting against apoptosis[30]. Additional evidence for the importance of lytic replication includes the fact that inhibition of active HHV-8 replication by gancyclovir reduces the incidence of HHV-8 in HIV-infected individuals[31].

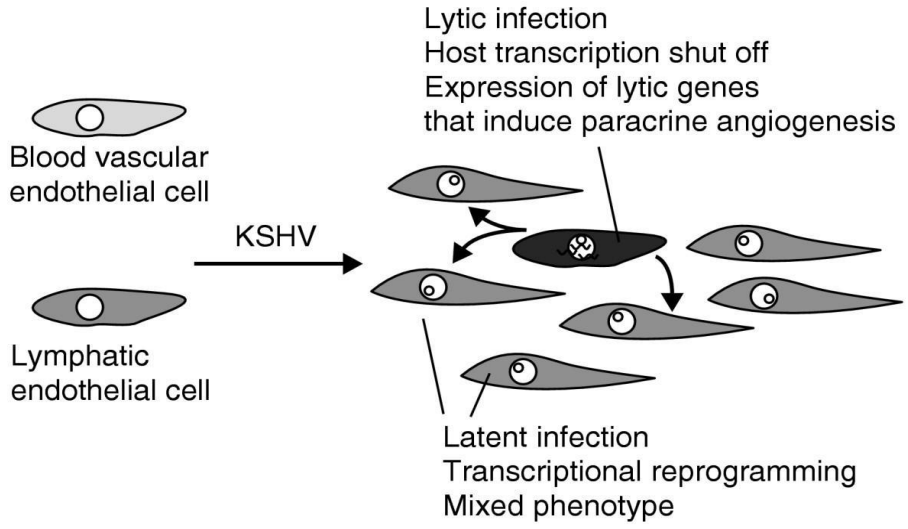

Figure 14: Cellular transformation after HHV-8 infection.

- *Kaposi's sarcoma*

KS was first described by Moritz Kaposi in the 1870s[32] and was described as an aggressive tumour affecting patients younger than those currently observed. For all epidemiological forms of KS, the tumour presents as an highly vascularised neoplasm that can be polyclonal, oligoclonal, or monoclonal. Its antigenic profile suggests either

endothelial, lymphoendothelial, or macrophage origins[8]. All forms of KS lesions contain a variety of cell types, including endothelium, extravasated erythrocytes, infiltrating inflammatory cells, and characteristic "spindle" cells of endothelial origin[33]. The spindle cells express both endothelial and macrophagic markers.

Extensive and aberrant neoangiogenesis in KS lesions is accompanied by elevated levels of many cytokines, including basic fibroblast growth factor (bFGF), interleukin-1 (IL-1), IL-6, IL-8, platelet-derived growth factor (PDGF), tumour necrosis factor (TNF), gamma interferon (IFN-γ), and vascular endothelial growth factor (VEGF). Many of these cytokines are secreted by spindle cells, are essential for spindle cell viability in culture, and are themselves proangiogenic.

HIV infection increases the risk for development of KS, and therefore, the incidence of KS has increased substantially during the HIV pandemic, particularly in younger HIV-infected patients[34].

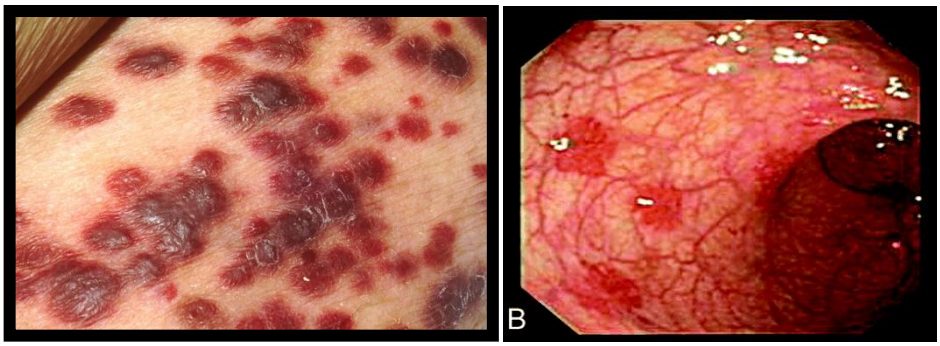

Figure 15: Cutaneous and visceral manifestations of Kaposi's sarcoma.

Four forms of Kaposi's sarcoma are known, differentiated on clinical parameters and epidemiology:

Classic KS: is an indolent tumour affecting the elderly population, preferentially men, in Mediterranean countries. The lesions tend to be found in the lower extremities and the disease, due to its non-aggressive course, usually does not kill those afflicted.

AIDS-KS: in the context of the acquired immunodeficiency syndrome (AIDS), KS is the most common malignancy and is an AIDS defining illness[35]. AIDS-KS is a more aggressive tumour than classic KS and can disseminate into the viscera with a greater likelihood of death. It presents more often multifocally and more frequently on the upper body and head regions.

*Endemic K*S: HHV-8 was prevalent in Africa prior to the HIV epidemic. Prior to HIV coinfections, endemic KS affected men with an average age of 35 and very young children[36]. HIV coinfection has raised the prevalence of KS significantly in Africa, where endemic KS is found more often in women and children than in other areas of the world[37].

Iatrogenic KS: Immunosuppression, as that occurring in transplant recipients, is known to facilitate reactivation of herpesviruses and therefore transplant patients under immunosuppressive therapy can develop KS. Withdrawal of the therapy can cause the KS to regress[38].

- *Multicentric Castleman disease*

MCD is a rare polyclonal B-cell angiolymphoproliferative disorder. Most of the B-cells in the tumour are not infected with HHV-8, and the HHV-8 infected cells are primarily located in the mantel zone of the lymphatic follicle. It is thought that uninfected cells are recruited into the tumour through HHV-8 paracrine mechanisms, such as vIL-6, a known growth factor for the tumour. More than 90% of AIDS patients with MCD are HHV-8 positive, whereas MCD in the context of no HIV infection has a HHV-8 prevalence of approximately 40%[39].

- *Primary effusion lymphoma*

First identified as a subset of body-cavity-based lymphomas (BCBL), PELs contain HHV-8 DNA sequences[6]. These lymphomas are distinct from malignancies that cause other body cavity effusions. PEL cell lines have 50–150 copies of HHV-8 episomes per cell[40].

2.7. HHV-8 and angiogenesis

The effects of acute HHV-8 infection on endothelial cell functions, induction of angiogenesis, and triggering of inflammatory processes are still largely unknown.

In our laboratory, we demonstrated that HHV-8 selectively triggers the expression and secretion of high levels of monocyte chemoattractant protein 1 (MCP-1). We also found that this event is accompanied by virus-induced capillary-like structure formation at a very early stage of acute infection[41].

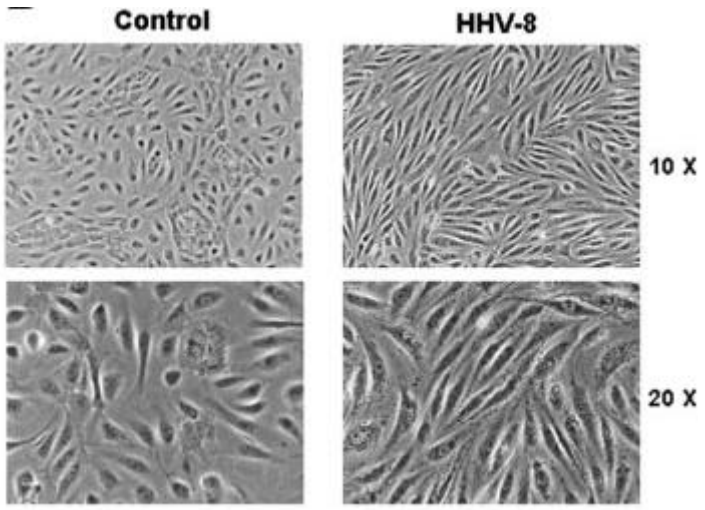

Figure 16: HUVEC monolayer not infected or infected with HHV-8 [41].

The MCP-1 expression is controlled by the nuclear factor kB (NF-kB), that induces the expression of chemokines promoting cell migration and angiogenesis, such as IL-8 and vascular endothelial growth factor (VEGF), several matrix metalloproteinases (MMPs) that promote tumour invasion of surrounding tissue. NF-kB is a critical regulator of the immediate early response to HHV-8, playing an important role in promoting inflammation, in the control of cell proliferation and survival, and in the regulation of virus replication. Several studies show that transfection of different HHV-8 genes results in NF-kB activation in different cell types, and in our laboratory we demonstrated that HHV-8 acute infection induces NF-kB activation in endothelial cells.

The human MCP-1 gene contains 2 NF-kB-binding sites in the enhancer region. The kB binding sites are required for TPA-induced expression. In HHV-8 infection we observed that the NF-kB pathway is involved in the enhancement of MCP-1 expression and is required for maximal production of the chemokine. However, mutations in both NF-kB sites in the enhancer region did not result in the complete loss of promoter induction in HHV-8 infected cells, and inhibitors of NF-kB do not prevent MCP-1 activation following HHV-8 infection suggesting that at least another signalling pathway may be involved in the control of MCP-1 expression in the course of acute HHV-8 infection.

3. The cellular activating transcription factor 4

ATF4 (also called cAMP responsive element binding 2, CREB2) belongs to the ATF/CREB family of transcription factors that represent a large group of basic region-leucine zipper (bZip) proteins. The basic region of the bZIP protein interacts with DNA, and they dimerize by their leucine zipper domains forming homodimers, heterodimers or both[42].

CREB/ATF family members include ATF1 (also known as TREB36), CREB/CREM, CREB314 (also known as Aibzip or Atce1), CREB-H, ATF2 (also known as CRE-BP1), ATF3, ATF4, ATF6, ATF7, B-ATF and ATFX (also known as ATF5).

ATF4 gene is in chromosome 22 at the cytogenetic band 22q13.1, located at 38,241,069–38,243,191 bp, with a genomic size of 2122 and is constitutively expressed in many cells.

The structure of human ATF4 mRNA includes three short open reading frames (uORFs) in the 5'UTR that precede the functional coding sequence[43] and are out of frame with the main protein-coding region. The organization of the 5'UTR uORFs in ATF4 is essential for the response of ATF4 to stress such as ER stress and hypoxia.

ATF4 protein consists of 351 amino acids. The protein is structured into several domains/motifs that are essential for ATF4 homo/heterodimerization and DNA binding. A transcriptional activation domain has been located at the N-terminus of ATF4[44].

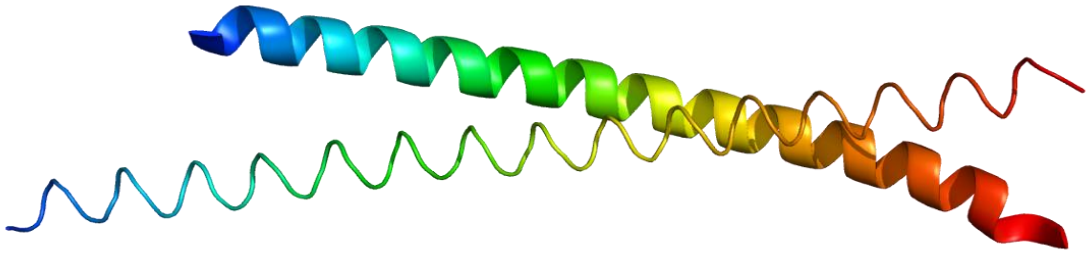

Figure 17: Representation of ATF4.

The mammalian ATF4 can form a homodimer, and heterodimers with members of the AP-1 and C/EBP family of proteins, including Fos[42] and Jun[45], and several C/EBP proteins[46]. ATF4 has a very short half-life of about 30-60 minutes.

ATF4 has several interacting partners, which include p300[47], RNA polymerase II subunit RPB3[48], ZIP kinase, a serine/threonine kinase, which mediates apoptosis[49], HTLV1 transactivator Tax, which activates the expression of viral mRNA through a three 21 bp repeat enhancer located within the HTLV-1 LTR[50]. Tax transactivates the HTLV-1 promoter via the Tax responsive elements that contain the consensus ATF/CRE core sequence. ATF4 enhances the ability of Tax to transactivate the HTLV-1 promoter. The numerous dimerization and interaction partners determine the diverse functions of ATF4.

ATF4 can function as a transcriptional activator, as well as a repressor. It is a stress responsive gene, which is upregulated by several factors/stressors, including oxygen deprivation (hypoxia/anoxia), amino acid deprivation, endoplasmic reticulum stress (ER stress), oxidative stress, and by the growth factor heregulin[51].

In mammalian cells, hypoxia/anoxia and perturbation of ER homeostasis induces a complex transcriptional program and triggers a reduction in protein translation (UPR: unfolded protein response). A central mediator of this translational response to anoxia is phosphorylation of the eukaryotic initiation factor 2α (eIF2α) by PERK protein kinase. Although the phosphorylation of eIF2α results in global translational reduction, it specifically increases the translation of ATF4 mRNA[43]. The various stress signals

integrate in a common pathway of increased translation of ATF4, which subsequently ensures supply of amino acids for protein biosynthesis and protects cells against oxidative stress, by modulating a number of genes involved in mitochondrial function (e.g., Lon mitochondrial protease homologue), amino acid metabolism and transport (e.g., asparagine synthetase), as well as in redox chemistry (e.g., NADH cytochrome B5 reductase homolog)[52]. As a result of metabolic and ER stress that activate the PERK pathway of translational inhibition, ATF4 initiates a feedback regulatory loop to ensure the transient nature of protein synthesis inhibition. ATF4 induces GADD34 transcription, a component of the phosphatase complex that dephosphorylates eIF-2alpha.

Some of the genes that are induced by ATF4 include receptor activator of nuclear factor-kappa B (RANK) ligand (RANKL), osteocalcin, E-selectin, VEGF, Gadd153, gadd34, asparagine-synthesase, TRB3, and several genes involved in mitochondrial function, amino acid metabolism and redox chemistry[52].

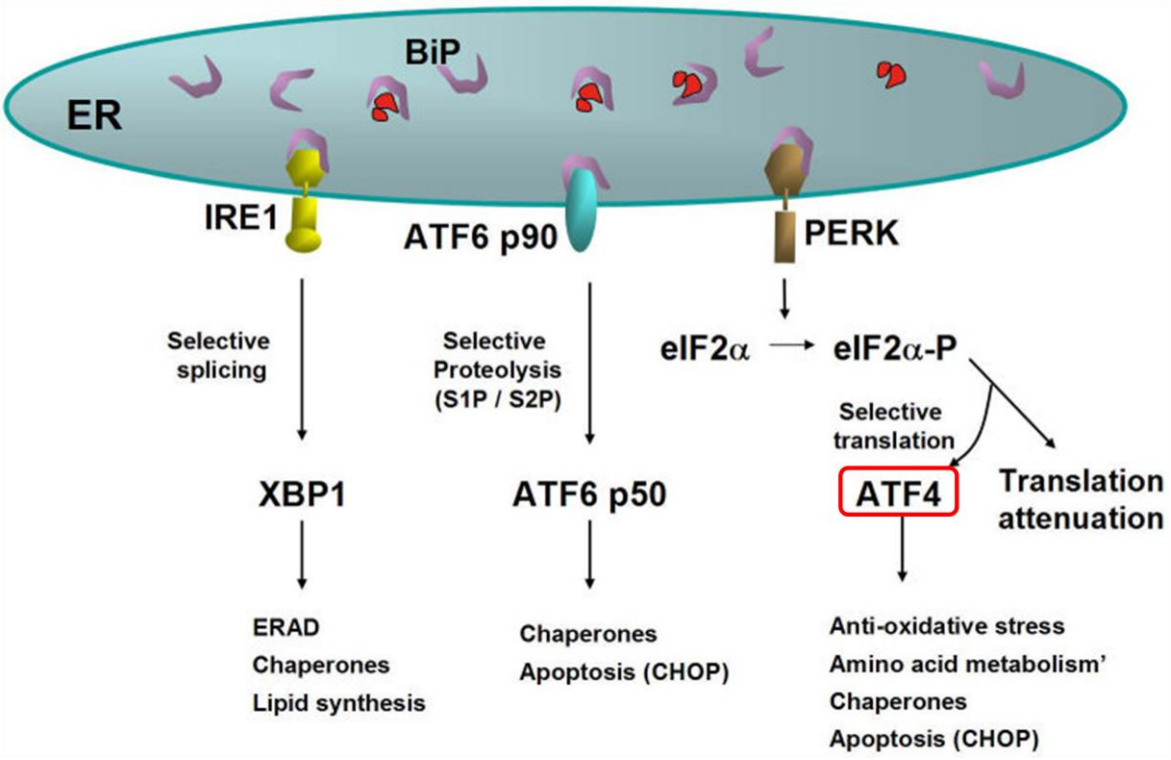

Figure 18: Three proximal sensors IRE1, PERK and ATF6 regulate the UPR through their respective signalling cascades.

One important stress factor relevant to cancer progression is hypoxia and more extremely, anoxia. Tumour hypoxia/anoxia is associated with a more aggressive clinical phenotype, and ATF4 protein has been observed to be in much greater levels in primary human tumours compared to normal tissues[53].

ATF4 induces VEGF and E-selectin which may be associated with increased metastasis. Since ATF4 protein has shown to be present at greater levels in cancer compared to normal tissue, and it is upregulated by signals of the tumour microenvironment such as hypoxia/anoxia, oxidative stress, and ER stress, it could potentially serve as a specific target in cancer therapy. As a target ATF4 is attractive because it is also potentially involved in angiogenesis and adaptation of cancer cells to hypoxia/anoxia, which are major problems in cancer progression. The induction of VEGF (vascular endothelial growth factor) has a key role in angiogenesis, and preliminary study in our laboratory demonstrate that transfection of ATF4 induces capillary-like structure formation in vitro.

Many viruses have been shown to induce ER stress and activate the UPR: these include three members of the flavivirus, C hepatitis and HCMV. Viral infection induces the cell response to stress, which should lead to an attenuation of viral replication. However, some aspects of the UPR can be regulated and limited by the virus. For example, infection with HCMV (betaherpesvirus) induces the UPR by regulating specifically three signalling pathways: PERK, ATF6 (activating transcription factor 6) and Ire-1[54].

Cells infected with this betaherpesvirus show an increase in ATF4 protein levels, leading to the activation of genes involved in metabolism and redox reactions and helping the virus to maintain a cellular environment permissive to infection.

Studies demonstrate that also HHV-8 can interact with ATF4. LANA, the latency associated nuclear antigen, encoded by ORF73, represses the transcriptional activation activity of ATF4 and the interaction requires the bZIP domain of ATF4. Repression by LANA is independent from the DNA-binding ability of ATF4[55].

AIM OF THE RESEARCH

Human herpesvirus 8 is the primary etiologic agent of Kaposi's sarcoma, a highly vascularised neoplasm of endothelial origin characterized by inflammation, neoangiogenesis, and by the presence of characteristic spindle cells.

HHV-8 infection of endothelial cells causes changes in cellular phenotype and leads to capillary-like structures formation. This angiogenic activity of HHV-8 is due to the activation of NF-kB and the subsequent induction of MCP-1 synthesis.

MCP-1 is a chemokine produced by macrophages and endothelial cells in response to different stimuli, and is a direct mediator of angiogenesis. The MCP-1 promoter contains an enhancer region with two NF-kB sites. MCP-1 production after HHV-8 infection is accompanied by virus-induced capillary-like structure formation in endothelial cells, and HHV-8-induced angiogenesis is MCP-1 dependent.

Previous studies demonstrate that HHV-8 activates the MCP-1 promoter also in absence of the enhancer region containing the NF-kB binding sites, in fact, mutations in NF-kB sites do not result in a complete loss of MCP-1 transcription. Moreover, treatment with NF-kB-inhibitors does not prevent MCP-1 activation in HHV-8 infected cells.

Therefore, HHV-8 activation of MCP-1 is not completely dependent on NF-kB induction and another cellular factor is involved.

A potential candidate is the cellular activating transcription factor 4 (ATF4), a stress responsive gene. ATF4 is upregulated in several condition, including ER-stress, viral infection (e.g. CMV) and in tumours.

Previous data obtained by gene array in stable Jurkat cell clones transfected with ORF50 gene (major transactivator of HHV-8), indicated that HHV-8 upregulates ATF4.

The aim of the research was therefore to determine whether the viral infection of HHV-8 increases the expression of the transcription factor ATF4 and clarify if this increase is functional for the replication of HHV-8. The results showed that HHV-8

(and ORF50) causes a significant increase of ATF4, and that this increase leads to increased virus replication in infected cells.

ATF4 is not able to reactivate HHV-8 from latency, being unable to activate the major gene promoters. This “indirect” effect on HHV-8 activity can be explained by investigation of interactions between ATF4 and MCP-1. In fact, we found that ATF4 activates the MCP-1 promoter, and this activity is NF-kB-independent.

MATERIALS AND METHODS

1. Cell cultures

The B cell lines BC-3 and BCBL-1, derived from PEL and chronically infected with HHV-8, were used as representative of HHV-8 target of infection. Lymphoid T (Jurkat cells) and B cell lines were grown in RPMI medium (Gibco) supplemented with 10% inactivated fetal bovine serum (FBS), 2 mM L-glutamine, 100 U/ml penicillin and 100 mg/ml streptomycin.

HeLa cell line (human cervix carcinoma cells) and 293 cell line (human embryonic kidney cells) were grown in Dulbecco's Modified Eagle medium (Gibco) supplemented with 10% inactivated fetal bovine serum (FBS), 2 mM L-glutamine, 100 U/ml penicillin and 100 mg/ml streptomycin.

All cells were cultured at 37°C in the presence of 5% CO_2.

2. Plasmids

Transfection experiments were performed using recombinant plasmids pCR-50sp, pGL-PR57, pGL-PR50, pGL-PRT1.1, pGLM-PRM, pGLM-ENH, pGLM-MA1MA2, pRL-SV40 and pCG-ATF4.

Spliced forms of ORF50 were cloned in the expression vector pCR3.1-Uni (Invitrogen) in our laboratory[25]. Briefly, spliced genes were obtained from TPA-activated BCBL-1 cells by specific retrotranscription of polyA RNA followed by PCR amplification. Amplified fragments were sequenced to verify their integrity and were then inserted into the vector pCR3.1-Uni to obtain the recombinant plasmid pCR-50sp.

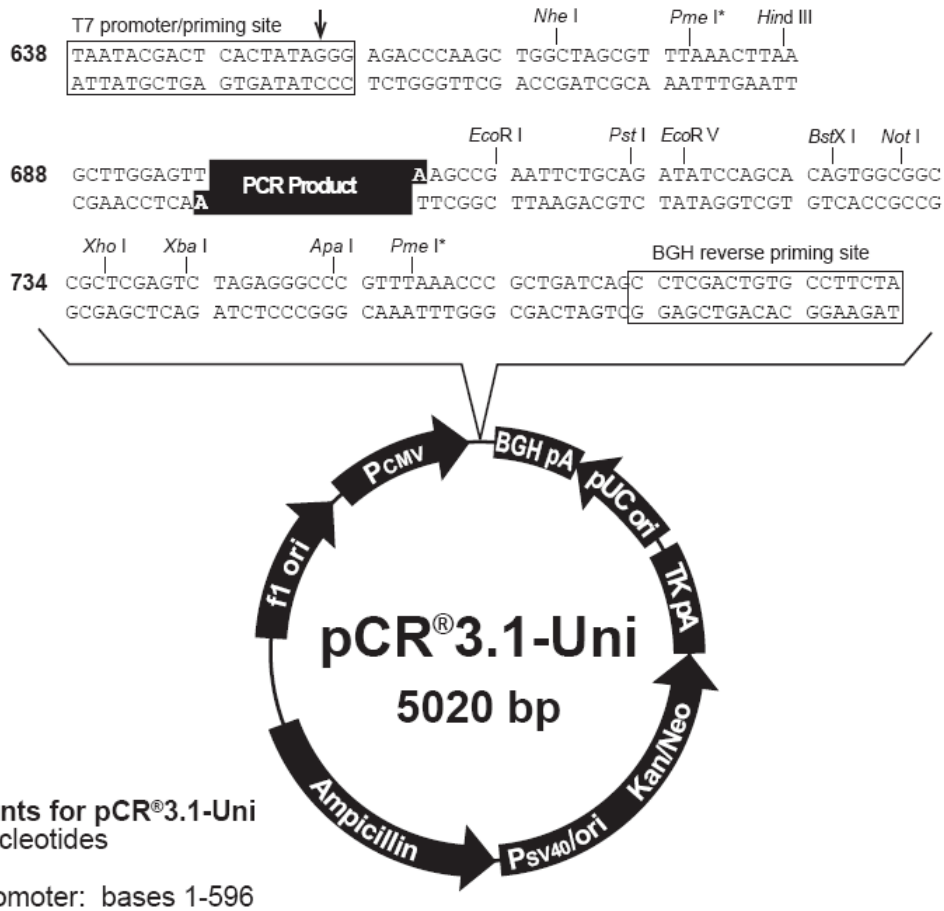

Comments for pCR®3.1-Uni
5020 nucleotides

CMV promoter: bases 1-596
Putative transcriptional start: bases 620-625
T7 promoter/priming site: bases 638-657
Multiple cloning site: bases 670-761
TA Cloning® site: bases 697-698
BGH reverse priming site: bases 773-791
BGH polyadenylation site: bases 772-986
pUC origin: bases 1076-1749
SV40 promoter and origin: bases 3492-3154 (complement)
Neomycin/kanamycin resistance gene (ORF): bases 3119-2331 (complement)
Thymidine kinase polyadenylation site: bases 2156-1886 (complement)
Ampicillin resistance gene (ORF): bases 4431-3571 (complement)
f1 origin: bases 4562-5018

*There is more than one *Pme* I site in the polylinker.

Figure 19: pCR3.1-Uni map.

HHV-8 gene promoters were cloned in the reporter vector pGL3-Basic in this laboratory[56], containing the Firefly luciferase gene cloned under the transcriptional control of HHV-8 promoters.

The MCP-1 promoter-luciferase constructs (provided by Dr. T. Yoshimura)[57] contain the proximal promoter (pGLM-PRM), the proximal promoter and the distal enhancer (pGLM-ENH), the proximal promoter and the distal enhancer in which both NF-kB sites are mutated (pGLM-MA1MA2).

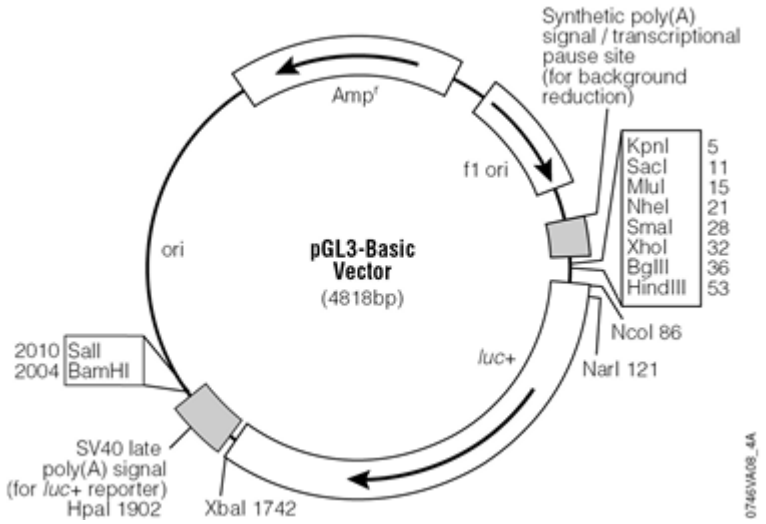

Figure 20: Firefly luciferase pGL3-Basic vector.

pRL-SV40 vector (Promega) was used as an internal transcriptional control, and contains the Renilla luciferase gene cloned under the transcriptional control of the SV40 virus promoter.

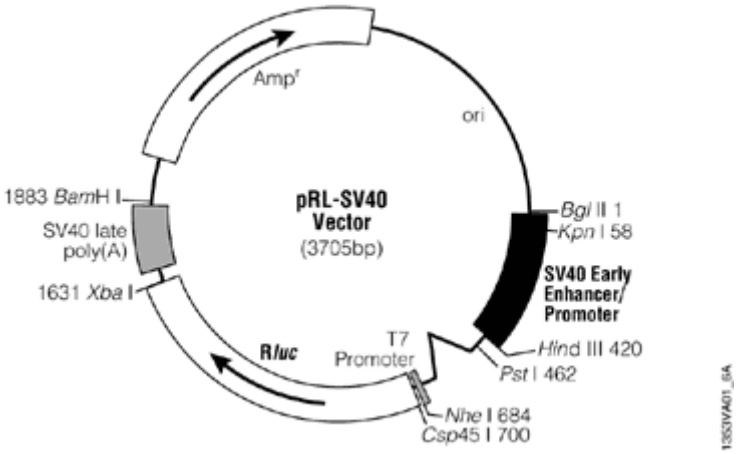

Figure 21: Renilla luciferase pRL-SV40 vector.

pCG-ATF4 plasmid contains the ATF4 gene cloned under the transcriptional control of the CMV promoter[51].

3. Cell transfections

Jurkat, BC-3 and BCBL-1 cells were seeded 24 hours before transfection to obtain optimal cellular density (10^6 cells/mL) and 10^6 cell samples were transfected with 1 μg of plasmid DNA by electroporation (Nucleofector, Amaxa), following the manufacturer's instructions. This method permits to obtain high efficiency of transfection, carrying the exogenous DNA into the cells and directly into the nucleus. Efficiency of transfection determined in parallel samples by transfection with pmax-GFP plasmid (Amaxa).

HeLa and 293 cells were seeded in 24-well plates 24 hours prior to transfection to obtain optimal confluence, then were transfected with 1μg of plasmid DNA by GeneJuice Transfection Reagent (Novagen), based on polyamine formulation, following the manufacturer's instructions.

4. Virus purification and cell infection

Cell-free HHV-8 inoculum was obtained by stimulation of BC-3 cells for 3 days with 20 ng/mL 12-O-tetradecanoyl-phorbol-13-acetate (TPA; Sigma). Cells were collected by centrifugation and lysed by rapid freezing and thawing followed by sonication (3 cycles of 5 seconds at medium power with 10-second intervals in a water bath sonicator). Cleared cellular content was added to culture supernatant, and virions were collected by centrifugation for 30 minutes at 20000 xg at 4°C.

Virus particles were purified by density centrifugation on Optiprep self-forming gradients (Sentinel), at 58000 xg for 3,5 hours at 4°C. Purified virions were washed in phosphate buffered saline (PBS) and collected by centrifugation at 20000 xg for 30 minutes at 4°C.

Virions were suspended in sterile PBS containing 0,1% bovine serum albumin (BSA) and stored at -80°C until use. To obtain 1 mL of purified virus, $4\text{^}10^8$ BC-3 cells were stimulated. The same ratio between cells and final suspension volume was maintained in all virus preparations to avoid variations in virus concentration between different stocks.

Virus particles were morphologically intact, and the preparation was cell debris-free, as assessed by electron microscope observation.

Prior to use, virus stock was treated with DNase-I and RNase-A, to eliminate free viral nucleic acids eventually present in the preparation.

Infectivity of virus preparation was evaluated by specifically designed infection experiments performed in different cell types, using PCR, rtPCR and immunofluorescence assays to evaluate virus presence, transcription, and expression of antigens.

Quantification of virus genomes present in the stock preparation was obtained by real-time polymerase chain reaction (qPCR)[58].

HHV-8 DNA standard was obtained by serial dilutions of pCR-ORF26 plasmid containing a cloned fragment of HHV-8 DNA (ORF26, nucleotides 47127 to 47556). The absence of human gDNA was assessed by amplification of the β-actin gene. The purified cell-free virus inoculum contained an average of $4{,}7\text{^}10^5$ copies of viral DNA/μL.

T and B cells were seeded 24 hours before infection to obtain optimal density of 10^6cells/mL and then were infected with a m.o.i. (multiplicity of infection, referred to equivalent genomes) of 1:10. After 3 hours of absorption at 37°C, the HHV-8 inoculum was removed, cells were washed with PBS and incubated in fresh medium. Cell samples were harvested at specific time points and processed for DNA or RNA extraction.

5. DNA extraction

Genomic DNA was extracted from 10^6 cell samples.

Cells were lysed in 500µL lysis buffer (10 mM Tris-HCl pH 8.0, 10 mM disodium EDTA pH 8.0, 10 mM NaCl, 0.6% SDS and 100 µg/ml proteinase K) and incubated at 37°C for a minimum time of 4 hours. After three cycles of phenol:chloroform:isoamyl alcohol (25:24:1) extractions, DNA was recovered by ethanol precipitation, resuspended in sterile water, and RNase A was added to a final concentration of 100 µg/ml. Following 1 hour incubation at 37°C, RNase A was removed by phenol extraction. After precipitation with ethanol, DNA pellets were dissolved in sterile water and stored at -20°C until PCR or qPCR analysis.

DNA concentration was determined by reading optical density at 260 nm.

6. RNA extraction and retrotranscription

Total RNA was extracted with RNAzol B (Tel-Test), following the protocol provided by the manufacturer. Briefly, 10^6 cell samples were lysed with RNAzol, then, chloroform in ratio 1:5 was added. The mixture was centrifuged 20 minutes at 8500 xg and the aqueous phase was collected and RNA precipitated with isopropanol. After two washes with 75% ethanol and DNAse treatment (4 U/mg RNA, 3 x 20 min. at room temperature), RNA was precipitated with isopropanol 20 minutes at 8500 xg at 4°C. RNA quality was checked by electrophoretic analysis on a 0.8% agarose gel. The absence of contaminating DNA was checked by PCR

amplification of human β-actin gene before retrotranscription (RT-). Negative PCR results for β-actin ensured that the RNA sample was completely free from DNA sequences. First strand cDNA synthesis was carried out with MuLV reverse transcriptase and random hexamer primers (Applied Biosystems), following the manufacturer's instructions, retrotranscribing 2 μg of total RNA from all the samples. The mixture was incubated for 1 hour at 42°C. Efficiency of retrotranscription was assessed by analysis of dilutions of cDNA with PCR specific for human β-actin gene (RT+).

7. PCR and rtPCR

The presence and the level of transcription of HHV-8 were analyzed by PCR and reverse transcription PCR (rtPCR) amplification of the *ORF26* and *ORF50* genes. PCR amplification was performed using 100 ng total DNA or 200 ng total cDNA extracted from infected cells. Amplification of the housekeeping β-actin gene was used as a control. The transcription of ATF4 was analysed by rtPCR amplification of the ATF4 gene. Specific primers and PCR conditions are described in Table 2. The absence of contaminating DNA was checked by PCR amplification of human β-actin gene before retrotranscription. Negative PCR results for β-actin ensured that the RNA sample was completely free from DNA sequences, and that positive amplification after retrotranscription was positively associated to viral transcripts.

Particular care was taken to avoid sample-to-sample contamination: different rooms and dedicated equipment were used for DNA extraction and processing, for PCR set-up and gel analyses, all pipette tips had filters for aerosol protection.

GENES	PRIMERS	SEQUENCES	AMPLICONS
ORF50	ORF50-Forw ORF50-Rev	5'-TTGGTGCGCTATGTGGTCTG-3‘ 5'-GGAAGGTAGACCGGTTGGAA-3'	420 bps
ORF26	ORF26-Forw ORF26-Rev	5'-GCCGAAAGGATTCCACCAT-3‘ 5'-TCCGTGTTGTCTACGTCCAG-3'	232 bps
ATF4	ATF4-Forw ATF4-Rev	5’-GTGGCCAAGCACTTCAAACC-3’ 5’-GGAATGATCTGGAGTGGAGG-3’	414 bps
b-actin	HACT-Forw HACT-Rev	5’-TCACCCACACTGTGCCCATCT-3’ 5’-GACTACCTCATGAAGATCCTCAC-3’	674 bps

GENES	CONDITIONS	CYCLES	$[MgCl_2]$
ORF50	94°C 5min 94°C 30 sec, 57°C 1 min, 72°C 1 min + ext. 3 sec/cycle 72°C 10 min, 4°C >>>	1 35 1	2mM
ORF26	94°C 5min 94°C 1min, 57°C 1 min, 72°C 1 min + ext. 3 sec/cycle 72°C 10 min, 4°C >>>	1 45 1	1.5 mM
ATF4	94°C 5min 94°C 1min, 57°C 1 min, 72°C 1 min + ext. 3 sec/cycle 72°C 10 min, 4°C >>>	1 35 1	2mM
b-actin	94°C 5min 94°C 1min, 57°C 1 min, 72°C 1 min + ext. 3 sec/cycle 72°C 10 min, 4°C >>>	1 30 1	1.25mM

Table 2: Primer sets and thermal conditions used for PCR and rtPCR reactions.

8. Real time PCR (qPCR)

Real time PCR or quantitative PCR (qPCR) was used to determine the amount of ORF26 and ATF4 genes. β-actin housekeeping gene was used as internal control in order to normalize the results.

qPCR using the TaqMan probes was performed using the 7700 ABI Prism (Applied Biosystems).

The DNA or cDNA copy numbers were quantified by comparison with a 10-fold serial dilutions of known concentrations of pCG-ATF4 or pCR-ORF26 plasmids. The concentration of the standard DNA was assessed by spectrophotometer and plasmid copy numbers were calculated to prepare standard curves (10^7 to 10 copies).

Amplifications were carried out in a 50 μL total volume containing 25 μL 2X TaqMan Universal PCR Master Mix (Applied Biosystems), 5 μL of primer and probes, and 20 μL template. The target genes were amplified using TaqMan FAM-labelled probe at the 5'-end and TAMRA quencher at the 3'-end. The β-actin housekeeping gene was simultaneously amplified using a 5'-VIC-labelled probe. Primers and probes used are shown in Table 3. Concentrations of the primers and probes were 900 nM of each primer and 200 nM of each probe.

The reaction conditions for all templates were 10 minutes at 95°C for enzyme activation, and 40 cycles with 15 seconds at 95°C for DNA denaturation and 1 minute at 60°C for annealing and extension. Fluorescence data were collected in the primer elongation phase at 60°C.

To normalise the data, the cycle threshold (Ct) values of the housekeeping gene were subtracted from the target gene Ct value of the sample.

GENES	PRIMERS & PROBES	SEQUENCES
ORF26	H8-Forward	5'-CTCGAATCCAACGGATTTGAC-3‘
	H8-Reverse	5'-TGCTGCAGAATAGCGTGCC-3'
	H8-Probe	5’-(6Fam) CCATGGTCGTGCCGCAGCA (Tamra)-3’
ATF4	ATF4-Forward	5’-CCCCCCTAGTCCAGGAGACT-3’
	ATF4-Reverse	5’-CTGGGAGATGGCCAATTGG-3’
	ATF4-Probe	5’-(6Fam) ATAAGCAGCCCCCCCAGACGG (Tamra)-3’
β-actin	h-ACT-Forward	5'-TCACCCACACTGTGCCCATCT-3'
	h-ACT-Reverse	5'-GACTACCTCATGAAGATCCTCAC-3'
	h-ACT-Probe	5’-(Vic) ATGCCCTCCCCCATGCCATCCTGCGT (Tamra)-3’

Table 3: Primer and probe sets used for real time PCR quantifications.

9. Luciferase assay

The Luciferase assay was performed using the Dual-Glo Luciferase Assay System (Promega). Luciferase and Renilla were used as co-reporters to measure gene expression. In order to generate luminescence Firefly luciferase requires luciferin, ATP, magnesium and molecular oxygen. Renilla luciferase requires coelenterazine and molecular oxygen.

Cells were seeded into 24-well plates 24 hours prior to transfection, then, they were co-transfected with the reporter constructs, pRL-SV40, and with the expression plasmids. 48 hours post-transfection, Dual-Glo Luciferase Reagent was added to each well in ratio 1:1 with the medium and cells were transferred to 96-well plate. After at least 10 minutes of incubation, the firefly luminescence was measured. Following the first measurement, an equal volume of Dual-Glo Stop&Glo Reagent was added and after 10 minutes incubation, the Renilla luminescence was measured.

The results were expressed as Luciferase activity, normalized using the Renilla emission.

10. Western blotting

Cell samples (1-2^10^6) were harvested and centrifuged 2 minutes at 8000 xg. Pellets were resuspended in lysis buffer (6,7 M urea, 10 mM Tris-HCl pH 6.8, 5 mM DTT, 1% SDS, 10% glycerol, protease inhibitors cocktail) and debris was eliminated by centrifugation. 6X loading buffer was added to 20 μg cellular total lysated, and the mixture was subjected to 10% SDS-PAGE electrophoresis. Following electrophoresis, proteins were transferred in the Hibond-P PVDF-membrane (Amersham) in an electroblotter (Biorad). After transfer, the membrane was probed with the rabbit anti-ATF4 antibody (SantaCruz Biotechnology) 1:200 diluted, 90 minutes at room temperature. After three washes, the membrane was incubated with the anti-rabbit HRP conjugated antibody (SantaCruz Biotechnology) 1:1000 diluted for 90 minutes at room temperature. After three washes the antibody was revealed by luminol staining (SuperSignal West Pico Chemiluminescent Substrate, Pierce). ATF4 molecular weight is 38 kDa.

RESULTS

1. HHV-8 infection increases ATF4 expression

Results previously obtained by gene array in stable clones of Jurkat cells transfected with plasmid pCR-ORF50sp indicated that the expression of transactivator ORF50 of HHV-8 upregulates the transcription factor ATF4 (unpublished data).

Based on this preliminary observation, we verified whether the infection with the entire HHV-8 could have the same effect on ATF4 expression. To study the effect of HHV-8 infection we used the cell-free inoculum obtained in our laboratory to infect Jurkat cells in vitro and analyze the effect of the viral infection on ATF4 transcription.

Briefly, Jurkat cells were seeded at optimal density (10^6 cells/mL) 24 hours before infection and were then infected with HHV-8 (1:10 of m.o.i.) as described in Materials and Methods. Samples were then collected for analysis of cellular transcription of ATF4 at different times post-infection (p.i.) 0, 4, 8, 24 and 48 hours p.i..

Total RNA was extracted by organic solvent extraction (RNAzol) from each cell sample (10^6 cells), and RNAs were treated with DNase to eliminate possible genomic DNA contamination. To verify the absence of DNA contamination, a PCR was carried out using 200 ng of RNA as template (RT-) and amplifying the gene for β-actin, constitutively present and ubiquitous in the cells used (housekeeping gene). After verifying the absence of contaminating DNA, shown by the absence of amplification product, RNA was reverse-transcribed into cDNA. ATF4 was amplified using the specific primers and temperature conditions described in Materials and Methods. ATF4 transcript was quantitated by semi-quantitative rtPCR, performing PCR amplification reactions on 10-fold serially diluted cDNA templates. The absence of the amplification products identifies the dilution in which targets are below the sensitivity threshold.

In parallel, the same dilutions of template were used to amplify the house-keeping β-actin gene as a control. PCR products were run in a 2% agarose gel and visualized by ethidium bromide staining.

Fig. 22 shows the results of the samples collected at 24, 48 hours p.i. and semi-quantitative rtPCR specific for β-actin, which is necessary in order to normalize the results obtained by rtPCR specific for ATF4.

Infection with HHV-8 induces a 10-fold increase of ATF4 transcription at 24 hours and 48 hours post infection, compared to control uninfected cells.

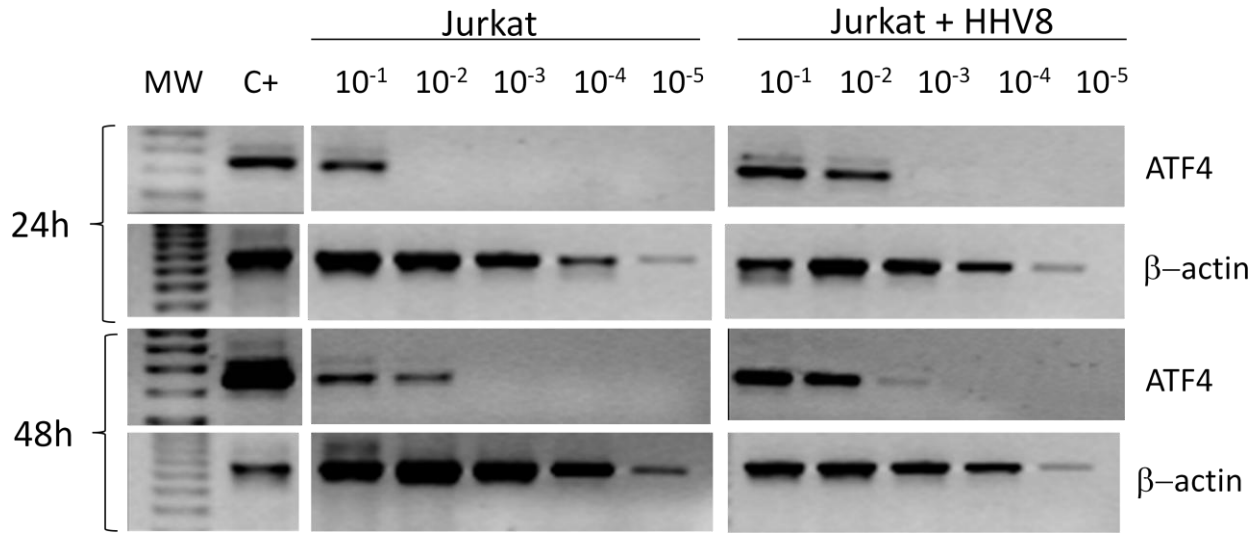

Figure 22: Semiquantitative rtPCR on ATF4 transcript and β-actin in Jurkat cells HHV-8 infected or not infected; rtPCR products are ethidium bromide stained in 2% agarose gel.

The results obtained by semi-quantitative rtPCR showed an increase in the ATF4 transcript induced by infection with HHV-8. To confirm these data, we repeated the experiments using the real-time PCR, to quantify more precisely ATF4 transcripts. Compared with PCR, the real-time PCR has an important advantage: the results are normalized with the simultaneous amplification of the housekeeping gene β-actin, avoiding errors due to over or underestimation of template.

Twenty µl of cDNA-template (corresponding to 200 ng of total RNA) were amplified in 30 µl of reaction mix, as described in Materials and Methods.

The results, summarized in Figure 23, showed that infection with HHV-8 causes an increase of the ATF4 transcript by approximately 1,3 fold at 8 hours p.i., 9,5 fold at 24 hours p.i. and 6,7 fold at 48 hours p.i..

This result confirmed data obtained by semiquantitative rtPCR, showing a peak of upregulation at 24 hours p.i..

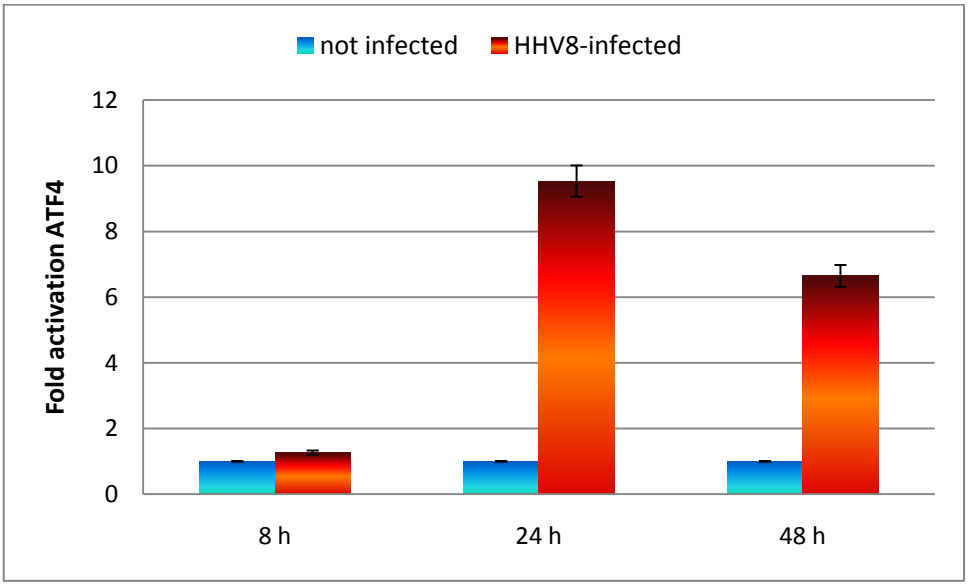

Figure 23: ATF4 transcription levels in Jurkat cells HHV-8-infected or not-infected at 8, 24 and 48 hours post infection, analysed by real time PCR.

To determine whether infection with HHV-8 had effect also on the levels of ATF4 protein, a western blot analysis was performed using a monoclonal antibody anti-ATF4/CREB2 (Santa Cruz Biotechnology). 20 μg of total protein extract, derived from HHV-8 infected Jurkat cells, was electrophoretically separated, transferred to Hybond-P membrane (Amersham) and hybridized with the monoclonal antibody anti-ATF4. The results showed an increase of ATF4 protein levels in infected cells compared to non-infected.

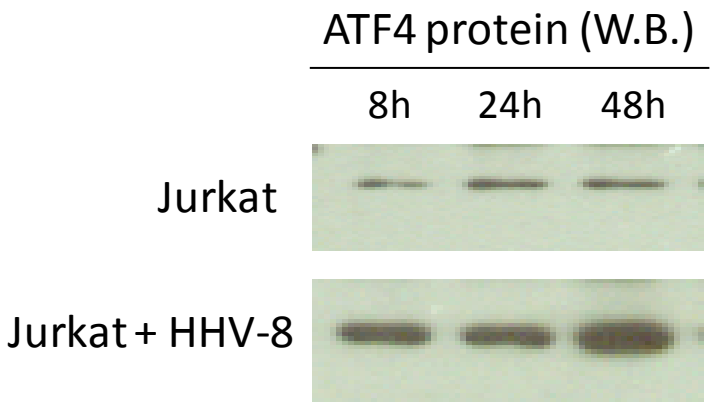

Figure 24: Western blotting analysis of ATF4 protein levels in non-infected and HHV-8-infected Jurkat cells.

2. ATF4 induces HHV-8 replication

Based on the results showing the increase of ATF4 transcription after HHV-8 infection, we further investigated whether this increase was functional to viral replication and if the overexpression of ATF4 could have a positive effect on replication of HHV-8.

To verify this hypothesis, Jurkat cells were transfected with pCG-ATF4 plasmid, containing the full length ATF4 gene cloned under the transcriptional control of early promoter of human cytomegalovirus (CMV). Jurkat cells were seeded at optimal confluence 24 hours before transfection. Cell samples of $2\text{^}10^6$ were transfected by nucleofection with 2 μg of pCG-ATF4 plasmid DNA. Control cells were nucleofected with 2 μg of the vector pCR3.1-Uni, containing only the CMV early promoter. In parallel, to assess the transfection efficiency, cells were transfected with the pmax-GFP plasmid containing the gene encoding GFP (green fluorescent protein), cloned under the transcriptional control of early promoter of CMV. 24 hours post transfection, cells expressing GFP (green) compared to the number of total cells were more than 50%.

The viability was verified by the exclusion assay Trypan Blue 24 hours after transfection, and was about 80%.

To verify the production of ATF4 messenger, cell samples were analyzed by rtPCR 24 and 48 hours after transfection. The results show the ability of the plasmid to produce a 100 fold enhancement of ATF4 levels in the transfected cells (Fig. 25).

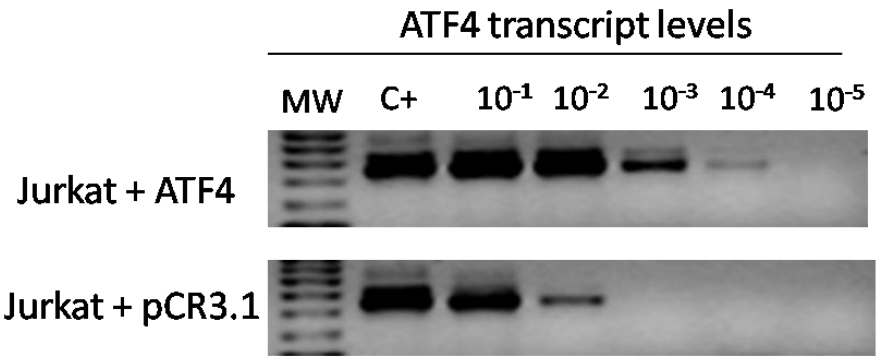

Figure 25: Semiquantitative rtPCR on ATF4 transcripts in Jurkat transfected with pCG-ATF4 and in Jurkat transfected with "empty" vector pCR3.1-Uni, 24 hours post transfection.

In order to investigate the effect of ATF4 overexpression on HHV-8, Jurkat cells were seeded at optimal confluence and were then transfected with pCG-ATF4 plasmid or with control pCR3.1-Uni empty vector. After verifying vitality and efficiency of transfection, cells were infected with HHV-8 (1:10 of m.o.i.). After 3 hours adsorption, the virus inoculum was removed. Cell samples were then collected at 0, 8, 24 and 48 hours p.i.. To evaluate the replication and transcription of HHV-8, respectively, DNA and RNA extracted from cells were analyzed. To investigate viral replication, total DNA was extracted from 10^6 cell samples collected at different times p.i. and was used as template in real-time PCR to quantify the presence of virus by amplification of late viral ORF26 gene (using 1μg of DNA as template). The results showed that the overexpression of ATF4 leads to a 15 fold increase in viral replication at 24 hours p.i., and 9,7 fold at 48h.

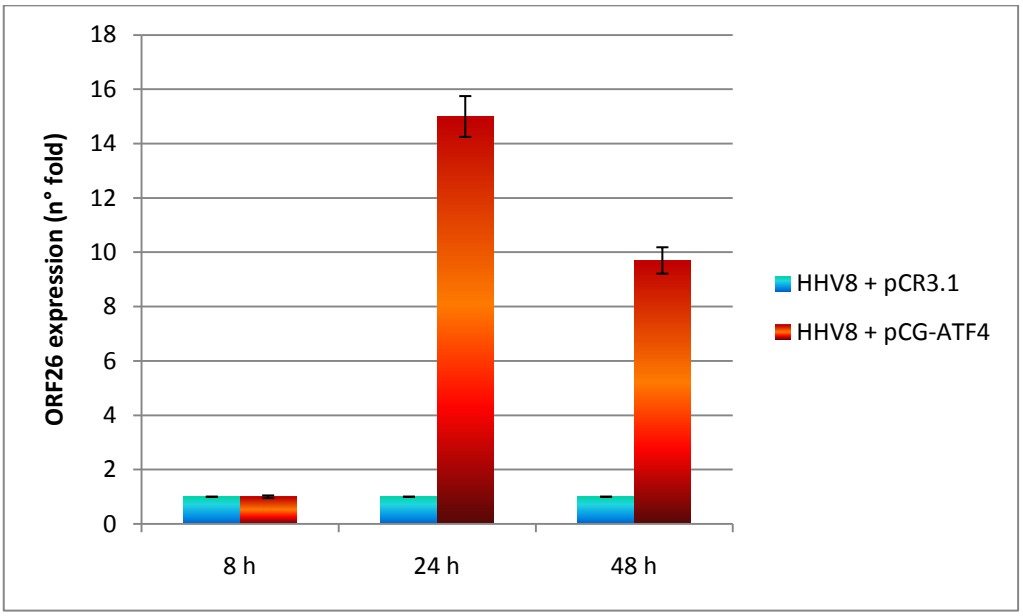

Figure 26: Analysis of ORF26 expression by real time PCR on DNA of HHV-8-infected Jurkat cells, tranfected with ATF4 plasmid or with pCR3.1 empty vector. Collection times were: 8, 24 and 48 hours.

To investigate transcription of HHV-8 in presence or absence of ATF4, total RNA from cell samples was extracted, reverse transcribed to cDNA and analysed by rtPCR, searching for viral transcripts corresponding to ORF50 and ORF26 genes. As described above, rtPCR was performed using serial dilutions of template. In parallel, the same dilutions of template were amplified for the β-actin gene (housekeeping gene) as control. Amplification products were run in 2% agarose gel and ethidium bromide stained. Fig. 27 shows the results of rtPCR at 24 and 48 hours p.i..

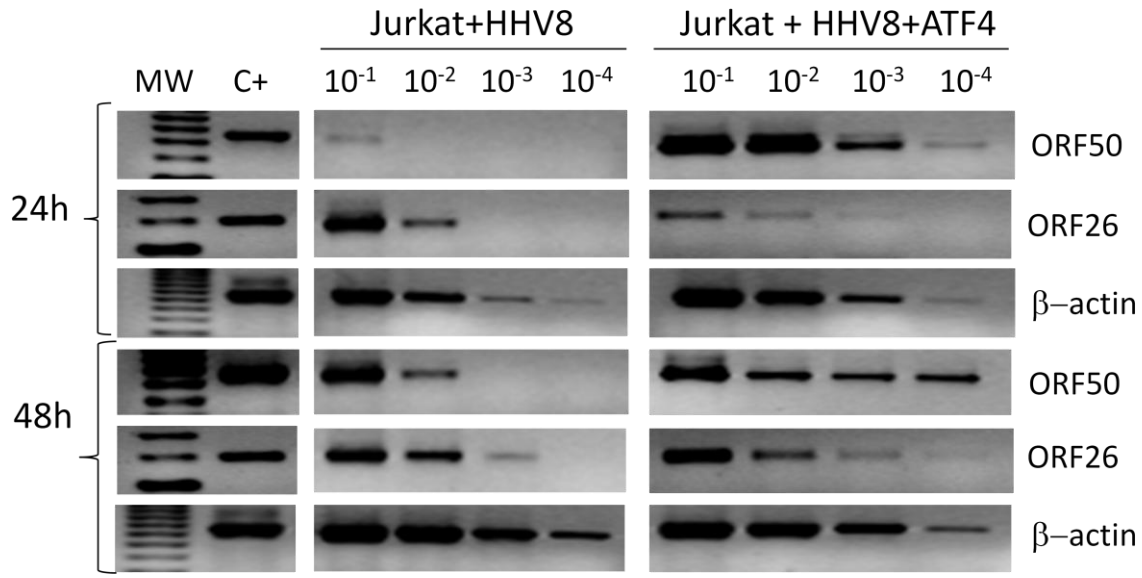

Figure 27: Analysis of ORF50 and ORF26 transcripts by semiquantitative rtPCR in Jurkat cells transfected with ATF4 plasmid and HHV-8 infected.

The increase of HHV-8 ORF50 transcripts is evident at all times, whereas the increase of ORF26 is most evident at 48 hours p.i.. Two independent experiments were performed with samples in duplicate. The data show that the overexpression of ATF4 increases the HHV-8 transcription.

3. The expression of ATF4 does not reactivate HHV-8 from latency

The results obtained showed that ATF4 is able to increase replication of HHV-8 in infected cells. Based on this observation, we investigated whether ATF4 is also able to directly reactivate the productive cycle of HHV-8 in latently infected cells.

For this purpose cell lines BC-3 and BCBL-1 were used, both derived from PEL, containing HHV-8 in a latent state. The reactivation of the virus can be obtained by treatment with phorbol esters, e.g. TPA, which is the method used to produce the cell-free viral inoculum used in the experiments of infection in vitro. Samples of $2\text{^}10^6$ BCBL-1

cells were transfected by nucleofection with 2 µg of pCG-ATF4 plasmid or pCR3.1-Uni empty vector. Samples were collected at different times (1, 2, 3 and 6 days) post-transfection, and DNA was extracted to quantify viral genome by real time PCR specific for the viral gene ORF26 of HHV-8. As a positive control of reactivation, cells were stimulated with TPA (20 ng/ml).

The results (Fig. 28) show that the expression of ATF4 does not induce viral reactivation, as proven by a similar amount of HHV-8 DNA molecules in control cells and in those transfected with ATF4.

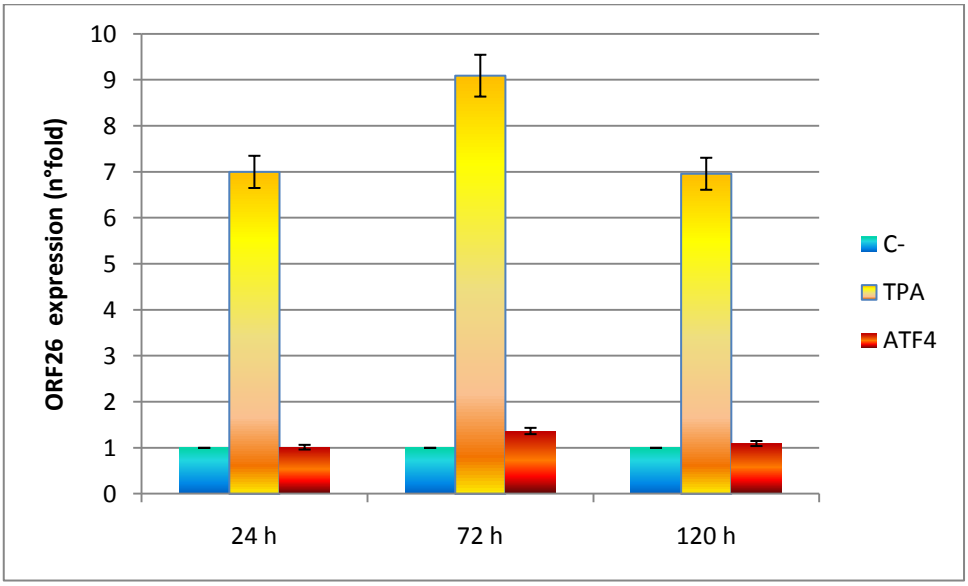

Figure 28: Real time PCR of BCBL-1 DNA. C-: untreated BCBL1 cells; TPA: cells treated with TPA (reactivation from latency); ATF4: cells transfected with pCG-ATF4 plasmid.

In contrast, as expected, treatment with TPA (used as a positive control) reactivated viral replication, causing about 10 fold increase of viral genomes copy numbers into the cells.

To verify that this "negative" result was not due to cell type used, we repeated the experiment with BC-3 cells, which also contain HHV-8 in a latent state. The results confirmed that nucleofection with ATF4 does not increase the number of genomes compared to cells transfected with empty plasmid, thus confirming that ATF4 is not able to directly induce the reactivation of HHV-8 (data not shown).

4. ATF4 does not activate HHV-8 promoters

Because of the results of the in vitro HHV-8 infection showing that ATF4 promotes viral replication, we investigated whether ATF4 acts at transcriptional level, inducing the activation of major gene promoters of HHV-8, ORF50, ORF57 and T1.1 promoters.

Jurkat cells were seeded at optimal density and then transfected with pCG-ATF4 plasmid and with reporter plasmids containing the reporter gene *luc* (encoding the luciferase enzyme of Firefly) cloned under the transcriptional control of different gene promoters (PR) of HHV-8: pGL-PR50 (ORF50 promoter), pGL-PR57 (ORF57 promoter), pGL-T1.1 (T1.1 promoter that encodes a nuclear polyadenylation RNA, PAN mRNA, a non-coding transcript that represents the most abundant lytic cycle transcript). These plasmids were previously obtained in our laboratory[56].

Nucleofection was performed in duplicate on samples of $2\text{^}10^6$ cells with 2 μg total DNA consisting of: a fixed amount (500 ng) of reporter pGL-PR plasmid series of HHV-8, with different concentrations (500 ng, 1 μg) of pCG-ATF4 plasmid or control vector pCR3.1-Uni, and a constant concentration (500 ng) of pGL-SV40 reporter plasmid containing the luciferase reporter gene of Renilla.

The Renilla luciferase is cloned under the transcriptional control of SV40 promoter and expresses an enzyme that acts at a different pH from the Firefly luciferase (respectively pH 9-10 and pH 7.8): for this reason the two reactions can be carried out at different times and PGL-SV40 was used as internal control to normalize the results, being proportional to the efficiency of transfection. The expression plasmid pCR-50sp, encoding ORF50, a known transactivator of the promoters tested[56] was used as a positive control.

After transfection, cells incubated for 48 hours at 37° C were then collected for luciferase assay. In this experiment, 10^6 cells samples were harvested and lysed following the manufacturer's instructions (Dual Glo luciferase assay System) as described in Materials and Methods. Sample lysates were measured by luminometer. The signal emitted from the Firefly luciferase was measured after 20 minutes incubation at room temperature. Subsequently the Stop & Glo Reagent, containing the Renilla luciferase substrate was added and incubated for 10 minutes at room temperature, to perform the measurement of the Renilla luciferase emission necessary to standardize the results.

The results (Fig. 29) shows that ATF4 does not activate the promoter tested, and no synergic activity is observed in co-expression with ORF50.

A.

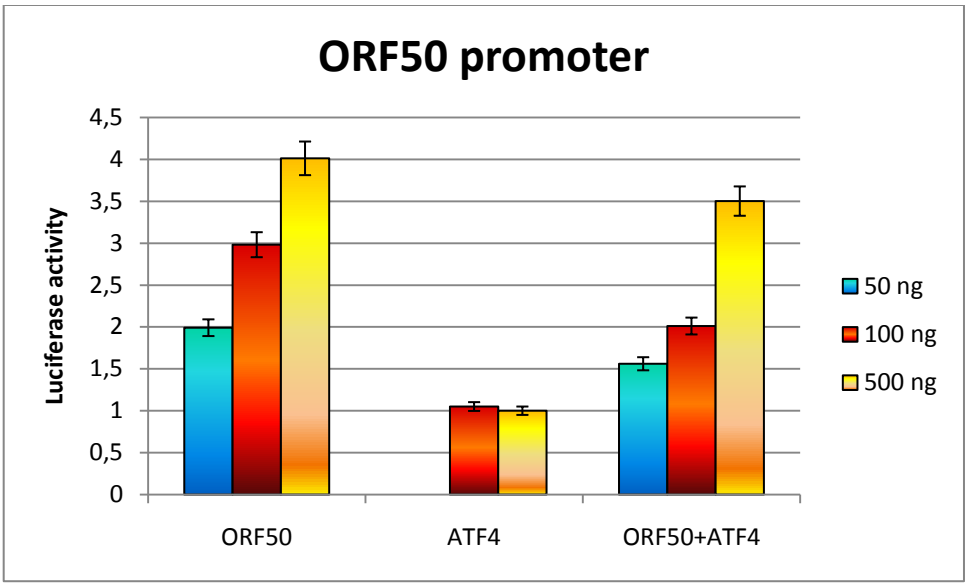

B.

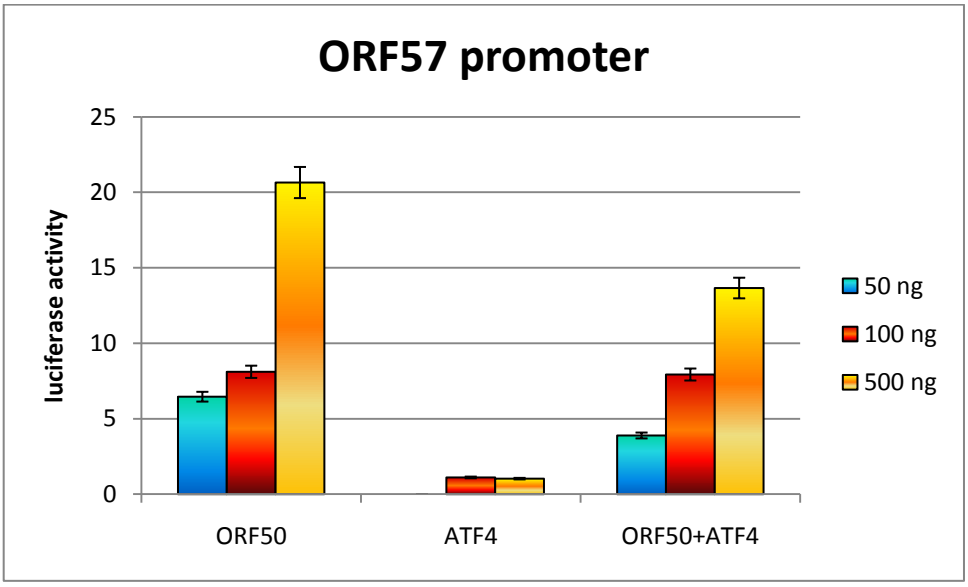

C.

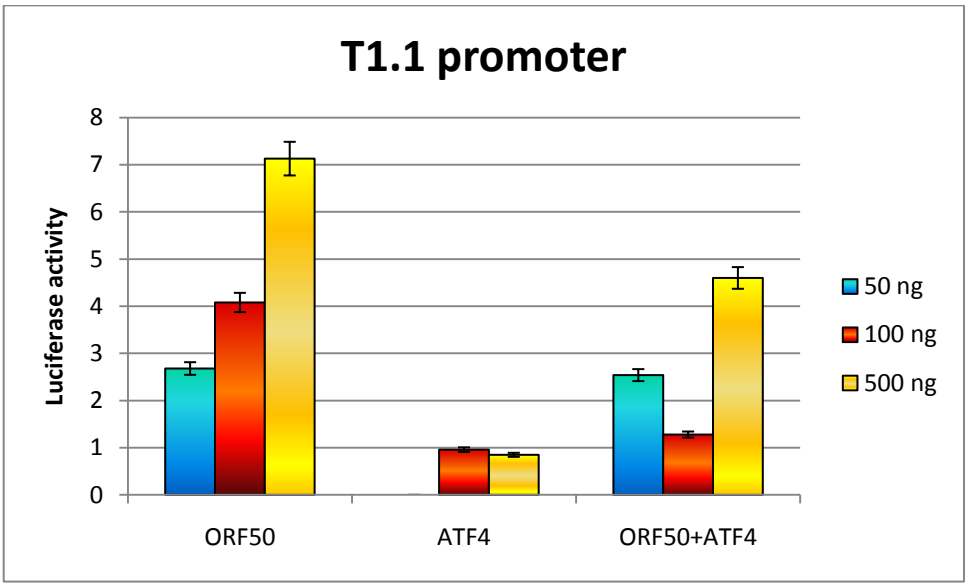

Figure 29: Luciferase assays on Jurkat cells co-transfected with HHV-8 promoter report plasmids (pGL-PR50, pGL-PR57, pGL-PRT1.1) and ORF50 or ATF4 or both. A: ATF4 activity on ORF50 promoter. B: ATF4 activity on ORF57 promoter. C: ATF4 activity on T1.1 promoter.

5. ATF4 activates MCP-1 promoter

Since the results demonstrated that ATF4 increases replication and transcription of HHV-8, but does not act on HHV-8 promoter and HHV-8 reactivation, we investigated whether ATF4 was involved in the activity of MCP-1.

MCP-1 is a cytokine upregulated by HHV-8[41] involved in angiogenesis.

To study the activation of MCP-1 promoter, different constructs were used (provided by T. Yoshimura, National Cancer Institute, Frederick, MD)[57]. The MCP-1 promoter-luciferase constructs contain the proximal promoter of MCP-1 (pGLM-PRM), the proximal promoter and the distal enhancer (pGLM-ENH), and the promoter and the enhancer with mutations of the NF-kB sites (pGLM-MA1A2).

Hela cells were seeded at optimal confluence and co-transfected with 1 µg total DNA consisting of: 400 ng of the MCP-1 promoters (pGLM-PRM, pGLM-ENH or pGLM-MA1MA2), 400 ng pCG-ATF4 plasmid (or control vector pCR3.1-Uni), and 200 ng of pGL-SV40 reporter plasmid containing the Renilla luciferase.

After transfection, cells incubated for 48 hours at 37° C, were then collected for luciferase assay. Cells samples were harvested and lysed following the kit instructions (Dual Glo luciferase assay System) as described in Materials and Methods. Sample lysates were measured by luminometer. The signal emitted from the Firefly luciferase was measured after 10 minutes incubation at room temperature. Subsequently the Stop & Glo Reagent containing the substrate of Renilla luciferase was added and incubated 10 minutes at room temperature, to perform the measurement of the Renilla luciferase signal in order to standardize the results.

ATF4 induces a 3,1-fold activation of the MCP-1 promoter in Hela cells, as shown in Figure 30, whereas no activation of the MCP-1 promoter with the enhancer and with the mutated enhancer is observed, suggesting that the NF-kB sites are not required for ATF4 activity.

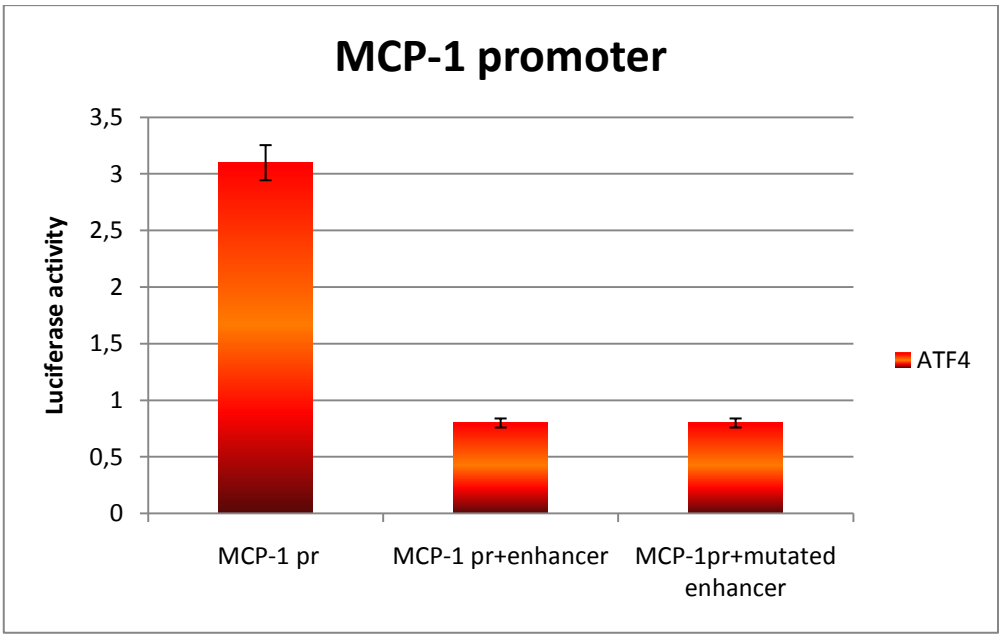

Figure 30: Luciferase assay on Hela cells co-transfected with ATF4 and MCP-1 promoter report plasmid pGLM-PRM, pGLM-ENH and pGLM-MA1MA2.

DISCUSSION

HHV-8, also known as Kaposi's sarcoma associated herpesvirus (KSHV), is a gamma-herpesvirus initially identified by Chang et al. in 1994 from a Kaposi sarcoma biopsy[5]. HHV-8 is considered the primary etiologic agent of Kaposi sarcoma, a highly vascularised neoplasm characterised by the presence of spindle cells of endothelial origin, angiogenesis and inflammatory infiltrates. HHV-8 is also implicated in other malignancies like primary effusion lymphoma (PEL) and multicentric Castleman's disease (MCD) and is associated with immunodeficiency and immunosuppression. The viral genome contains several genes homologous to oncogenes that induce malignant tumours. Development of HHV-8 associated tumours is related to the replicative activity of the virus. In fact, a critical step in HHV-8 oncogenesis is represented by the activation of virus replication, mediated by the switch between latent and lytic phases. The major transactivator genes ORF50 and ORF57 play an important role in the regulation of virus replication and reactivation. Both genes are expressed at early stages of infection.

Previous results obtained in our laboratory by gene array on Jurkat cells stably expressing ORF50 gene showed that ORF50 upregulates the activating transcription factor ATF4 (unpublished data).

ATF4 is a signal-responsive member of the basic leucine zipper family of transcription factors. ATF4 is activated in response of several forms of cellular stress, such as hypoxia, amino acid deficiency and ER stress. ATF4 expression is upregulated in many tumours and is involved in angiogenesis by interaction with VEGF. Since angiogenesis is a key event in the development of Kaposi's sarcoma induced by HHV-8 infection, we have focused our attention on this aspect, showing that HHV-8 induces a rapid and potent angiogenesis in cultured endothelial cells[41]. Induction of angiogenesis is due to the activation of MCP-1 and NF-kB pathways. HHV-8 acute infection induces NF-kB activation in endothelial cells at levels comparable to those reached with the NF-kB inducer TPA. NF-kB controls the expression of several proinflammatory genes, and is a critical regulator of the immediate early response to HHV-8. MCP-1 is a cytokine NF-kB dependent and human MCP-1 gene contains two NF-kB binding sites in the enhancer region, required for TPA-induced

expression. Previous studies[41] also demonstrated that HHV-8 infection selectively triggers the increase of MCP-1 levels. NF-kB is involved in this activation, and is required for maximal production of the cytokine. However, mutations in both NF-kB binding sites in the enhancer region did not result in the complete failure of promoter induction in HHV-8 infected cells, moreover, inhibitors of NF-kB did not prevent MCP-1 activation, suggesting that other pathways are involved.

Thus, due to the properties of ATF4, we explored the possibility of a role of this transcriptional factor in the angiogenesis induced by the virus.

Firstly, to explain how HHV-8 and ATF4 interact, we investigated the effect of infection with HHV-8 on ATF4 expression in Jurkat cells, using a cell-free inoculum obtained in our laboratory, and we found that HHV-8 triggers the expression of ATF4 with a 10-fold increase 24 hours post infection.

To further investigate whether the increase of ATF4 was functional to HHV-8 replication, we transfected Jurkat cells with the pCG-ATF4 plasmid and analysed the replication of the virus by real time PCR and rtPCR. The results showed a 15-fold increase of viral replication 24 hours post transfection, and a 10-fold augment of HHV-8 transcription.

These data suggested an important role of ATF4 on HHV-8 replication, so we investigated whether ATF4 reactivated the virus from latency. In order to verify this hypothesis, we transfected PEL-derived cells BC-3 and BCBL-1, containing latent HHV-8, with the pCG-ATF4 plasmid and analysed by real time PCR the viral replication.

ATF4 did not induce reactivation of HHV-8 from latent state. To confirm this result, we analysed the effect of ATF4 on HHV-8 promoters. Three viral promoters were tested by luciferase assay: ORF50 promoter, ORF57 promoter and T1.1 promoter. ATF4 did not activate any of the promoter tested.

Thus, to further understand how HHV-8 takes advantage from ATF4, we considered another important aspect of HHV-8 infection and ATF4 activity: angiogenesis.

In order to investigate whether ATF4 was involved in the MCP-1 pathway of HHV-8 infected cells, we studied the activation of MCP-1 promoter after overexpression of ATF4 by luciferase assay. We analysed both MCP-1 promoter and MCP-1 promoter with mutation in the NF-kB binding sites and we found that ATF4 activates the enhancerless MCP-1 promoter. In addition, NF-kB binding sites are not required for this activation.

Therefore, we describe for the first time that ATF4 is a transcription factor important for HHV-8 replication. It is not yet possible to determine whether ATF4 is absolutely necessary or only an enhancing factor for virus replication, since ATF4 is constitutively expressed in the cell lines used in these experiments. Further experiments, performed by silencing ATF4, will elucidate this important novel aspect of HHV-8 replication.

Furthermore, ATF4 might to be implicated in HHV-8 induced tumorigenesis, being involved in several aspects of viral replication, and could represent a potential therapeutic target for HHV-8 induced transformation.

REFERENCES

1. Roizman B., Sears A. (1998) - Herpes simplex viruses and their replication. In: *Virology (vol.2) - III Edition.* Fields BN., Knipe DM. Howley PM. (eds.) Lippincot-Raven Publishers, Philadelphia-New York, pp.2231- 2342.
2. Furlong D, Swift H, Roizman B: Arrangement of herpes virus deoxyribonucleic acid in the core. *Journal of Virology*, 1972. 10 (5): 1071-1074.
3. McCombs RM, Brunschwig JP, Mirkovic R, Benyesh-Melnick M: Electron microscopic characterization of a herpeslike virus isolated from three shrews. *Virology*, 1971. 45 (3): 816-820.
4. Deiss LP, Chou J, Frenkel N: Functional domains within the a sequence involved in the cleavage-packaging of the herpes simplex virus DNA. *Journal of Virology*, 1986. (3): 605-618.
5. Chang Y, Cesarman E, Pessin MS, Lee F, Culpepper J, Knowles DM, Moore PS. Identification of herpesvirus-like DNA sequences in AIDS-associated Kaposi's sarcoma. *Science*, 1994. 266 (5192): 1865-1869.
6. Cesarman E, Chang Y, Moore PS, Said JW, Knowles DM: Kaposi's sarcoma-associated herpesvirus-like DNA sequences in AIDS-related body-cavity-based lymphomas. *The New England journal of medicine*, 1995. 332 (18): 1186-1191.
7. Soulier J, Grollet L, Oksenhendler E, Cacoub P, Cazals-Hatem D, Babinet P, d'Agay MF, Clauvel JP, Raphael M, Degos L, et al. Kaposi's sarcoma-associated herpesvirus-like DNA sequences in multicentric Castleman's disease. *Blood*, 1995. 86 (4): 1276-1280.
8. Antman K, Chang Y. Kaposi's sarcoma. *The New England journal of medicine*, 2000. 342 (14): 1027-1038.
9. Luppi M, Barozzi P, Santagostino G, Trovato R, Schulz TF, Marasca R, Bottalico D, Bignardi L, Torelli G. Molecular evidence of organ-related transmission of Kaposi sarcoma-associated herpesvirus or human herpesvirus-8 in transplant patients. *Blood*, 2000. 96 (9): 3279-3281.

10. Wu L, Lo P, Yu X, Stoops JK, Forghani B, Zhou ZH: Three-dimensional of the human herpesvirus 8 capsid. *Journal of Virology*, 2000. 74 (20): 9646-9654.
11. Renne R, Lagunoff M, Zhong W, Ganem D: The size and conformation of Kaposi's sarcoma associated herpesvirus (human herpesvirus 8) DNA in infected cells and virions. *Journal of Virology,* 1996. 70 (11): 8151-8154.
12. Moore PS, Gao SJ, Dominguez G, Cesarman E, Lungu O, Knowles DM, Garber R, Pellett PE, McGeoch DJ, Chang Y: Primary characterization of a herpesvirus agent associated with Kaposi's sarcoma. *Journal of Virology,* 1996. 70 (1): 549-558.
13. JP, Peruzzi D, Edelman IS, Chang Y, et al.: Nucleotide sequence of the Kaposi sarcoma-associated herpesvirus (HHV-8). *PNAS USA*, 1996. 93 (25): 14862-14867.
14. Arvanitakis L, Geras-Raaka E, Varma A, Gershengorn MC, Cesarman E: Human herpesvirus KSHV encodes a constitutively active G-protein-coupled receptor linked to cell proliferation. *Nature*, 1997. 385 (6614): 347-350.
15. Coscoy L, Ganem D: Kaposi's sarcoma-associated herpes virus encodes two proteins that block cell surface display of MHC class I chains by enhancing their endocytosis. *PNAS USA*, 2000. 97 (14): 8051-8056.
16. Birkman A, Mahr K, Ensser A, Yaguboglu S, Titgemeyer F, Fleckenstein B, Neipel F: Cell surface heparan sulfate is a receptor for human herpesvirus 8 and interacts with envelope glycoprotein K8.1. *Journal of Virology*, 2001. 75 (23): 11583-11593.
17. Decker LL, Shankar P, Khan G, Freeman RB, Dezube BJ, Lieberman J, et al. The Kaposi sarcoma-associated herpesvirus (KSHV) is present as an intact latent genome in KS tissue but replicates in the peripheral blood mononuclear cells of KS patients. *The Journal of experimental medicine*, 1996.184: 283–288.
18. Ballestas ME, Chatis PA, Kaye KM. Efficient persistence of extrachromosomal KSHV DNA mediated by latency-associated nuclear antigen. *Science*, 1999. 284: 641–644.

19. Lu F, Day L, Gao SJ, Lieberman PM. Acetylation of the latency-associated nuclear antigen regulates repression of Kaposi's sarcoma-associated herpesvirus lytic transcription. *Journal of Virology*, 2006. 80: 5273–5282.
20. Zhu FX, Cusano T, Yuan Y. Identification of the immediate early transcripts of Kaposi's sarcoma-associated herpesvirus. *Journal of Virology*, 1999. 73 (7): 5556-5567.
21. Lukac DM, Kirshner JR, and Ganem D. Transcriptional activation by the product of the open reading frame 50 of Kaposi's-associated herpesvirus is required for lytic viral reactivation in B cells. *Journal of Virology*, 1999. 73: 9348–9361.
22. Lukac DM, Garibyan L, Kirshner JR, Palmeri D, Ganem D. DNA binding by Kaposi's Sarcoma-associated herpesvirus lytic switch protein is necessary for transcriptional activation of two viral delayed early promoters. *Journal of Virology*, 2001. 75 (15): 6786–6799.
23. Chang PJ, Shedd D, Gradoville L, Cho MS, Chen LW, Chang J, Miller G. Open reading frame 50 protein of Kaposi's sarcoma-associated herpesvirus directly activates the viral PAN and K12 genes by binding to related response elements. *Journal of Virology*, 2002. 76 (7): 3168-3178.
24. Sakakibara S, Ueda K, Chen J, Okuno T, Yamanishi K. Octamer-binding sequence is a key element for the autoregulation of Kaposi's sarcoma-associated herpesvirus ORF50/Lyta gene expression. *Journal of Virology*, 2001. 75: 6894-6900.
25. Caselli E, Menegazzi P, Bracci A, Galvan M, Cassai E, Di Luca D. Human herpesvirus-8 (Kaposi's sarcoma associated herpesvirus) ORF 50 interacts synergistically with the tat gene product in transactivating the human immunodeficiency virus type 1 LTR. *Journal of General Virology*, 2001. 82 (8): 1965- 1970.
26. Caselli E, Galvan M, Santoni F, Rotola A, Caruso A, Cassai E, Di Luca D. Human herpesvirus-8 (Kaposi's sarcoma-associated virus) ORF50 increases in vitro cell susceptibility to human immunodeficiency virus type 1 infection. *Journal of General Virology*, 2003. 84 (5): 1123-1131.

27. Kirshner JR, Lukac DM, Chang J, Ganem D. Kaposi's sarcoma - associated Herpesvirus ORF57 encodes a posttrascriptional regulator with multiple distinct activities. *Journal of Virology*, 2000. 74 (8): 3586-3597.
28. Pauk J, Huang ML, Brodie SJ, Wald A, Koelle DM, Schacker T, Celum C, Selke S, Corey L: Mucosal shedding of human herpesvirus 8 in men. *The New England journal of medicine*, 2000. 343 (19): 1369-1377.
29. Lacoste V, de la Fuente C, Kashanchi F, Pumfery A. Kaposi's sarcoma-associated herpesvirus immediate early gene activity. *Frontiers in Bioscience*, 2004. 9: 2245–2272.
30. Damania B. DNA tumor viruses and human cancer. *Trends Microbiology*, 2007. 15: 38–44.
31. Laman H, Boshoff C. Is KSHV lytic growth induced by a methylation-sensitive switch? *Trends Microbiology*, 2001. 9: 464–466.
32. Kaposi M: Idiopathic multiple pigmented sarcoma of the skin. *Archiv fur Dermatologie und Syphilis*, 1872. 4: 265-273.
33. Ensoli b, Sgadari C, Barillari G, Sirianni MC, Sturzl M, Monini P. Biology of Kaposi's sarcoma. *European Journal of Cancer*, 2001. 37: 1251-1269.
34. Tappero JW, Conant MA, Wolfe SF, Berger TG: Kaposi's sarcoma. Epidemiology, pathogenesis, histology, clinical spectrum, staging criteria and therapy. *Journal of the American Academy of Dermatology*, 1993. 28 (3): 371-395.
35. Goedert JJ: The epidemiology of acquired immunodeficiency syndrome malignancies. *Seminars in Oncology*, 2000. 27 (4): 390-401.
36. Wabinga HR, Parkin DM, Wabwire-Mangen F, Mugerwa JW: Cancer in Kampala, Uganda, in 1989–91: changes in incidence in the era of AIDS. *International Journal of Cancer*, 1993. 54 (1): 26-36.
37. Dourmishev LA, Dourmishev AL, Palmeri D, Schwartz RA, Lukac DM: Molecular genetics of Kaposi's sarcoma-associated herpes virus human herpesvirus-8) epidemiology and pathogenesis. *Microbiology & Molecular Biology Reviews*, 2003. 67 (2): 175-212. table of contents

38. Hengge UR, Ruzicka T, Tyring SK, Stuschke M, Roggendorf M, Schwartz RA, Seeber S: Update on Kaposi's sarcoma and other HHV-8 associated diseases Part 1: epidemiology, environmental predispositions, clinical manifestations, and therapy. *The Lancet Infectious Diseases*, 2002. 2 (5): 281-292.
39. Katano H, Sato Y, Kurata T, Mori S, Sata T: Expression and localization of human herpesvirus 8-encoded proteins in primary effusion lymphoma, Kaposi's sarcoma, and multicentric Castleman's disease. *Virology*, 2000. 269 (2): 335-344.
40. Renne R, Zhong W, Herndier B, McGrath M, Abbay N, Kedes D, Ganem D. Lytic growth of Kaposi's sarcoma-associated herpesvirus (human herpesvirus 8) in culture. *Nature Medicine* 1996. 2 (3): 342-346.
41. Caselli E, Fiorentini S, Amici C, Di Luca D, Caruso A, Santoro MG. Human herpesvirus 8 acute infection of endothelial cells induces monocyte chemoattractant protein 1-dependent capillary-like structure formation: role of the IKK/NF-kB pathway. *Blood*, 2007. 109 (7): 2718-2726.
42. Hai T, Curran T. Cross-family dimerization of transcription factors Fos/Jun and ATF/CREB alters DNA binding specificity. *PNAS USA*, 1991. 88: 3720-3724.
43. Harding HP, Zhang Y, Bertolotti A, Zeng H, Ron D. PERK is essential for translation regulation and cell survival during unfolded protein response. *Molecular Cell*, 2000. 5 (5): 897-904.
44. Schoch S, Cibelli G, Magin A, Steinmuller L, Thiel G. Modular structure of cAMP response element binding protein 2 (CREB2). *Neurochemistry International*, 2001. 38: 601-608.
45. Chevray PM, Nathans D. Protein interaction cloning in yeast: identification of mammalian proteins that react with the leucine zipper of Jun. *PNAS USA*, 1992. 89: 5789-5793.
46. Vallejo M, Ron D, Miller CP, Habener JF. C/ATF, a member of the activating transcription factor family of DNA-binding proteins, dimerizes with CAAT/enhancer-binding proteins and directs their binding to cAMP response elements. *PNAS USA*, 1993. 90: 4679-4683.

47. Lassot I, Estrabaud E, Emiliani S, Benkirane M, Benarous R, Margottin-Goguet F. p300 modulates ATF4 stability and transcriptional activity independently of its acetyltransferase domain. *Journal of Biological Chemistry*, 2005. 280: 41537-41545.
48. De Angelis R, Iezzi S, Bruno T, Corbi N, Di Padova M, Floridi A. Functional interaction of the subunit 3 of RNA polymerase II (RPB3) with transcription factor 4 (ATF4). *FEBS Letters*, 2003. 547: 15-19.
49. Kawai T, Matsumoto M, Takeda K, Sanjo H, Akira S. ZIP kinase, a novel serine/threonine kinase which mediates apoptosis. *Molecular and Cellular Biology*, 1998. 18: 1642-1651.
50. Reddy TR, Tang H, Li X, Wong-Staal F. Functional interaction of the HTLV-1 transactivator Tax with activating transcription factor-4 (ATF4). *Oncogene*, 1997. 14: 2785-2792.
51. Hai T, Hartman MG. The molecular biology and nomenclature of the activating transcription factor/cAMP responsive element binding family of transcription factor: activating transcription factor proteins and homeostasis. *Gene*, 2001. 273: 1-11.
52. Harding HP, Zhang Y, Zeng H, Novoa I, Lu PD, Calfon M, Sadri N, Yun C, Popko B, Paules R, Stojdl DF, Bell JC, Hettmann T, Leiden JM, Ron D. An integrated stress response regulates amino acid metabolism and resistance to oxidative stress. *Molecular Cell*, 2003. 11 (3): 619-633.
53. Bi M, NaczKi C, Koritzinsky M, Fels D, Blais J Hu N. ER stress-regulated translation increases tolerance to extreme hypoxia and promotes tumour growth. *The Embo Journal*, 2005. 24: 3470-3481.
54. Isler JA, Skalet AH and Alwine JC. Human Cytomegalovirus Infection Activates and Regulates the Unfolded Protein Response. *Journal of Virology*, 2004. 79 (11): 6890-6899.
55. Lim C, Sohn H, Gwack Y, Choe J. Latency associated nuclear antigen of Kaposi's sarcoma-associated herpesvirus (human herpesvirus-8) binds ATF4/CREB2 and inhibits its transcriptional activation activity. *Journal of General Virology*, 2000. 81, 2645-2652.

56. Santoni F, Lindner I, Caselli E, Goltz M, Di Luca D, Ehlers B. Molecular interaction between porcine and human gammaherpesviruses: implication for xenografts? *Xenotransplantation*, 2006. 13 (4): 308-317.
57. Ueda A, Ishigatsubo Y, Okubo T, Yoshimura T. Transcriptional regulation of the human monocyte chemoattractant protein-1 gene. Cooperation of two NF-kappaB sites and NF-kappaB/Rel subunit specificity. *Journal of Biological Chemistry*, 1997. 272: 31092-31099.
58. White IE, Campbell TB. Quantitation of cell-free and cell-associated Kaposi's sarcoma-associated herpesvirus DNA by real-time PCR. *Journal of clinical microbiology*, 2000. 38: 1992-1995.

PART II

REAL TIME PCR TO ASSESS TOTAL BACTERIAL LOAD IN CHRONIC WOUNDS

INTRODUCTION

1. Microbial diversity in chronic wounds

Chronic wounds are wounds that do not heal in a predictable amount of time the way most wounds do. Usually, wounds that do not heal within three months are considered chronic, and may never heal or may take years to do so. These wounds cause severe emotional and physical stress to patients, and are a major health care problem. In fact, non healing wounds lead to disability, decrease quality of life and are very expensive both on the health care system and on patients and their families. In the United States, the cost of chronic wounds exceeds 10 billion $ per year and constitutes over half of the total cost for all skin diseases[1,2]. There are also heavy indirect costs through loss of income, depression, impact on friends and family.

The vast majority of chronic wounds can be classified into three categories: venous ulcers, diabetic and pressure ulcers. A small number of wounds that do not fall into these categories may be due to different causes such as exposure to radiations or ischemia. Venous ulcers, which usually occur in the legs, account for about 70% to 90% of chronic wounds and mostly affect the elderly. They are thought to be due to venous hypertension caused by improper function of venous valves, therefore prevent blood from flowing backward.

Another major cause of chronic wounds is diabetes. Chronic wounds in diabetic patients are increasing in prevalence. Diabetics have a 15% higher risk for amputation than the general population due to chronic ulcer. Diabetes causes neuropathy, which inhibits nociception and the perception of pain. Thus, patients may not initially notice small wounds to legs and feet, and may therefore fail to prevent infection or repeated injury[3]. Further, diabetes damages small blood vessels, preventing adequate oxygenation of tissue, which can cause chronic wounds. Pressure also plays a role in the formation of diabetic ulcers.

Another leading type of chronic wounds is pressure ulcer, which usually occurs in bedridden patients and in people with conditions such as paralysis, inhibiting movement of body parts that are commonly subjected to pressure such as heels, shoulder blades and

sacrum. Pressure ulcers are caused by ischemia that occurs when pressure in the tissue is greater than the pressure in capillaries, and thus restricts blood flow into the area. Muscle tissue, which needs more oxygen and nutrients than skin does, shows the worst effects from prolonged pressure.

Chronic wounds affect mostly people over the age of 60. The incidence is 0,78% of the population and the prevalence ranges from 0,18 to 0,32%[4]. As the population ages, the number of chronic wounds is expected to rise[5].

Chronic wounds usually occur in patients with predisposing conditions, such as neuropathy, vascular compromission and venous disease, diabetes. In addition, other systemic conditions affect wound healing, such as trauma, inflammatory diseases, metabolic abnormalities, coagulopathies, etc. The main effect of these predisposing factors is the impairment of blood flow, resulting in local hypoxia and consequent decrease of leukocyte bactericidal action.

Chronic wounds are colonized by polymicrobial flora, comprising commensal bacteria normally present in local skin flora and urogenital tract, but also obligate anaerobic bacteria, that can proliferate in the wound due to the combination of necrotic tissue and low oxygen tension. Some of the bacteria more frequently detected in chronic wounds are reported in Table 1.

The role of bacteria in wound healing depends on their concentration, species composition and host response. Although bacterial colonization occurs in all chronic wounds, the differentiation between colonization and infection is not well defined.

AEROBES AND FACULTATIVE ANAEROBES	ANAEROBES
Coagulase-negative Staphylococci ***Staphylococcus aureus***	***Peptostreptococcus spp. (P. magnus, P. micros, P. prevotii, P. indolicus, P. asaccharolyticus)***
Beta-hemolytic Streptococci ***Streptococcus spp.***	***Clostridium perfrigens, C. difficile, C. baratii, C. cadaveris, C. ramosum, C. hystolyticum, C. sporogenes.***
Micrococcus spp.	***Eubacterium limosum***
Corynebacterium spp. ***C. xerosis***	***Propionibacterium acnes***
Escherichia coli	***Bacteroides fragilis, B. ureolyticus, B. uniformis, B. stercoris, B. capillosus***
Serratia liquefaciens	***Prevotella oralis, P. oris, P. biviae, P. buccae, P. corporis, P. melaninogenica***
Klebsiella pneumoniae ***K. oxytoca***	***Porphyromonas asaccharolytica***
Enterobacter cloacae ***E. aerogenes***	**Gram-negative pigmented bacillus**
Citrobacter freundii	***Fusobacterium necrophorum***
Proteus mirabilis ***P. vulgaris***	***Veillonella spp.***
Providencia stuarti	
Morganella morganii	
Acinetobacter calcoaceticus	
Pseudomonas aeruginosa	
Sphingobacterium multivorum	

Table 1: Bacteria frequently detected in chronic wounds.

The exposure of subcutaneous tissue to external environment provides a favourable setting for colonization by microorganisms. As previously mentioned, growth conditions become ideal when tissue is necrotic, or when the immune response is impaired. The most important sources of contamination are the external environment (for example bacteria in air, soil or on objects), the tissue surrounding the lesion (skin commensal flora) and endogenous sources, especially for lesions in proximity of body orifices (gastrointestinal tract, urogenital mucosa, oropharynx). Even if bacteria colonize the wounds and replicate, pathologic infection does not necessarily ensues. Infection takes place when virulence factors produced by colonizing bacteria prevail over local immune defences. An important contribution in promoting the passage from colonization to infection is represented by an elevate bacterial burden.

The progression from colonized lesion to infected wound depends on several host and microbic factors, including characteristics of the lesion (extension, depth, site), host systemic conditions and immune status, microbial load, and synergies among different bacterial species. Further complications of the local ecology of chronic wounds are their metabolic characteristics, which can affect the genotype expression of the wound bacteria.

Usually, chronic wounds show modifications of their bacterial flora over time. In the first phases, the wound is colonized by normal commensal flora from the skin, but in few weeks a significant increase of Gram-positive cocci take place. Subsequently, polymicrobial mixtures develop, comprising both aerobic and anaerobic bacteria.

Many studies focused on the detection of bacteria by standard culture methods, but search for specific pathogens by qualitative microbiology has failed to differentiate colonizers from invading pathogenic microorganisms (reviewed by Martin et al, 2010)[6]. For example, chronic venous leg ulcer harbour staphylococci, enterococci and pseudomonas[7]. However, no pathogen is consistently detected in the majority of samples, and also comparisons among different studied is difficult, since they are based on different sampling methods, culturing procedures and often selecting specific bacterial groups.

Furthermore, most studies investigated aerobic pathogens. However, also anaerobic bacteria are frequently present, even if fewer studies document their presence[8,9], due the difficulties in isolating and identifying anaerobes in comparison to aerobes.

In fact, methods of specimen collections and transport to the laboratory are critical for viability of obligate anaerobes. Furthermore, the time required for their culture and isolation is prolonged and more resource demanding than investigation for aerobes.

Until recently, the complexity of wound bacterial flora was underestimated, because standard culture techniques cannot identify all bacteria, particularly anaerobic bacteria that are difficult to isolate, and culture conditions might select bacterial species that are less represented in the in vivo lesion. Therefore, it has been difficult to establish the role of microorganisms in wound persistence, and to differentiate pathogenic bacteria that delay or prevent wound healing from innocent colonizers. Recently, several reports have strengthened the notion that the polymicrobic nature of infection, and the still undetermined interactions among colonizing bacteria, may play a major role in the absence of healing of chronic wounds[6,10].

Due to the impossibility of growing all bacteria, it is difficult to substantiate with precision a threshold of significance, but there is a growing perception that the presence of 10^5 or more bacterial cells-per gram of tissue (determined by classic culture-based analysis) is a key determinant in delayed wound healing[11].

2. Rapid molecular method for quantifying bacteria.

Many different techniques have been applied to identify microorganisms in chronic wounds. Table 2 (published originally by Martin et al, 2010)[6] summarizes the advantages and disadvantages of the most used methods. Traditionally, identification of wound bacteria has relied on standard bacteriological culture-based methods. These qualitative cultures are inexpensive, easy and quick to perform, however they completely miss the unculturable population that may be present. An important problem is given by the search of anaerobic bacteria, that frequently infect chronic wounds, but require specific culture conditions, suffer from transportation to the laboratory and can be refractory to in vitro growth. Furthermore, standard culture methods are insufficient for characterising complex polymicrobial communities, since many bacteria cannot be cultured. Moreover, bacteria that are present in only small quantities in most environments, including chronic wounds,

may proliferate readily in culture, whereas major populations, especially anaerobic ones, may require very specialised conditions to propagate under laboratory conditions.

Method	Technique description	Processing time and costs	Advantages	Disadvantages	Practice implications
Qualitative cultures	Swab culture of wound; Standard bacteriology culture	1 h for Gram stain; 1–3 days for culture results. Inexpensive	Inexpensive, widely available	Low sensitivity, not quantitative	Rapid and widely available, used to screen for methicillin-resistant *S. aureus* or *Pseudomonas*
Quantitative culture	Tissue specimen homogenized and organisms identified and quantified	3–4 days for speciation and quantification; expensive	Accurate and reproducible	Labor intensive, requires specialized facilities and not widely available. Long lag time	Widely used in Burn units, but clinical correlation not well defined
Nucleic acid amplification-PCR	DNA is extracted from specimens and amplified, using organism-specific primers	4–6 h; moderate cost	Rapid turnaround, highly sensitive. Equipment increasingly available	Requires testing for known organisms. Not useful for identifying ''unknowns'', not clinically standardized	Research settings largely. Used for methicillin-resistant *S. aureus* surveillance
Metagenomic methods	DNA is extracted from wound specimens, amplified and sequenced. All bacterial clones in specimen are sequenced	Several days; requires dedicated facility and personnel; expensive	Identifies all bacterial sequences within a specimen, including fastidious organisms and organisms in low numbers	Expensive, long turnaround time, not standardized. Sequences identified may include surface contaminants and nonviable organisms	Research settings at present, needs clinical correlation

Table 2: Common methods used to analyze bacterial populations in chronic wounds (Martin et al, 2010)[6].

Quantitative cultural methods, aiming to define a threshold value of significance of bacterial burden, require at first the identification of bacteria, and subsequently quantification. This approach, in addition to the problems outlined above for standard bacteriological analysis, are labor intensive and clinical correlations are not well defined. Standard culturing methods depend on diagnostic growth conditions (nutrient, inhibitors, temperature, gases, pressure, etc.), and characterize only viable and culturable bacteria, while molecular methods, depending on diagnostic macromolecules (DNA), can characterize viable and non-viable, culturable and unculturable bacteria, fastidious or dormant. A widely used molecular method is polymerase chain reaction (PCR), a culture-free molecular technique amplifying specific targets of DNA. However, PCR requires the use of oligonucleotide primers specific for a given bacterial species, and is not quantitative. Very recently, the use of metagenomic methods has been proposed. This approach requires

amplification of DNA and subsequent sequencing. Therefore, it is very labor-intensive, requires specialized laboratories, is expensive and time-consuming.

Another method that is increasingly applied to bacterial determination in chronic wounds is real-time PCR, that allows precise quantification of bacterial load. This approach has been used to detect and quantify specific pathogens in chronic wounds[12,13], but as outlined above for classic PCR, it requires the use of primers (and in this case also probes) specific for each bacterial species of interest. An important development of real-time PCR has been the design of "universal" primers, focused on the 16S rRNA gene[14]. This is a region, conserved across a wide range of bacterial genome, that can be employed, and therefore allows to determine the total bacterial burden, with simultaneous quantification of bacterial DNA without distinguishing among different species. This approach, so far not yet applied to the study of chronic wounds, offers several advantages:

- High sensitivity (about 100 fold more than classic culture methods)
- Rapid results (the analysis can be performed in few hours)
- Independent on the bacteria viability (transport methods are not relevant)
- Detection of all bacteria present in the wounds, aerobic and anaerobic, easy to culturing and fastidious ones.

The real time PCR used in this study amplifies the conserved region 16S ribosomal DNA. The 16S rRNA gene is highly conserved among the Domain Bacteria and different universal probes can be constructed to enumerate complex bacterial populations.

The 16S rRNA is a part of the ribosomal RNA, component of the small prokaryotic ribosomal subunit 30S; it has a structural role, acting as a scaffold defining the positions of the ribosomal protein. It interacts with 23S to promote the binding of the two ribosomal subunits 50S and 30S.

3. Cutimed Sorbact

For many years chronic wounds have been treated with antibiotic therapies. Now it is known that antibiotic treatments have several disadvantages, such as selection for bacterial resistance, inability to penetrate in the wound because of the barrier created by the biofilms

formed by the microorganisms, toxicity and increase in the general costs and time of healing[15,16].

These limitations suggest the need to develop new treatments as a suitable alternative without the issue of the cost and bacterial resistance.

Cutimed Sorbact, produced by BSN Medical GmbH (Hamburg, Germany), is an innovative dressing, coated with DACC (dialkyl-carbamoyl-chloride), a fatty acid derivative which makes the dressing highly hydrophobic.

It is recognised that both aerobes and anaerobes are largely hydrophobic in nature and express cell-surface hydrophobicity. Once in physical contact with the wound bed, and in the presence of moisture, such as wound exudates, bacteria are hydrophobically attracted by DACC and bind to the dressing (Fig. 1), thus reducing the overall concentration of microbes in the wound. The binding starts 10 minutes after contact and reaches a maximum at 2 hours. Moreover, bacteria remain stably bound for several days, with a very low extent of replication.

This unique mechanism of action means that Cutimed Sorbact is a useful dressing for reducing bacterial loads and can be an alternative to silver and other antimicrobials.

There is no risk of bacterial resistance and no limitations of use in the patients.

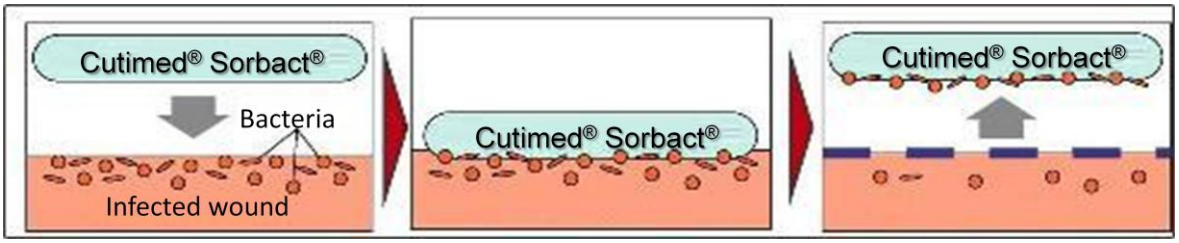

Figure 1: mechanism of action of Cutimed Sorbact.

A hydrophobic dressing is a non-allergic, non-toxic alternative for reducing bacterial load in open wound without enhancing nosocomial spread and can reduce the use of antibiotics. Hydrophobic microorganisms bind to the dressing, preferably in a moist environment, and are removed with it. They multiply to quite a low extent when adsorbed in the dressing, and may not produce extracellular toxins and enzymes[17].

AIM OF THE RESEARCH

Chronic wounds usually occur in patients with predisposing conditions, such as neuropathy, vascular compromission and venous disease, diabetes. They are characterized by the fact that usually do not heal like normal wounds do and persist for long period of time. Chronic wounds are colonized by polymicrobial flora, comprising commensal bacteria normally present in local skin flora and urogenital tract, but also of obligate anaerobic bacteria, that can proliferate in the wound due to the combination of necrotic tissue and low oxygen tension. However, the role of bacteria in the pathogenesis of these lesions is still unclear. Even if all wounds are colonized by bacteria, it is practically impossible to differentiate between colonizing and invading microorganisms. Standard bacteriologic analysis is not always sensitive enough, and not all microorganisms grow in culture conditions. In fact, culturing techniques depend on diagnostic growth conditions, and although anaerobic bacteria often constitute a significant proportion of the total microflora in wounds, their culture is prolonged and more resource demanding. As a consequence, the need of new techniques to assess the total microbial load in wounds is increasing. Therefore, molecular approaches represent a promising alternative to the traditional time-consuming cultivation methods, and have been applied to the study of microbiology of chronic wounds. This work aimed to assess the usefulness of a pan-bacterial quantitative real time PCR reaction to precisely quantitate the total bacterial load in chronic wounds treated with Cutimed Sorbact, a novel therapeutic approach based on hydrophobic binding of bacteria to a membrane, and to correlate the total bacterial burden with the clinical results obtained using this dressing.

A highly conserved region of the bacterial gene 16S, present in all bacteria, was amplified with an universal set of primers and probe. The aim of the study was to verify whether determination of bacterial load could be an useful prognostic parameter to analyse biopsies and swabs derived from patients with chronic ulcers.

MATERIALS AND METHODS

1. Clinical study

A non comparative double-blind pilot study was carried out by the Vascular Disease Center (Ferrara, St. Anna Hospital), guided by Prof. P. Zamboni. Ethical approval was obtained from the Ethical Committee of the University of Ferrara by Prof. P. Zamboni. The aim of the pilot study was to assess the efficacy of a novel antibiotic-free treatment on chronic venous leg ulcers in a 4-week period.

Nineteen patients (for a total of 20 wounds) affected by chronic venous leg ulcers were enrolled in the study and gave written informed consent. Specimens were transported to the laboratory under code to ensure patient's privacy.

Wounds were treated with Cudimed Sorbact (BSN Medical, Hamburg, Germany), an innovative non-antibiotic approach for chronic wound treatment. Cutimed Sorbact is a hydrophobic coated dressing that binds and removes microbes from the wound by hydrophobic interactions.

The dressings were changed twice a week and the study was performed during a 4-week period.

2. Wound sampling

Punch biopsies were taken at the beginning and at the end of the treatment with Cutimed Sorbact, swabs were taken once a week during the dressing change. Tissue is obtained aseptically and is then put into a sterile tube containing 500 μl of sterile phosphate buffered saline (PBS) and transported to the laboratory, where is weighted, homogenised and lysed.

Wound swabbing involves the use of Cutimed dressing to sample superficial wound fluid and tissue debris. Dressings are put into a sterile tube containing 2 ml of sterile PBS and transported to the laboratory.

3. DNA extraction

Biopsy and swab samples were respectively incubated in 2 ml and 3 ml lysis buffer (0,6% SDS, 10 mM Tris, 1 mM EDTA, 120 µg/ml proteinase K) at 37°C overnight.

Then, genomic DNA was extracted by four extractions with an equal volume of phenol: chloroform: isoamyl alcohol (25: 24: 1) mixture, using the Phase Lock Gel 15 ml tubes (Eppendorf). After isopropanol precipitation, DNA was centrifuged, washed with 75% ethanol and resuspended in 100 µl of sterile water. DNA quantity was assessed by optical density reading at 260 nm using a spectrophotometer and by a second reading using the Qubit fluorometer (Invitrogen). Qubit fluorometer is a highly sensitive fluorescence-based quantitation system that uses fluorescent dyes selective for dsDNA, avoiding incorrect reading due to the presence of RNA or proteins.

Purified DNAs were then stored at -20°C until real time PCR analysis.

4. Bacterial strains

Two bacterial strains used in this study were obtained from the American Type Culture Collection (ATCC, USA), including *Bacteroides fragilis* (ATCC 25285) and *Fusobacterium necrophorum* (ATCC 25286). Both strains were cultured in anaerobic condition for 48 or 72 hours at 37° C. The anaerobic conditions were created using the AnaeroGen sachet in the Anaerobic Jar (Oxoid), and assessed by the Anaerobic Indicator.

Both bacteria were grown in CDC Anaerobe Agar with 5% sheep blood plates and in BBL cooked meat medium (Becton-Dickinson).

5. Plasmid constructs

Two plasmids were constructed to have standard curves of *Bacteroides* and *Fusobacterium*. The amplicons containing target regions for real time PCR analysis were produced using qualitative PCR of *B. fragilis* and *F. necrophorum* DNA, and amplified a specific region of the 16S rRNA gene.

Primers sequences are shown in Table 3.

PRIMERS	SEQUENCES	AMPLICONS
B.Frag-Forw B.Frag-Rev	5'- GTCAGTTGCAGTCCAGTGAG -3‘ 5'- GTAACACGTATCCAACCTGC -3'	634 bps
F.Necr-Forw F.Necr-Rev	5'- GAGGTATGGAGACAGTGCTA-3‘ 5'- GACAACTGGTACATCAGAGG -3'	485 bps

SPECIES	CONDITIONS	CYCLES	[$MgCl_2$]
bacteroides	94°C 5min 94°C 30 sec, 63°C 1 min, 72°C 1 min + ext. 3 sec/cycle 72°C 10 min, 4°C >>>	1 35 1	2mM
fusobacterium	94°C 5min 94°C 1min, 60°C 1 min, 72°C 1 min + ext. 3 sec/cycle 72°C 10 min, 4°C >>>	1 35 1	2mM

Table 3: Primer sequences for ligations, and thermal conditions.

PCR products were run on a 1,5% agarose gel to confirm the specificity of the amplifications. Both amplicons were then purified using the QIAquick PCR Purification Kit (Qiagen) and ligated into pCR2.1 vector (Invitrogen, Figure 2) using the TA-cloning kit (Invitrogen). After ligations, the transformation into TOP10F’ competent *E. coli* cells was performed following the manufacturer’s instructions. Blue/white screening of transformants was done on Luria-Bertani agar containing 50 mg/ml ampicillin and top–spread with 20 mg/ml X-Gal solution.

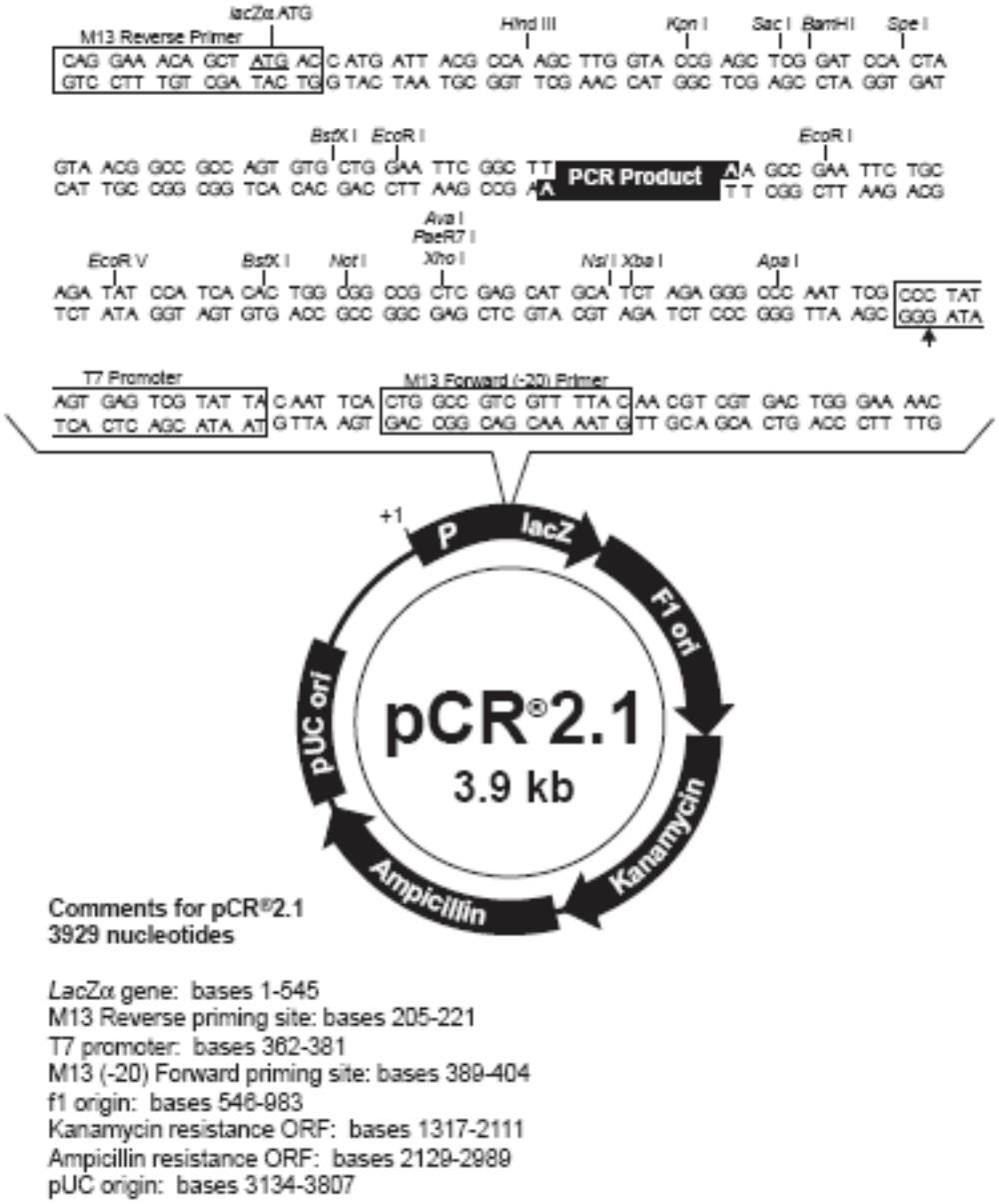

Figure 2: Representation of the pCR2.1 map.

Plasmid DNAs were extracted using the Zyppo Plasmid Miniprep Kit (Zymo Research), and EcoRI digestion to check the validity of cloning was performed.

6. Real time PCR

Real time PCR or quantitative PCR (qPCR) was used to determine either the amount of total bacterial genomes with a panbacterial consensus set of primers and probe, and the amount of *Bacteroides* and *Fusobacterium* genomes with specific reactions.

The reactions were performed using the 7300 Applied Biosystems PCR equipment.

- Eubacterial qPCR:

  The DNA copy numbers were quantified by comparison with a 10 fold serial dilutions of known concentration of *E. coli* (ATCC 10536) genomic DNA. The concentration of the standard DNA was assessed by spectrophotometer and genome copy number was calculated to prepare standard curve (10^7 to 10 copies). Efficiency of the reaction was similarly assessed using standard curves obtained with *S. aureus* (ATCC 25923), *P. aeruginosa* (ATCC 15442), *E. hirae* (ATCC 541), *S. agalactiae* (ATCC 12344) and *B. subtilis* (ATCC 6633) bacterial genomes. The 16S rRNA gene was amplified using TaqMan 5'-FAM-labelled and 3'-TAMRA-labelled probe. The RNAseP eukaryotic gene was amplified using a 5'-VIC-labelled and 3'-non fluorescent (MGB, Applied Biosystems) probe. Primers and probes for panbacterial qPCR were those described by Yang et al, 2002[18], except for modification of the reporter dye.

- *Bacteroides* and *Fusobacterium* qPCR:

  Primer and probe sets for qPCR were designed on the sequence of standard PCR amplification products. The DNA copy numbers were quantified by comparison with a 10 fold serially diluted pCR-bact and pCR-fuso plasmids. The concentration of the standard plasmids was assessed by spectrophotometer and plasmid copy number was calculated to prepare standard curves (10^7 to 10 copies). The targets were amplified using TaqMan 5'-FAM-labelled and 3'-TAMRA-labelled probe. The RNAseP eukaryotic gene was amplified using a 5'-VIC-labelled and 3'-non fluorescent (MGB, Applied Biosystems) probe.

RNAseP gene was simultaneously quantified to calculate the number of eukaryotic cells present in the samples, as an internal positive control to ensure that all samples were suitable for amplification.

Amplifications were carried out in a 50 µl total volume containing 25 µl 2X TaqMan Universal Master Mix (Applied Biosystems), 2,5 µl of primers and probes mix, 2,5 µl of 20X RNAseP mix and 20 µl template corresponding to 100 ng total DNA.

Sequences of primers and probes used are shown in Table 4. Concentrations were 900 nM of each primer, 100 nM each probe and 1X RNAseP.

The reaction condition for all template were: 10 minutes at 95°C for enzyme activation, 10 cycles with 15 seconds at 95°C for DNA denaturation and 60 seconds at 60°C for annealing and extension. Fluorescence data were collected in the primers elongation step at 60°C.

All samples were amplified in duplicate, and the average value was calculated.

GENES	PRIMERS & PROBES	SEQUENCES
16S rRNA*	UNI-Forward	5'-TGGAGCATGTGGTTTAATTCGA -3'
	UNI-Reverse	5'-TGCGGGACTTAACCCAACA -3'
	UNI-Probe	5'-(6Fam) CACGAGCTGACGACARCCATGCA (Tamra)-3'
Fusbacterium 23S rRNA	Fn-Q-Forward	5'- CCGCGCATTCCGTATGG-3'
	Fn-Q-Reverse	5'- CGGGTAGGATCAGCCTGTTATC -3'
	Fnecr-Probe	5'-(6Fam) TCGTCGCTCAACGGATAAAAGCTACCCT (Tamra)-3'
Bacteroides	BFr-Q-Forward	5'- TTCAGGCTAGCGCCCATT -3'
	BFr-Q-Reverse	5'- GGAACTGAGACACGGTCCAAAC-3'
	BFrag-Probe	5'-(6Fam) CCAATATTCCTCACTGCTGCCTCCCGTA (Tamra)-3'
RNAseP**	Endogenous reference for multiplex reactions	Pre-designed primers and VIC-labelled probe mix

Table 4: Oligonucleotide sequences of primers and probes used in the study.

* primer and probe set was taken from literature and used in our laboratory after modification of the reporter dye. (Yang et al, 2002)[18].

** RNAseP mix is optimized by Applied Biosystems.

7. Isolation of **Staphylococcus** *and* **Pseudomonas** *spp by culture methods*

Classic cultures were performed by Prof. P.G. Balboni (University of Ferrara).

Briefly, 1/10 volume of biopsies and swabs were plated in selective agar for the growth of *Staphylococcus* and *Pseudomonas* species. Detection of staphylococci was performed on Mannitol Salt agar plates (Oxoid), and *Pseudomonas* spp were selected on Cetrimide agar plates (Oxoid). After 24 and 48 (respectively) hours incubation at 37°C, the number of colony forming units (CFU) of each microorganism was counted for each plate.

8. Statistical analysis

Statistical analysis was performed by non-parametrical Mann-Whitney test, used for assessing whether two independent samples of observations come from the same population.

RESULTS

1. Sensitivity of eubacterial real time PCR

To assess the sensitivity of qPCR, the primers and probe for eubacterial detection were checked on standard curves obtained with different bacterial DNAs.

DNA was extracted as described in Material and Methods from:

- *E. coli* (gram negative)
- *S. aureus* (gram positive)
- *P. aeruginosa* (gram negative)
- *E. hirae* (gram positive)
- *S. agalactiae* (gram positive)
- *B. subtilis* (gram positive)

As negative controls, DNA extract from *C. albicans* (mycete, ATCC 10231) and from Jurkat cells (eukaryote) were used.

To assess the sensitivity of the broad range real time PCR, serial dilutions from 10^7 to 100 molecules of bacterial DNA were used in the reactions.

Fig. 3 shows the results of two representative standard curves obtained from purified DNA of *E. coli* and *B. subtilis*. All 6 bacterial species at each concentration tested were correctly amplified and detected (data not shown). The linear range of amplification was consistent regardless of the number of target molecules present in the amplification reaction.

DNA extracted from bacterial cultures was carefully quantified by spectrophotometric analysis and by Qubit fluorometer (Invitrogen).

Quantification was reliable starting from 100 up to 10^7 target DNA molecules. All different bacterial DNAs were amplified with the same efficiency. Negative controls failed to be amplified by qPCR, being detected over the 39^{th} amplification cycle (Ct, threshold of detectability).

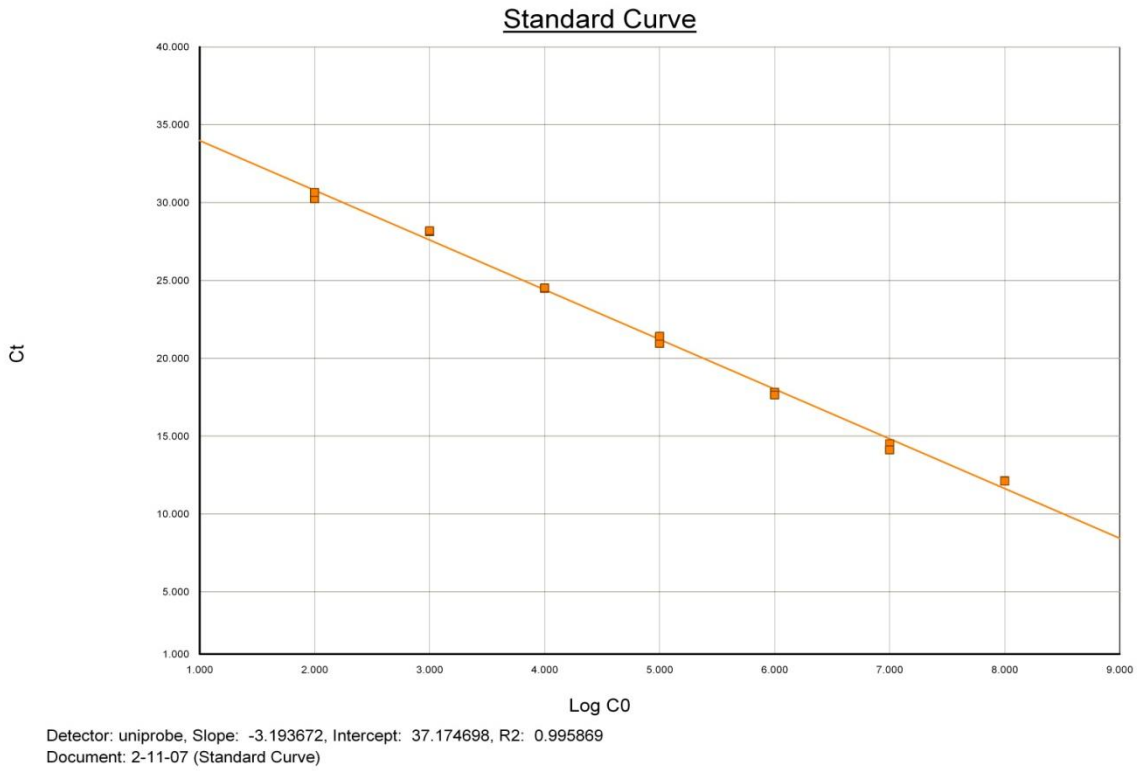

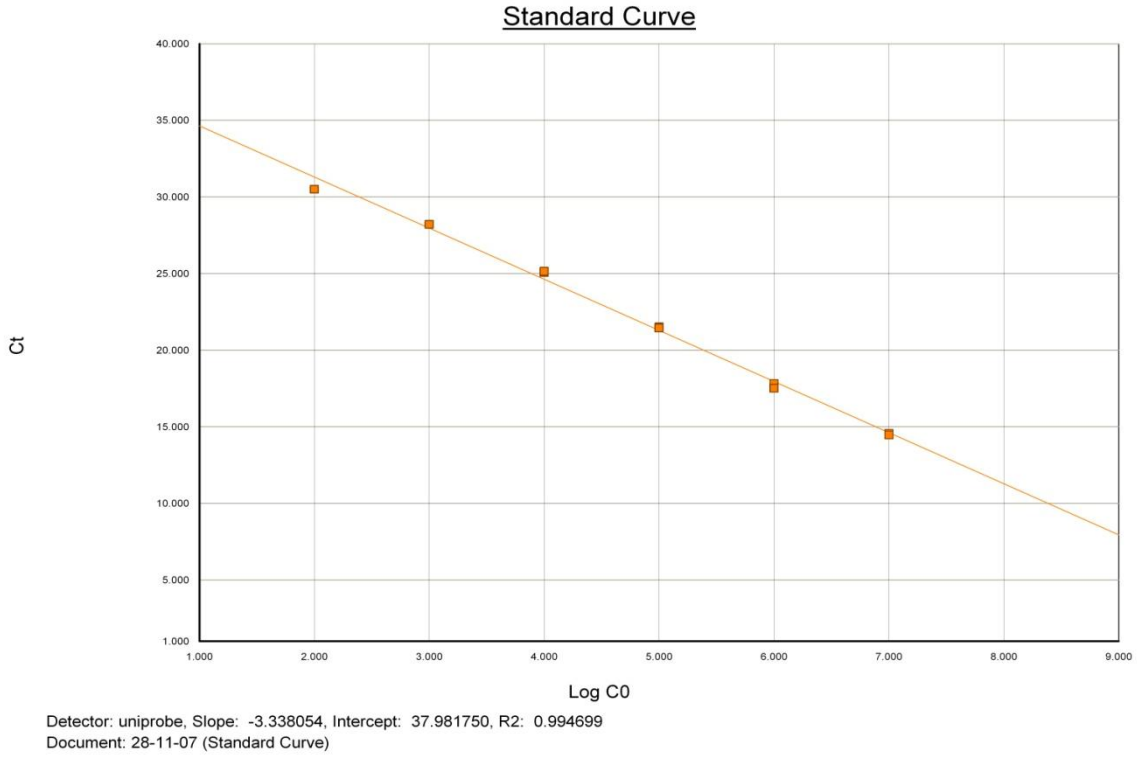

Figure 3: Representative standard curves obtained from purified DNA of *B.subtilis* and *E.coli.* The slopes (-3,19 and -3,33 respectively) obtained are in the linearity range required for correct quantification.

2. Clinical results

Clinical data were assessed by the medical team of Prof. P. Zamboni (Vascular Disease Center, University of Ferrara). In particular, the area affected by chronic lesion was measured at the time of first biopsy, and once a week, until the end of the study period, and the data were transferred to our laboratory under code, to protect the patient's privacy.

Treatment with Cutimed Sorbact resulted in a significant clinical outcome in 75% of wounds, defining a positive outcome when the affected area was reduced by 20% or more.

3. Total bacterial load in chronic wounds.

The total load of the bacterial DNA was quantified from biopsies and swabs of 20 chronic wounds. Swabs from 6 healthy skins were used as controls.

Quantification of total bacterial load was assessed by comparison to the standard curve obtained by 10-fold serially diluted purified DNA of *E. coli*.

In the case of biopsies, all reactions were performed on 100 ng of total DNA, simultaneously amplifying the highly conserved bacterial 16S rRNA gene and the eukaryotic RNAseP gene, used as internal control to assess that all the samples were suitable for amplification.

In the case of swabs, reactions were performed on 100 ng of total extracted DNA amplifying the bacterial 16S rRNA gene, and then the results were normalized to the total volume of extraction buffer where swabs were initially soaked.

The mean of the bacterial load in normal healthy skin was $4,5\text{^}10^5$ bacteria per swab, that represent the normal flora colonising our skin.

Figure 4 shows the total bacterial load of swabs and biopsies and the difference of the wound's area (clinical data) for each patient (enumerated 1 to 20) during 4 weeks of treatment with Cutimed Sorbact.

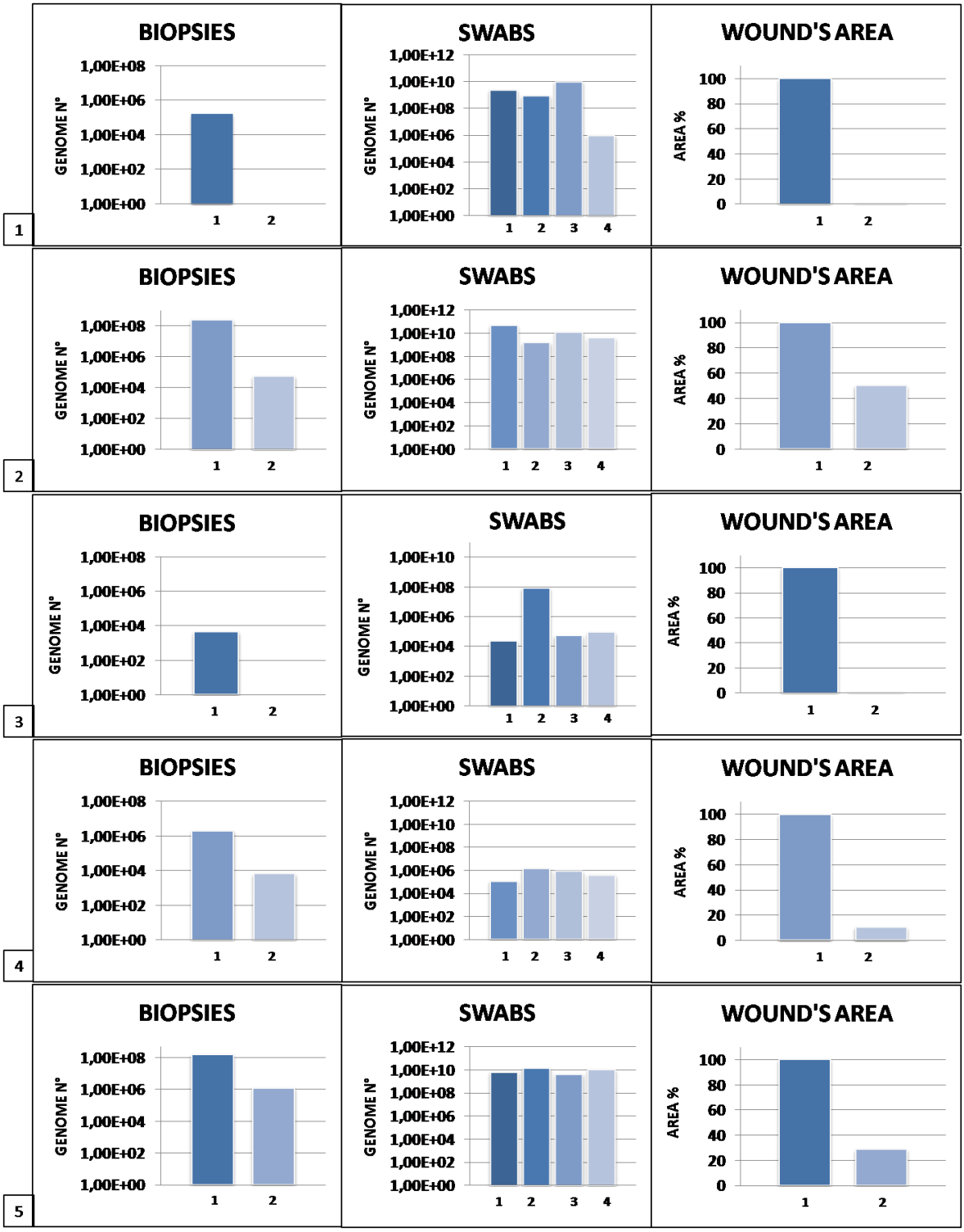
1
BIOPSIES
GENOME N°
1,00E+08
1,00E+06
1,00E+04
1,00E+02
1,00E+00
1 2
SWABS
GENOME N°
1,00E+12
1,00E+10
1,00E+08
1,00E+06
1,00E+04
1,00E+02
1,00E+00
1 2 3 4
WOUND'S AREA
AREA %
100
80
60
40
20
0
1 2
2
BIOPSIES
GENOME N°
1,00E+08
1,00E+06
1,00E+04
1,00E+02
1,00E+00
1 2
SWABS
GENOME N°
1,00E+12
1,00E+10
1,00E+08
1,00E+06
1,00E+04
1,00E+02
1,00E+00
1 2 3 4
WOUND'S AREA
AREA %
100
80
60
40
20
0
1 2
3
BIOPSIES
GENOME N°
1,00E+08
1,00E+06
1,00E+04
1,00E+02
1,00E+00
1 2
SWABS
GENOME N°
1,00E+10
1,00E+08
1,00E+06
1,00E+04
1,00E+02
1,00E+00
1 2 3 4
WOUND'S AREA
AREA %
100
80
60
40
20
0
1 2
4
BIOPSIES
GENOME N°
1,00E+08
1,00E+06
1,00E+04
1,00E+02
1,00E+00
1 2
SWABS
GENOME N°
1,00E+12
1,00E+10
1,00E+08
1,00E+06
1,00E+04
1,00E+02
1,00E+00
1 2 3 4
WOUND'S AREA
AREA %
100
80
60
40
20
0
1 2
5
BIOPSIES
GENOME N°
1,00E+08
1,00E+06
1,00E+04
1,00E+02
1,00E+00
1 2
SWABS
GENOME N°
1,00E+12
1,00E+10
1,00E+08
1,00E+06
1,00E+04
1,00E+02
1,00E+00
1 2 3 4
WOUND'S AREA
AREA %
100
80
60
40
20
0
1 2

6

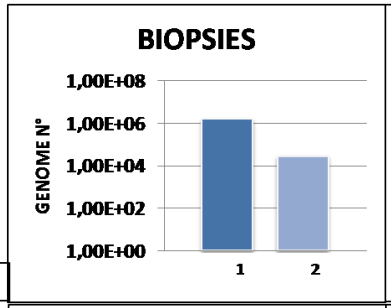
BIOPSIES
GENOME N°
1,00E+08
1,00E+06
1,00E+04
1,00E+02
1,00E+00
1
2

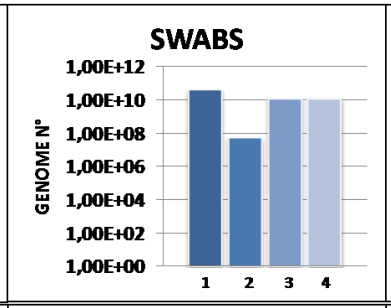
SWABS
GENOME N°
1,00E+12
1,00E+10
1,00E+08
1,00E+06
1,00E+04
1,00E+02
1,00E+00
1
2
3
4

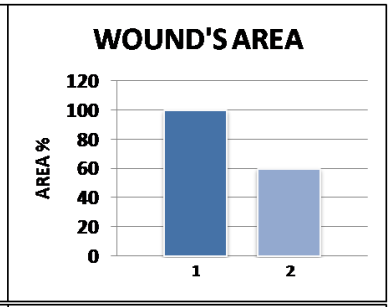
WOUND'S AREA
AREA %
120
100
80
60
40
20
0
1
2

7

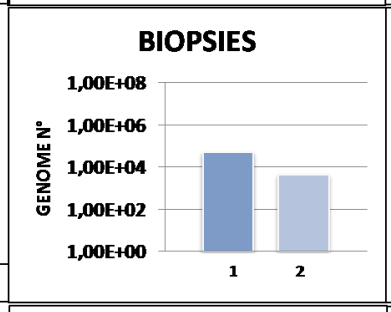
BIOPSIES
GENOME N°
1,00E+08
1,00E+06
1,00E+04
1,00E+02
1,00E+00
1
2

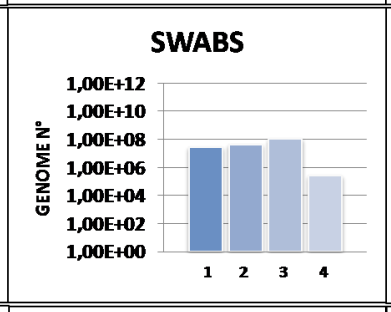
SWABS
GENOME N°
1,00E+12
1,00E+10
1,00E+08
1,00E+06
1,00E+04
1,00E+02
1,00E+00
1
2
3
4

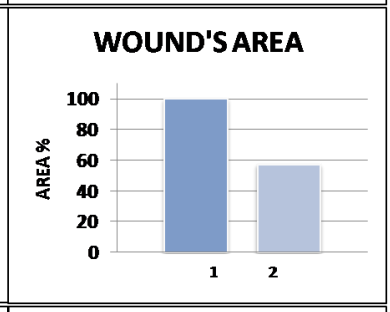
WOUND'S AREA
AREA %
100
80
60
40
20
0
1
2

8

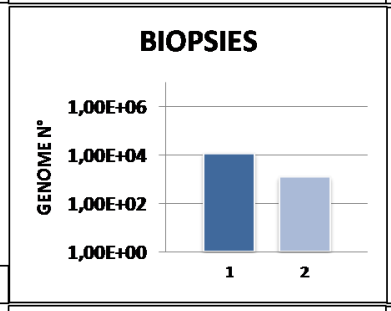
BIOPSIES
GENOME N°
1,00E+06
1,00E+04
1,00E+02
1,00E+00
1
2

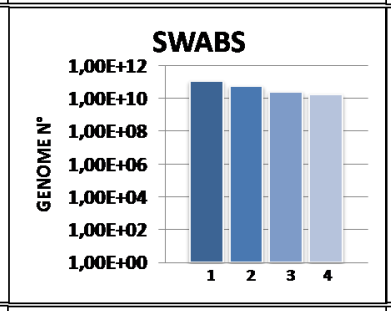
SWABS
GENOME N°
1,00E+12
1,00E+10
1,00E+08
1,00E+06
1,00E+04
1,00E+02
1,00E+00
1
2
3
4

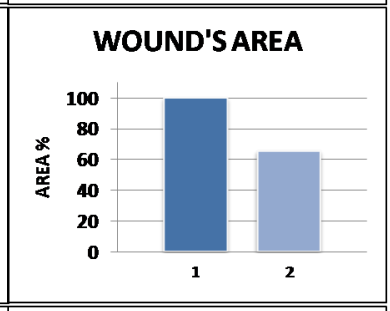
WOUND'S AREA
AREA %
100
80
60
40
20
0
1
2

9

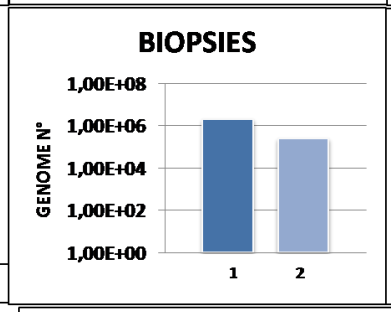
BIOPSIES
GENOME N°
1,00E+08
1,00E+06
1,00E+04
1,00E+02
1,00E+00
1
2

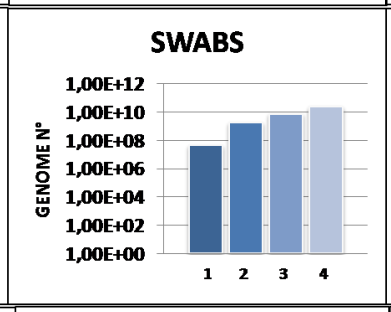
SWABS
GENOME N°
1,00E+12
1,00E+10
1,00E+08
1,00E+06
1,00E+04
1,00E+02
1,00E+00
1
2
3
4

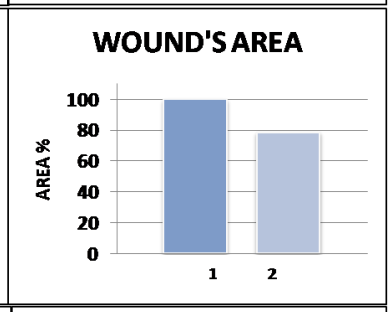
WOUND'S AREA
AREA %
100
80
60
40
20
0
1
2

10

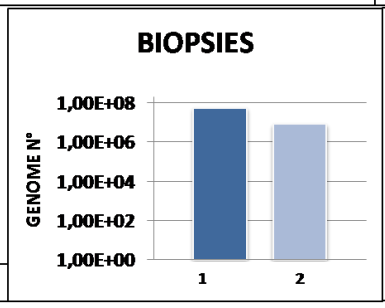
BIOPSIES
GENOME N°
1,00E+08
1,00E+06
1,00E+04
1,00E+02
1,00E+00
1
2

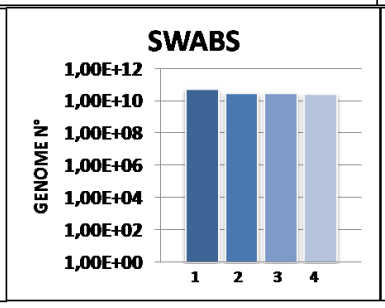
SWABS
GENOME N°
1,00E+12
1,00E+10
1,00E+08
1,00E+06
1,00E+04
1,00E+02
1,00E+00
1
2
3
4

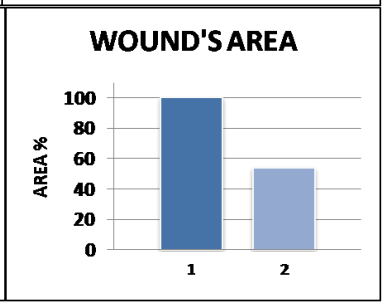
WOUND'S AREA
AREA %
100
80
60
40
20
0
1
2

11

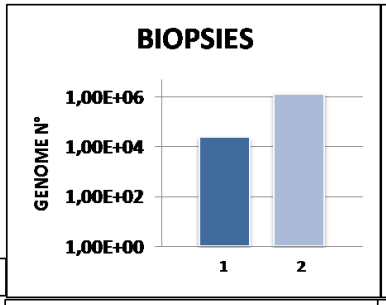
BIOPSIES
GENOME N°
1,00E+06
1,00E+04
1,00E+02
1,00E+00
1
2

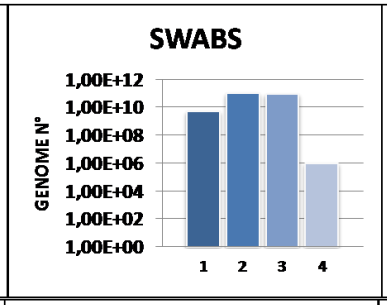
SWABS
GENOME N°
1,00E+12
1,00E+10
1,00E+08
1,00E+06
1,00E+04
1,00E+02
1,00E+00
1
2
3
4

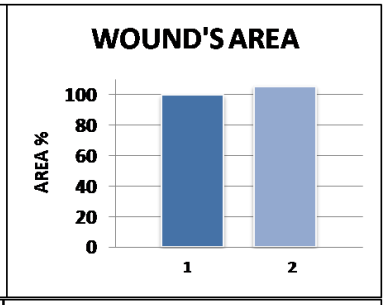
WOUND'S AREA
AREA %
100
80
60
40
20
0
1
2

12

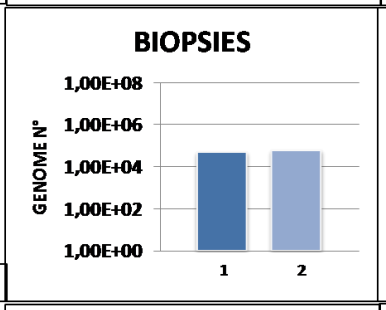
BIOPSIES
GENOME N°
1,00E+08
1,00E+06
1,00E+04
1,00E+02
1,00E+00
1
2

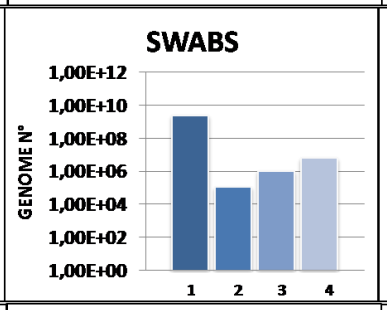
SWABS
GENOME N°
1,00E+12
1,00E+10
1,00E+08
1,00E+06
1,00E+04
1,00E+02
1,00E+00
1
2
3
4

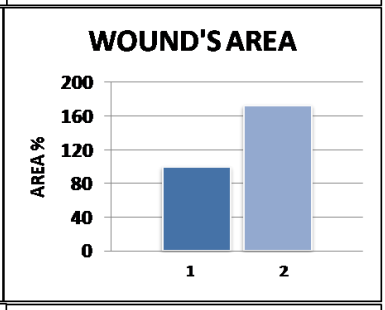
WOUND'S AREA
AREA %
200
160
120
80
40
0
1
2

13

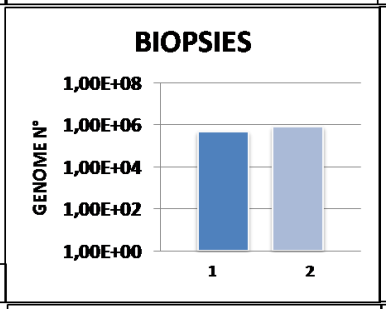
BIOPSIES
GENOME N°
1,00E+08
1,00E+06
1,00E+04
1,00E+02
1,00E+00
1
2

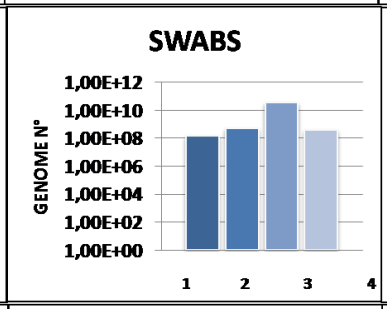
SWABS
GENOME N°
1,00E+12
1,00E+10
1,00E+08
1,00E+06
1,00E+04
1,00E+02
1,00E+00
1
2
3
4

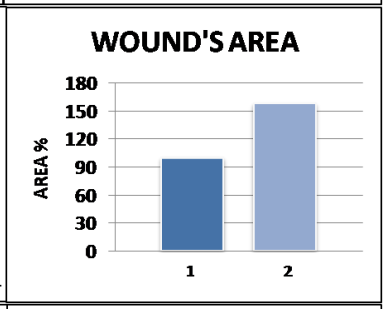
WOUND'S AREA
AREA %
180
150
120
90
60
30
0
1
2

14

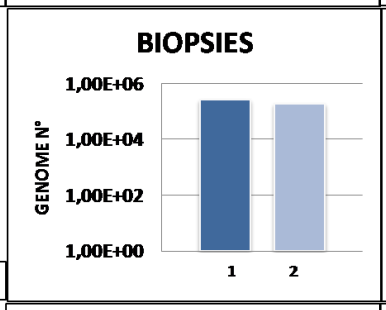
BIOPSIES
GENOME N°
1,00E+06
1,00E+04
1,00E+02
1,00E+00
1
2

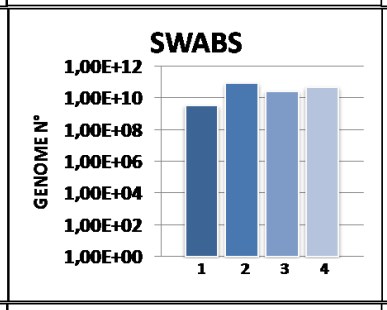
SWABS
GENOME N°
1,00E+12
1,00E+10
1,00E+08
1,00E+06
1,00E+04
1,00E+02
1,00E+00
1
2
3
4

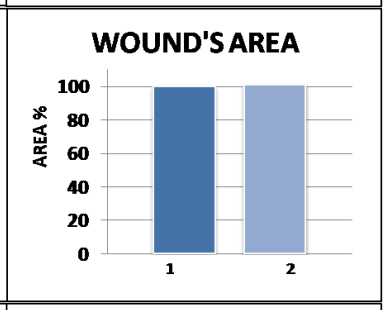
WOUND'S AREA
AREA %
100
80
60
40
20
0
1
2

15

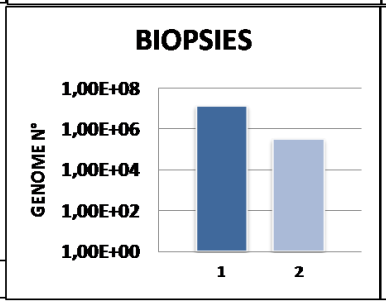
BIOPSIES
GENOME N°
1,00E+08
1,00E+06
1,00E+04
1,00E+02
1,00E+00
1
2

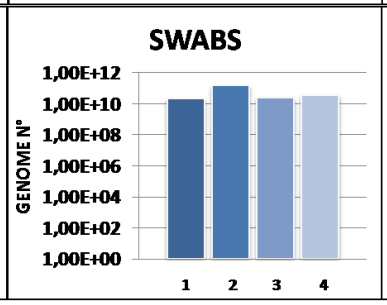
SWABS
GENOME N°
1,00E+12
1,00E+10
1,00E+08
1,00E+06
1,00E+04
1,00E+02
1,00E+00
1
2
3
4

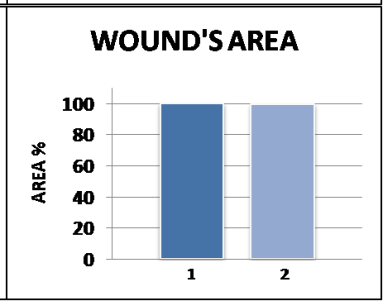
WOUND'S AREA
AREA %
100
80
60
40
20
0
1
2

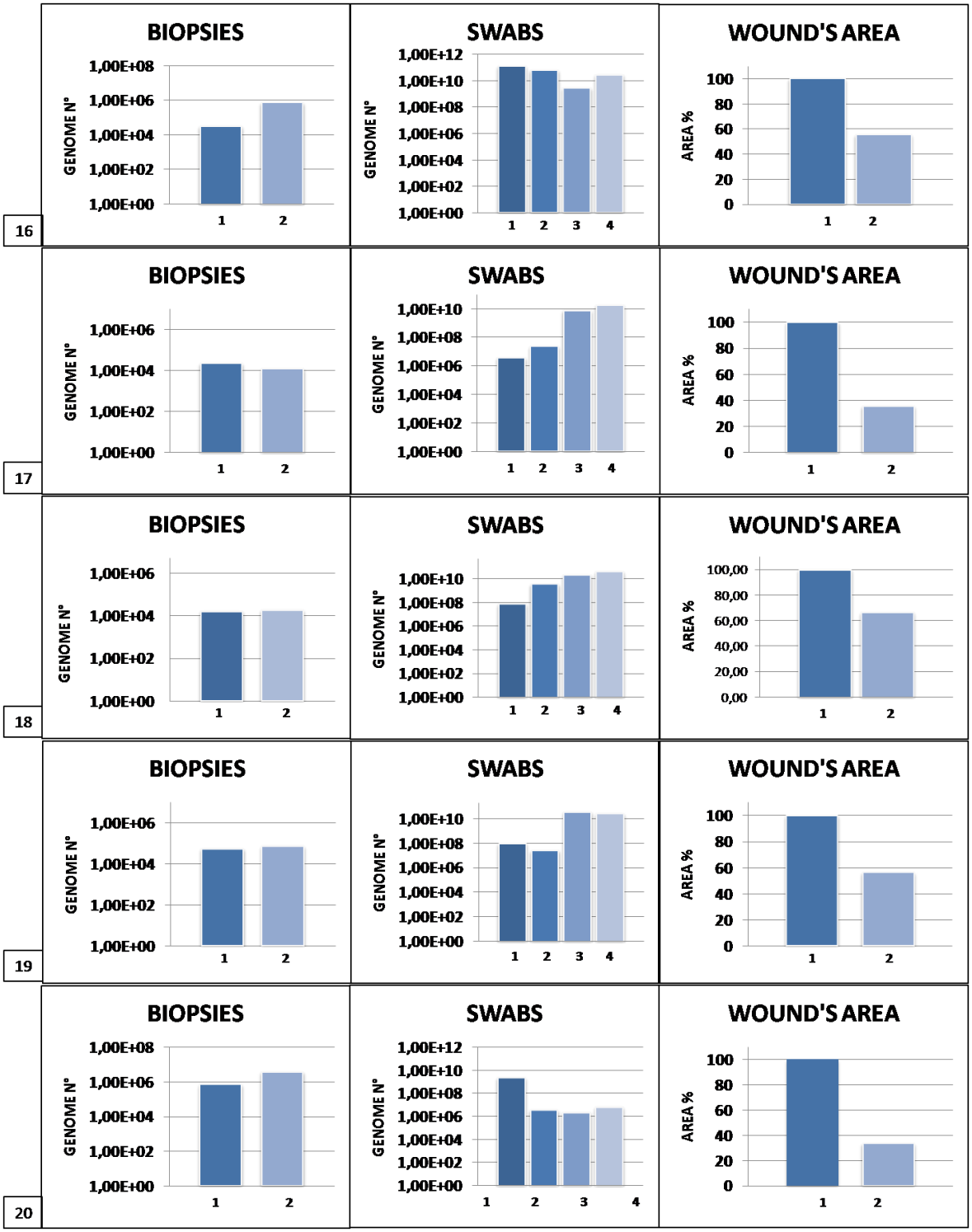

Figure 4: Summary of the results obtained for each patient. Numbers 1-20 represent patients. The first column of plots shows the total bacterial load of the first and the last biopsy; bacterial load is expresses by number of genomes detected per mg of tissue. The second column of plots shows the total bacterial load of the four swabs collected during the four weeks of treatment. The third column of plots represents the area of the wound (%) at the time of first and last biopsy, where the first measurement is assumed as 100%.

We evaluated the correlation between the molecular data obtained by real time PCR and the clinical data, in particular considering the area of the wound. The results allowed to divide the samples into 3 groups.

1. *Clinical positive results concordant with molecular data:*

   The first group is constituted by samples where the positive clinical outcome is concordant with molecular data. In particular, 10/15 wounds (66%) with a positive clinical outcome, with 58% mean reduction of the wound's area, showed a significant decreases of the total bacterial load. The initial bacterial load was considerably different in the samples, ranging from $4{,}38\text{^}10^3$ to $2{,}44\text{^}10^8$ bacterial genomes/mg of tissue. Nevertheless, the average of the total bacterial load at the beginning of treatment was $4{,}41\text{^}10^7$/mg of tissue, and at the end decreased to $1{,}73\text{^}10^5$/mg of tissue, corresponding to a 254-fold decrease of the total bacterial load (Fig. 5). The decrease of bacterial load was statistically significant (p=0,0243).

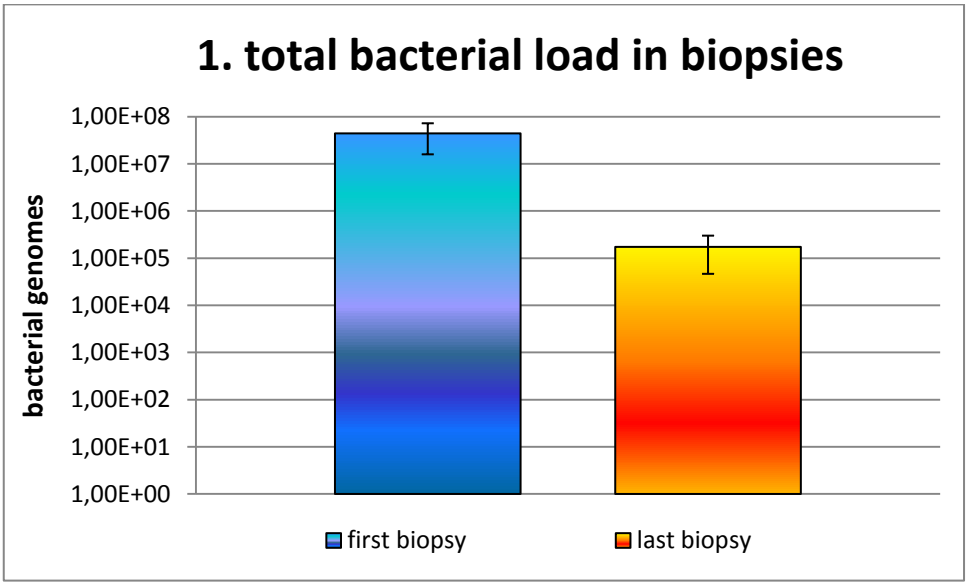

Figure 5: Total bacterial load of biopsies with concordant clinical and molecular results; p=0,0243. Bars represent standard errors.

Swabs of the same wounds were also considered. Swabs were collected once a week for 4 weeks. 100 ng of DNA extracted from swabs was amplified by real time PCR. In this case there was less variability among samples from different patients, and the majority of specimens yielded over 10^6 total bacteria in the first point. Analysis of the bacterial load in the course of clinical study failed to show any significant decrease. In fact, in spite of clinical positive outcome, the bacterial load remained constant, ranging from $2{,}63\text{^}10^{10}$ in the first samples to $9{,}37\text{^}10^9$ bacterial genomes/swab in the final samples (Fig. 6).

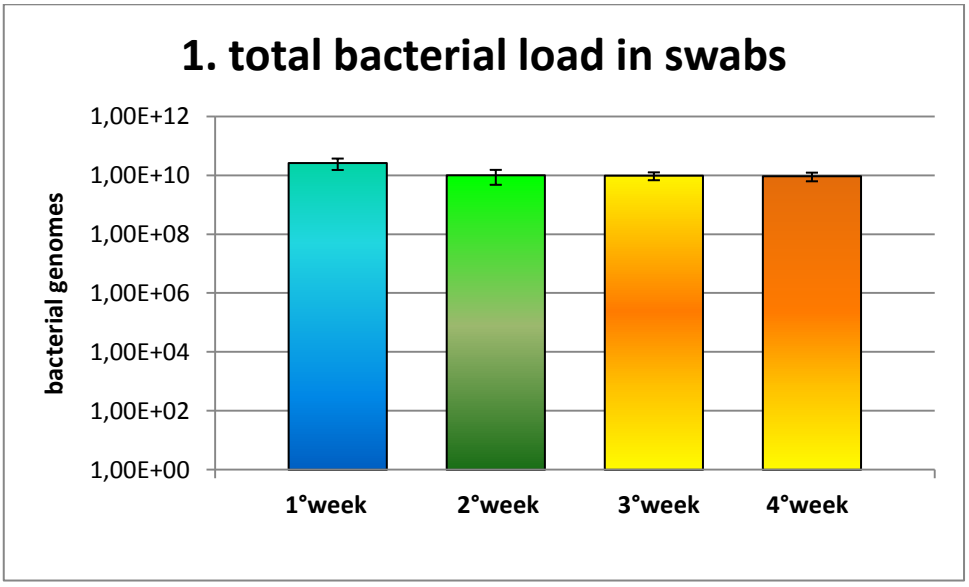

Figure 6: Total bacterial load of swabs representing the positive outcome of wounds (correlation between molecular and clinical data).

2. *Clinical negative results concordant with molecular data*

The second group is constituted by five chronic wounds that showed a negative clinical course, with no response to treatment, and averaged a 27% increase of the area.

The total bacterial load of biopsies of these five wounds showed a non-significant 5,2-fold decrease at the end of the treatment (2,73^10^6 to 5,22^10^5 bacterial genomes / mg of tissue; p=0,6)(Fig. 7).

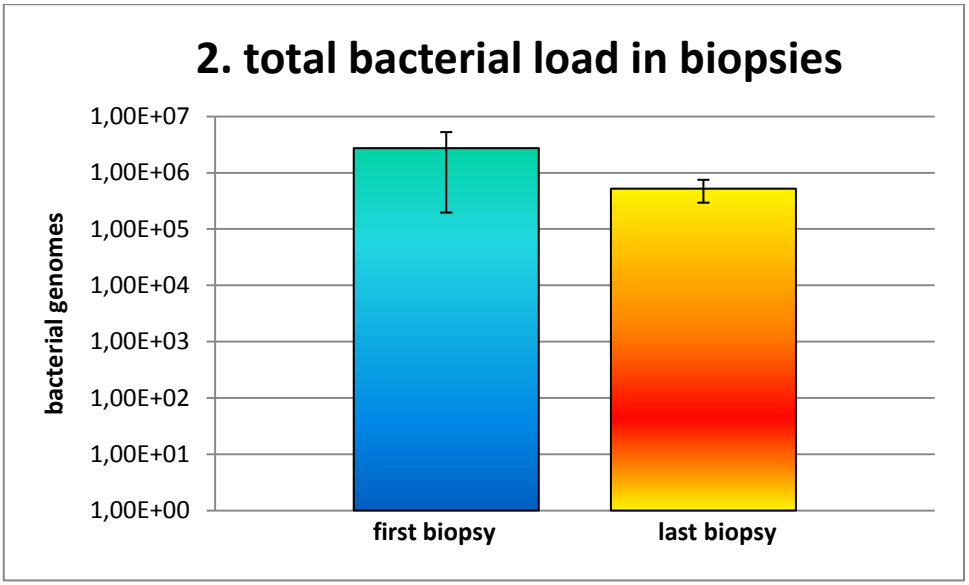

Figure 7: Total bacterial load in biopsies that did not have a positive clinical result (correlation between molecular and clinical data); p=0,6.

The swabs from these five wounds did not show any significant change in bacterial load, ranging from 6,50^10^9 to 1,71^10^{10} bacterial genomes/swab along the 4-weeks period of the study (Fig. 8).

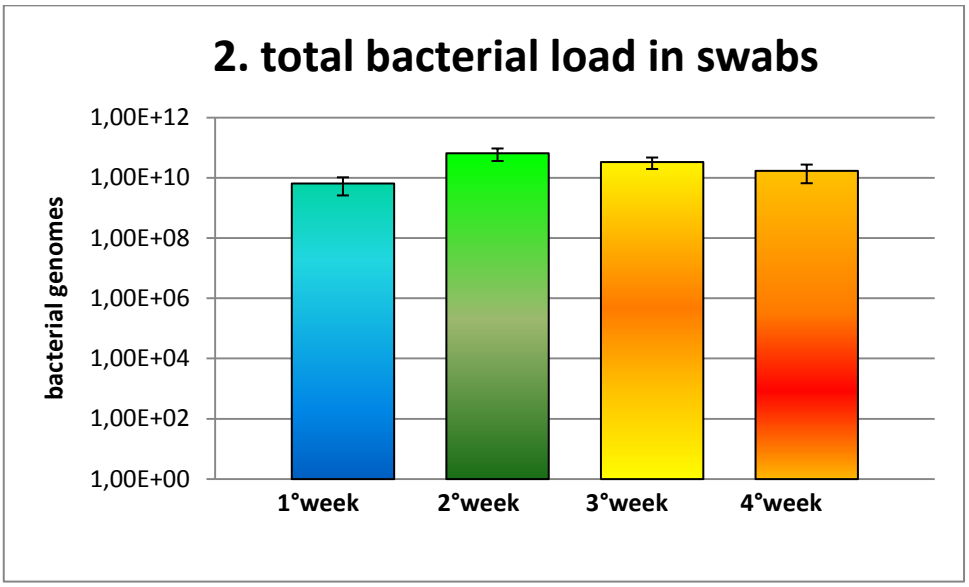

Figure 8: Total bacterial load of swabs representative for the negative outcome of wounds (correlation between molecular and clinical data).

3. Clinical positive results not correlating with molecular data

The last group of samples is represented by 5 chronic wounds that had a positive clinical outcome, with an average 50% decrease of the affected area, but there was no reduction of total bacterial load in biopsies. In fact, a slight, non significant 5,3-fold reduction was recorded (p=0,75)(Fig. 9).

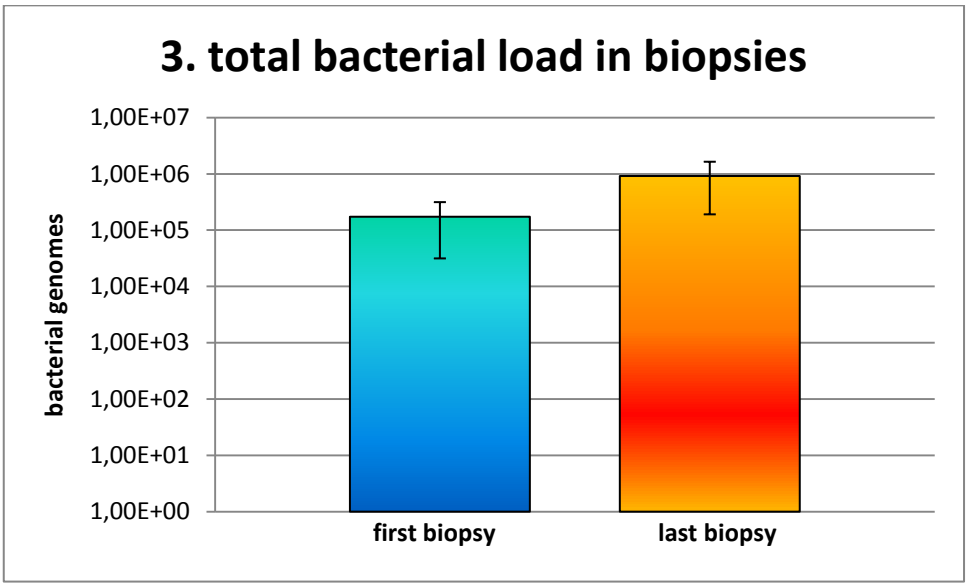

Figure 9: Total bacterial load in biopsies with discordant results between molecular and clinical data (positive clinical outcome and no reduction of bacterial load); p=0,75.

Similarly, the total bacterial load in swabs remained unchanged until the end of the treatment, at high levels of about 10^{10} bacterial genomes per swab (Fig. 10).

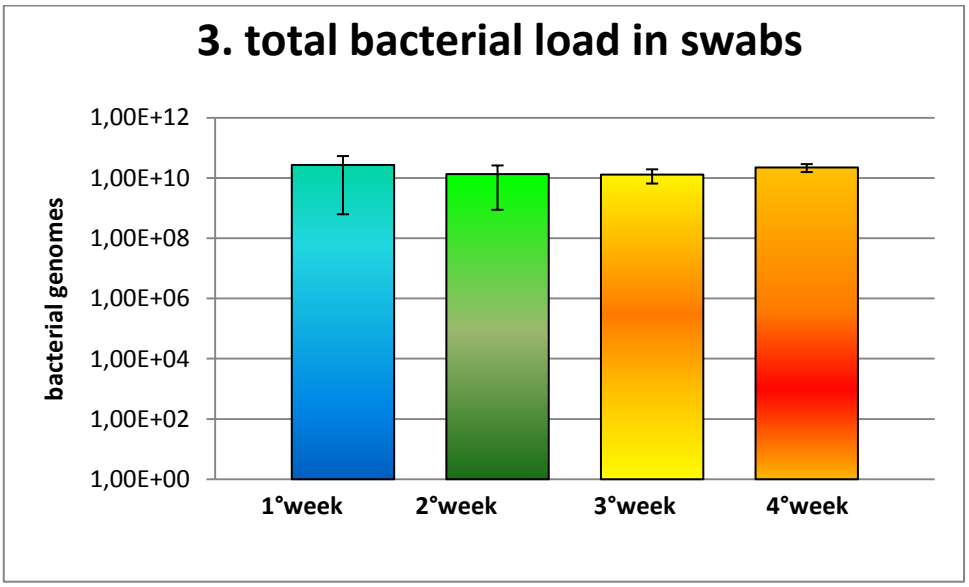

Figure 10: Total bacterial load in swabs representing the discordant results between molecular and clinical data.

4. Real time PCR sensitivity of anaerobic bacteria.

To quantify the bacterial load of two anaerobes frequently detected in chronic wounds, we used primers and probes specific for *Fusobacterium* and *Bacteroides* species. To test the sensitivity of reaction, and to build the standard curve, genomic DNA and pCR2.1 plasmids containing the amplified region of *Fusobacterium* and *Bacteroides* were serially diluted, and both reactions were sensitive enough to detect as few as 100 total genomes. No cross-reaction between primer and probe sets was observed, and no amplification of eukaryotic cell DNA and other bacterial DNA was present using these sets of primers. As shown in Figs 11 and 12, the linear range of amplification was achieved from 10^3 to 10^7 total molecules.

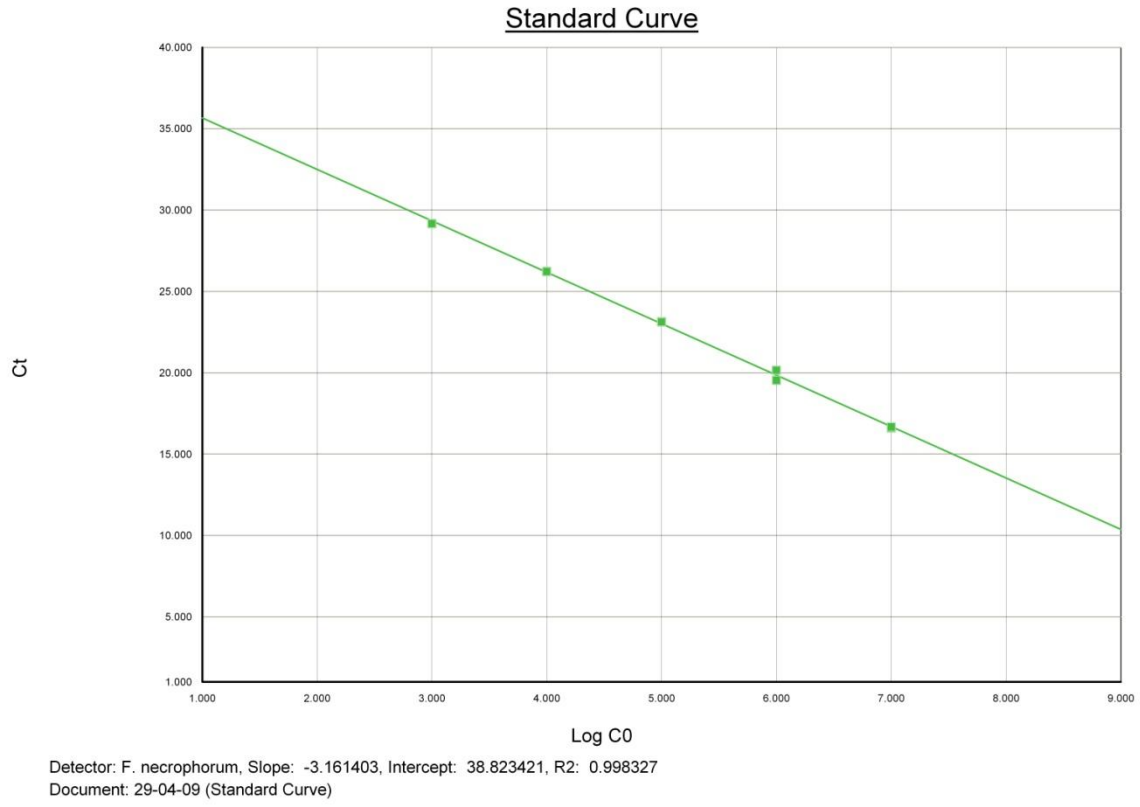

Figure 11: Representative standard curve of the real time PCR for the detection of *F. necrophorum*. 10-fold serially diluted DNA was obtained with the pCR-Fuso plasmid.

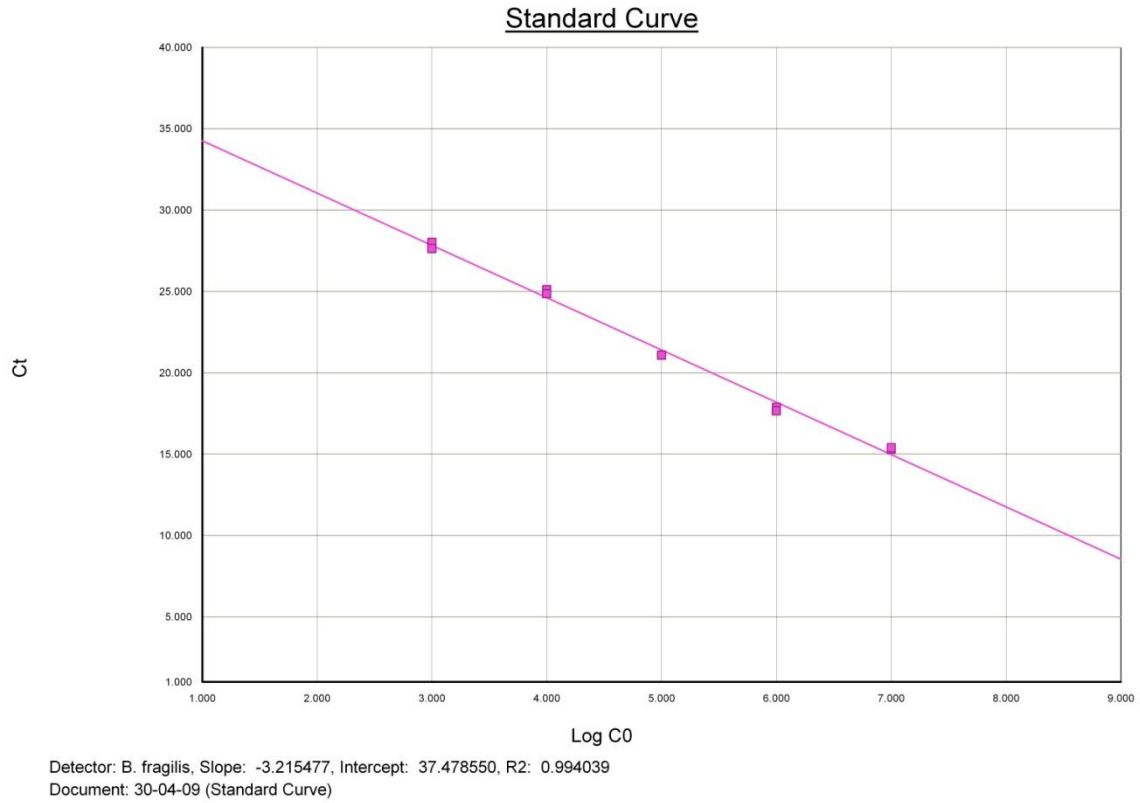

Figure 12: Representative standard curve of the real time PCR for the detection of *B. fragilis*. 10-fold serially diluted DNA was obtained with the pCR-Bact plasmid.

5. Quantification of anaerobes in chronic wounds.

- *Bacteroides* spp:

Bacteroides genomes were quantified in DNA extracted from biopsies.

The amount of DNA used was the same utilised in the eubacterial qPCR reactions (100 ng). Simultaneously, RNAseP gene was quantify to calculate the number of eukaryotic cells present in each specimen (internal control).

Bacteroides genomes were found in 10/20 (50%) of the wounds. The anaerobe's load showed a 197–fold decrease after treatment with Cutimed Sorbact, indicating that the dressing is also able to bind the anaerobic bacteria, but there was no statistical difference between the first and last biopsy (p=0,1)(Fig. 13).

More specifically, *Bacteroides* DNA was present in 6 wounds belonging to the first group of samples (positive correlation between total bacterial load and clinical outcome), in 3 wounds of the second group (absence of positive clinical result) and in one wound of the third group of samples (positive clinical result with no decrease in total bacterial load).

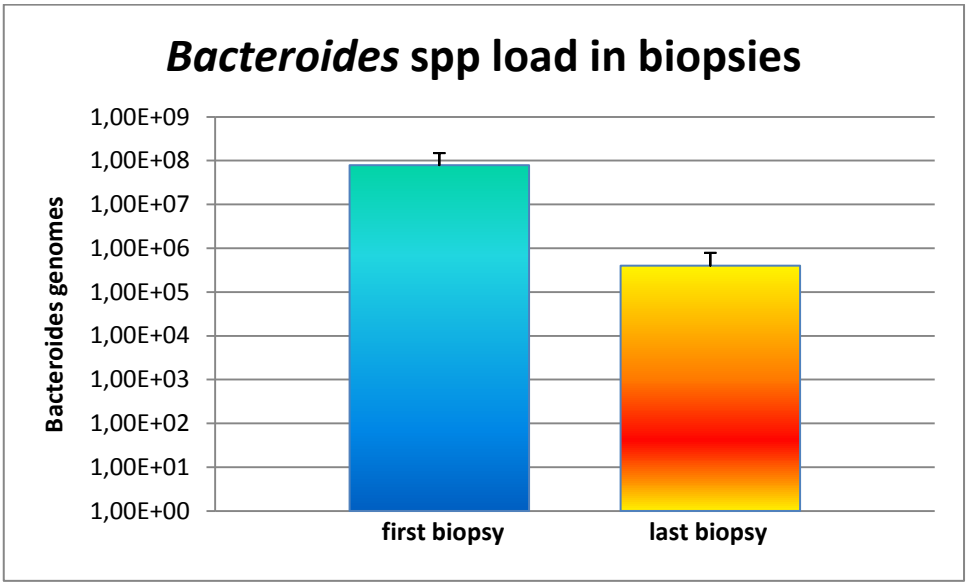

Figure 13: *Bacteroides* genome number present in 10/20 biopsies (p=0,1).

- *Fusobacterium* spp*:*

Fusobacterium genomes were quantified by qPCR in biopsies.

The amount of DNA used was the same utilised in the eubacterial qPCR reactions (100 ng). Simultaneously, RNAseP gene was quantified to calculate the number of eukaryotic cells present in specimens.

Fusobacterium species genomes were found in 10% of the wounds (2 patients), and the load showed a non significant 3,5–fold decrease after treatment with Cutimed Sorbact. The *Fusobacterium* genome number ranged from $1,7\text{^}10^4$ to $4,9\text{^}10^3$ genomes/mg of tissue (Fig. 14).

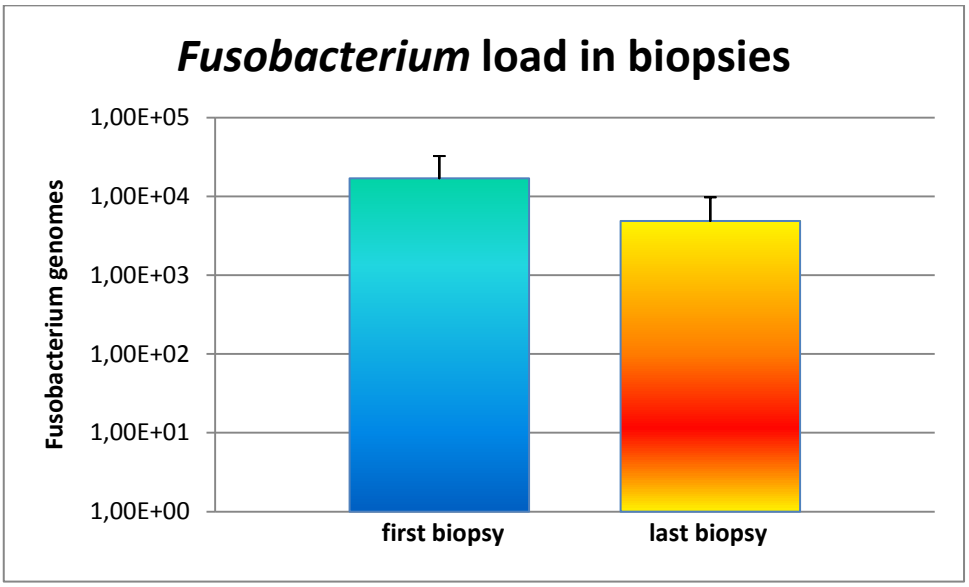

Figure 14: *Fusobacterium* genome number present in 2/20 biopsies.

6. Classic microbiologic culture results

Biopsies were also analysed by classical culture methods by plating on selective agar for the detection of *Staphylococcus* spp and *Pseudomonas* spp. The colony count in the normal healthy skin was under 100 CFU, thus, in wounds, we considered positive values over 100 CFU.

The results are summarized in Table 5, where the data obtained by culture are shown with the clinical and molecular data.

The results show that data from culture methods do not correlate with results from qPCR or with clinical ones.

For example, patient 1 had a complete clinical recovery, with a marked decrease of bacterial load by qPCR, in complete absence of *Staphylococcus* and *Pseudomonas spp* in both biopsies. By contrast, patient 2 had a significant clinical outcome and a corresponding decrease of bacterial load, with the presence of *Staphylococcus* and *Pseudomonas spp* both in the first and in the last biopsy.

			STAPHYLOCOCCUS		PSEUDOMONAS	
PATIENTS	Δ AREA (%)	Δ BACTERIAL LOAD (N°FOLD)	FIRST BIOPSY	LAST BIOPSY	FIRST BIOPSY	LAST BIOPSY
1	-100	-158000	-	-	-	-
2	-50	-4535	+	+	+	+
3	-100	-4380	-	-	-	-
4	-90	-313	-	-	-	-
5	-71,4	-120	+	-	-	-
6	-40	-58,2	+	-	-	-
7	-42,6	-11,7	+	-	-	-
8	-34,6	-12,6	-	-	-	-
9	-21,3	-8,2	-	-	-	+
10	-46,3	-6,1	+	+	-	-
11	+5,8	+56	+	+	-	-
12	+72,7	+1,2	-	-	-	-
13	+58,3	+1,7	+	+	-	-
14	-0,5	-42,7	-	-	+	-
15	+1,1	-1,4	-	-	-	-
16	-44,7	+22,4	+	+	+	+
17	-64,3	-1,8	+	-	-	-
18	-33,3	+1,1	+	-	-	-
19	-43,8	+1,3	+	+	-	-
20	-66,7	+5,1	-	+	-	-

Table 5: Grouping of clinical, molecular and microbiologic results. Area is expressed as percentage difference and bacterial load as fold difference. *Staphylococcus* and *Pseudomonas spp* are represented as positive where CFU exceed 100 units, and negative where CFU are below 100 units.

DISCUSSION

The impact of microorganisms on chronic wounds has been extensively studied using different approaches, aiming especially to elucidate their possible role in the lack of healing (reviewed by Howell-Jones et al, 2005)[19]. Often, it is difficult to compare studies, because of different methods of specimen collection and, especially, different methods of bacteriological analysis. A further complication is represented by the nature of infected chronic wounds, which present a polymicrobial population, with a complex ecology[20]. Studies performed by standard bacteriological techniques have shown that the mean number of bacterial species per wound ranges from 1.6 to 5.4[10,19], and that also wounds with no clinical sign of infection contain more than one bacterial species[21]. Therefore, even if several studies have described some bacteria as being the prevalent microorganism in chronic wounds, such as *Staphylococcus aureus*[22], *Pseudomonas aeruginosa*[23], and *Bacteroides spp*[24], their association with infection (vs colonization) and lack of healing is far from being established.

Until recently, the bacteria associated with chronic wounds have been analysed by standard, culture-dependent bacteriological methods, by taking a swab or biopsy from the wound and using it to inoculate different growth media. The development of molecular methods has demonstrated that culture-dependent methods underestimate the presence of bacteria, especially in the case of ulcers with slow-growing, fastidious or anaerobic microbes[25,26,27]. In particular, Davies et al (2004)[20] reported that 40% of microorganisms identified in chronic wounds by molecular methods could not be cultured by classical methods, even if most of them were species that are usually considered to grow well on agar plates. In a recent study, it was described that molecular methods detected anaerobic pathogen that had not been detected with anaerobic cultures[10]. The same study described that culture experiments showed the presence of 12 different species in chronic wounds compared with the 33 species found with molecular methods[10].

Molecular techniques applied to the study of microbiology of chronic wounds comprise (reviewed by Martin et al, 2010)[6]:

- normal PCR, which uses organism-specific primers and therefore different reactions are needed to detect each pathogen
- real time PCR, applied to selected pathogens, which also requires organism-specific primers but has the advantage of giving a precise quantitation of the specific pathogen
- metagenomic methods, either by large scale genomic pyrosequencing, or by denaturant gradient gel electrophoresis (DGGE) fingerprinting.

It is relevant to note that so far qPCR to evaluate the total bacterial load has not been applied to the study of chronic wounds.

While the main treatment of chronic wounds aims to address the underlying causes, often both compression bandages (to relieve edema) and antibiotics are prescribed to these patients. However, O'Meara et al (2000)[28] analysed existing studies on the use of antibiotics in chronic wounds and drew the conclusion that there is insufficient evidence for their use in wound healing. Furthermore, a more updated search of the literature found that conclusive studies regarding the use of systemic antibiotics have not been published in more recent years[19]. The need for treatment is strong, and the lack of established, proof-grounded guidelines has led to develop less conventional methods, such as debridement by using larvae from the fly Lucilia sericata to remove necrotic tissue and bacteria from the wound, thus aiding the healing process[29]. An innovative treatment is represented by Cutimed Sorbact, a membrane with hydrophobic properties allowing binding and retention of bacteria, enhancing the natural healing process. This approach has the advantage of having no unpleasant collateral effect and the inability of bacteria to develop resistance, invariably associated to the use of antibiotics.

This work aimed to verify the suitability of qPCR quantification of total bacterial load as a quick and sensitive laboratory parameter in the course of a clinical study on the use of Cutimed Sorbact for healing of chronic wounds. To achieve the goal, a panbacterial qPCR based on amplification of a conserved region of the 16S gene was set up, and verified on the genome of six different bacteria. The results (Fig. 3) show that this approach was sensitive and allows precise quantification over a broad range of concentrations (from 100 to 10^7 target molecules).

The clinical results show the success of the therapy in 15/20 patients. The laboratory results on panbacterial qPCR and identification of specific pathogens can be summarized as follows:

- Total bacterial load significantly decreased in 10/15 healing chronic wounds
- Total bacterial load did not change in 5/5 non healing chronic wounds
- Decrease of bacterial load was shown in biopsies, but not in swabs
- Classical microbiology for two aerobes widely predominant in chronic wounds (*S. aureus, P. aeruginosa*) did not show any correlation with the clinical outcome of the therapy
- Molecular quantification for two anaerobes often implicated in chronic wounds (*Bacteroides, Fusobacterium*) did not show any correlation with the clinical outcome.

Several interesting and original observations arise from this study.

The first result is that panbacterial qPCR can be a reliable method to assess the therapeutic success of chronic wound treatment. In fact, 10/15 chronic wounds with therapeutical success showed a significant decrease of total bacterial load, and no decrease was observed in 5/5 wounds with no clinical improvement. In total, the results of qPCR were concordant with clinical data in 15/20 chronic wounds, indicating that might be considered as an useful biomarker for treatment prognosis. This is an important observation. In fact, the scientific literature highlights the need of prognostic indicators for chronic ulcers. A recent review enumerates several potential biomarkers (cytokines, proteases and their inhibitors, senescence markers, oxidative stress, microbiological status, etc.) but concludes that no available data reflect wound progression or regression[30]. Our study indicates that panbacterial qPCR might fill this need.

Another observation is that quantification studies of chronic wounds by panbacterial real-time PCR require analysis of biopsies. In fact, no significant result was obtained by analysis of swabs (Figures 6, 8, 10). Even if this result cannot be explained at the moment, it is possible that chronic wounds, even at an advanced stage of healing, are still colonized by a high number of bacteria at the surface, while infection of deep tissues has been eliminated. According to this hypothesis, bacterial swabs would just indicate the presence of colonizing bacteria while infectious processes are being eliminated.

Furthermore, the analysis for specific pathogens is much less sensitive than panbacterial qPCR, and could even be misleading. In fact, by conventional culture *S. aureus* and *P. aeruginosa* were not detected in sample n° 12 (Table 5), and yet this lesion was refractory to treatment and showed a substantial increase of wound area. Furthermore, both bacteria continued to be present in sample n° 2, even if this lesion responded well to therapy with a significant decrease of affected area. A similar situation was observed by analysis of anaerobes by real-time PCR. No significant decrease of *Bacteroides* was recorded in healing wounds, and this anaerobic bacteria had similar loads in healing and non healing lesions (Fig. 13).

At the moment it is not possible to explain with convincing arguments the fact that 5 chronic wounds showed a positive clinical outcome with no decrease of total bacterial burden. One plausible explanation is that the bacterial population in these wounds was only a minor pathogenic component, or that the presence of bacteria reflected colonising, but not infecting, microorganisms. Alternatively, it is possible that there was a switch in the composition of the bacterial population, and that more aggressive bacteria present in the first biopsy had been replaced in the last biopsy by commensal microorganisms. However, it should be noted that *S. aureus*, *P aeruginosa* and *Bacteroides* were not involved in this hypothetical process.

In conclusion, these results show that panbacterial qPCR is a promising fast method for determining the total bacterial load in chronic wounds, and suggest that it might be an important biomarker for the prognosis of chronic wounds under treatment.

REFERENCES

1. Bickers DR, Lim HW, Margolis D, Weinstock MA, Goodman C, Faulkner E et al. The burden of skin diseases: 2004 a joint project of the American Academy of Dermatology Association and the Society for Investigative Dermatology. *Journal of the American Academy of Dermatology*, 2006. 55:490-500.
2. Kuehn BM. Chronic wound care guidelines issued. *JAMA*, 2007. 297: 938-939.
3. Moreo K. Understanding and overcoming the challenges of effective case management for patients with chronic wounds. *Case manager*, 2005. 16 (2): 62-67.
4. Crovetti G, Martinelli G, Issi M et al. Platelet gel for healing cutaneous chronic wounds. *Transfusion and Apheresis Science*, 2004. 30 (2): 145-150.
5. Supp DM, Boyce SR. Engineered skin substitutes: practices and potentials. *Clinics in Dermatology*, 2005. 23 (4): 403-412.
6. Martin JM, Zenilman JM, Lazarus GS. Molecular microbiology: new dimensions for cutaneous biology and wound healing. *Journal of Investigative Dermatology*, 2010. 130: 38-48.
7. Mangram AJ, Horan TC, Pearson ML, Silver LC, Jarvis WR. Guideline for prevention of surgical site infection. *American Journal of Infection control*, 1999. 27: 97-134.
8. Brook I, Frazier EH. Aerobic and anaerobic microbiology of chronic venous ulcers. *International Journal of Dermatology*, 1998. 37: 426-428.
9. Bowler PG. The anaerobic and aerobic microbiology of wounds: a review. *Wounds*, 1998. 10: 170-178.
10. Thomsen TR, Aasholm MS, Rudkjøbing VB, Saunders AM, Bjarnsholt T, Givskov M, Kirketerp-Møller K, Nielsen PH. The bacteriology of chronic venous leg ulcer examined by culture-independent molecular methods. *Wound Repair and Regeneration*, 2010. 18(1): 38-49.
11. Bowler PG. Bacterial growth guideline: reassessing its clinical relevance in wound healing. *Ostomy wound management*, 2003. 49 (1): 44-53.

12. Fang H, Hedin G. Rapid Screening and Identification of Methicillin-Resistant *Staphylococcus aureus* from Clinical Samples by Selective-Broth and Real-Time PCR Assay. *Journal of Clinical Microbiology*, 2003. 41(7): 2894-2899.
13. Boutaga K, van Winkelhoff AJ, Vandenbroucke-Grauls CMJE, Savelkoul PHM. Periodontal pathogens: a quantitative comparison of anaerobic culture and real-time PCR. *FEMS Immunology and Medical Microbiology*, 2005. 45: 191–199.
14. Wilson KH, Blitchington RB, Greene RC. Amplification of bacterial 16S ribosomal DNA with polymerase chain reaction. *Journal of Clinical Microbiology*, 1990. 28: 1942-1946.
15. Yoshikawa TT. Antimicrobial resistance and aging: beginning of the end of the antibiotic era? *Journal of the American Geriatrics Society*, 2002. 50(7 suppl): S226-229.
16. Ayliffe GA. The progressive intercontinental spread of methicillin-resistant Staphylocuccus aureus. *Clinical Infectious Disease*, 1997. 24 (suppl 1): S74-79.
17. Ljungh A, Yanagisawa N, Wadstrom T. Using the principle of hydrophobic interaction to bind and remove wound bacteria. *Journal of wound care*, 2006 15(4): 175-180.
18. Yang S, Lin S, Kelen GD, Quinn TC, Dick JD, Gaydos CA, Rothman RE. Quantitative multiprobe PCR assay for simultaneous detection and identification to species level of bacterial pathogens. *Journal of Clinical Microbiology*, 2002. 40 (9): 3449-3454.
19. Howell–Jones RS, Wilson MJ, Hill KE, Howard AJ, Price PE, Thomas DW. A review of the microbiology, antibiotic usage and resistance in chronic skin wounds. *Journal of Antimicrobial Chemotherapy*, 2005. 55: 143-149.
20. Davies CE, Hill KE, Wilson MJ Stephens P, Hill CM, Harding KG, Thomas DW. Use of 16S ribosomal DNA PCR and denaturing gradient gel electrophoresis for analysis of the microfloras of healing and nonhealing chronic venous leg ulcers. *Journal of Clinical Microbiology*, 2004. 42 (8): 3549-3557.
21. Hansson C, Hoborn J, Moller A, Swanbeck G. The microbial flora in venous leg ulcers without clinical signs of infection. Repeated culture using a validated

standardized microbiological technique. *Acta Dermato-Venereologica*, 1995. 75 (1): 24-30.

22. Bowler PG, Davies BJ. The microbiology of infected and non infected leg ulcers. *International Journal of Dermatology*, 1999. 38: 573-578.
23. Schmidt K, Debus ES, ST Jessberger, Ziegler U, Thiede A. Bacterial population of chronic crural ulcers: is there a difference between the diabetic, the venous, and the arterial ulcer? *VASA*, 2000. 29 (1): 62-70.
24. Kontiainen S, Rinne E. Bacteria in ulcera crurum. *Acta Dermato-Venereologica*, 1988. 68(3): 240-244.
25. James G, Swogger E, Wolcott R, Pulcini E, Secor P, Sestrich J, Costerton JW, Stewart PS. Biofilms in chronic wounds. *Wound Repair and Regeneration*, 2008. 16(1): 37-44.
26. Tolker-Nielsen T, Molin S. Spatial organization of microbial biofilm communities. *Microbial Ecology*, 2000. 40(2): 75-84.
27. Hill KE, Davies CE, Wilson MJ, Stephens P, Harding KG, Thomas DW. Molecular analysis of the microflora in chronic venous leg ulceration. *Journal of Medical Microbiology*, 2003. 52(Pt 4): 365-369.
28. O'Meara S, Cullum N, Majid M, Sheldon T. Systematic reviews of wound care management: (3) antimicrobial agents for chronic wounds; (4) diabetic foot ulceration. *Health Technology Assessment*, 2000. 4 (21): 1-237.
29. Church JCT, Courtenay M. Maggot debridement therapy for chronic wounds. *Lower Extremity Wounds*, 2002. 1: 129-134.
30. Moore K, Huddleston E, Stacey MC, Harding KG. Venous leg ulcer- the search for a prognostic indicator. *International Wound Journal*, 2007. 4: 163-172.